University of Mississippi

FLOOD MITIGATION ENGINEERING RESOURCE CENTER (FMERC) - PROJECT EC14-005

Final Report Appendix C- Hydrodynamic and Morpho-dynamic Model Data Sources, Acquisition and Development
Sandy Baseline Model and Simulation of Performance of Alternative Hard-Structures (Flood Walls and Barriers)

18 June, 2014

Submitted to:

NEW JERSEY DEPARTMENT OF ENVIRONMENTAL PROTECTION
Office of Engineering and Construction
Trenton, NJ
Attn: Dave Rosenblatt, Administrator
John Moyle, Manager of Dam Safety and Flood Control

Simulations of Storm Surges Driven by Hurricane Sandy and Sea Level Rise, Evaluation of Flood Protection Structures, and Modeling of Contaminant Leaching

Technical Report

April 28, 2014

Submitted to:

Department of Civil & Environmental Engineering, New Jersey Institute of Technology

Attn: **Dr. Fadi A. Karaa**

Submitted by:

National Center for Computational Hydroscience and Engineering

The University of Mississippi

Brevard Hall 327, University, MS 38677-1848

(662)915-8969

Attn: **Yan Ding, Mustafa S. Altinakar, Yaoxin Zhang, A.K.M. Azad Hossain, and Yafei Jia**

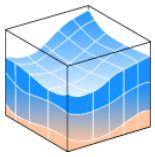

Table of Contents

Table of Figures

List of Tables

1 Objectives and Tasks

The main objective in this project is to evaluate the performance of the proposed engineering solutions for mitigating flood and inundation in the Hackensack area, including Moonachie and Little Ferry, by simulating storm surges driven by a Sandy-like hurricane, the possible dam break of the Oradell Reservoir, and the potential sea level rise (SLR) due to the future climate variations. The major tasks are outlined as follows:

I. Collection of various types of data for simulations of flood and inundation from the entire US East Coast to Northeast New Jersey including the Hackensack area,
II. Validation of the storm-surge model, CCHE2D-Coast, by reproducing storm surges and waves driven by Hurricane Sandy (2012) in the US East Coast,
III. Model validation by simulating flood and inundation induced by Sandy in the Hackensack area by using a high-resolution computational grid,
IV. Evaluation of flood mitigation measures by simulating flooding and inundation due to Sandy,
V. Prediction of flood and inundation under the combined conditions of Hurricane Sandy and the potential SLR scenarios,
VI. Evaluation of flood mitigation performance by installing the alternative solutions under the future conditions of hurricane and SLR,
VII. Simulation of flood and inundation by assuming that the Oradell dam-break happens in the peak of the Sandy's storm surge, and
VIII. Simulation of contaminant leaching processes from a potential leaching site in the period of Sandy.

2 Simulation of Flooding and Inundation Induced by Sandy and Sea Level Rise

2.1. Model Descriptions

2.1.1 CCHE2D-Coast for Storm-Surge Modeling

Storm surges are induced by wind and low air pressure during a storm or a hurricane. In a coast, storm surge waters are the amount of water pushed on shore by hurricane winds. Storm tide is a sum of astronomical tide and storm surge. Thus, coastal flooding and inundation can be measured by the flooding water depths, i.e., the amount of waters by substracting the teeain height from water surface elevation (or simply a storm tide elevation). Therefore, the range of coastal flooding and inundation generally varies with time and space. The most important index for measuring flooding and inundation is the flood water extent map, i.e. the map of maximum flood water depths (or water surface elevations).

Since coastal and ocean water motions are not just stimulated by astronomical tide and storm surges, coastal flood and inundation can be driven by multiple hydrodynamic processes (coastal and oceanographic processes) such as wind-induced currents, tidal flows, waves, earth rotation, river flows, etc, at the same time. The total water surface elevation increase during a hurricane is the sum of the expected high tide, storm surge caused by low barometric pressure and onshore winds, wave setup in the surf zone, and inflow caused by flooding rivers. To correctly and accurately compute the spatiotemporal variations of flood and inundation in coasts, one has to adopt an integrated coastal-ocean process model which is capable of taking into account various factors such as tide, wave, flow, wind, air pressure, and river flows if there are tributaries flowing to coasts.

Therefore, we use an integrated coast-ocean model developed in the NCCHE, called CCHE2D-Coast, to simulate the hydrodynamic processes in a hurricane, and to produce the flood water extent maps for different cases with the combined conditions of hurricane and SLR. This model consists of a multidirectional wave spectral model, a coastal hydrodynamic model, and a sediment transport and morphological change model (Ding et al. 2006, Ding and Wang 2008ab, Ding et al 2013c). It is capable of simulating hydrodynamic and morphodynamic processes in coasts, estuaries, rivers, and oceans such as (1) storm surges and waves driven by cyclonic wind which is calculated by a parametric cyclonic wind and air pressure model (Ding et al. 2013b), (2) irregular wave deformations and transformation, (3) tidal and river flows, (4) nearshore currents and wave setup/setdown, and (5) sediment transport and morphological

changes induced by waves and currents. This model generally employs a non-orthogonal grid that can model complex coastlines (Ding and Wang 2008a, Zhang and Jia 2009). This integrated coastal process model can run through a graphical user interface, CCHE2D-Coast GUI. The details of the GUI and the user guidance can be found in Ding et al. (2013c) and Zhang (2013). Hereafter, the wave and flow models of CCHE2D-Coast are adopted for computing hurricane wind, storm surges, and waves; the sediment transport model for morphodynamic processes modeling was not used in this project.

Figure 1 presents a flow chart and structure of the integrated wind-storm-surge model. The wind and pressure field model is to produce the hurricane conditions for the coast-ocean model. In addition to the parameters for calculating the wind field, the required data for simulating storm surges in a coast region include bathymetrical/topographic data, hydrological data (tides, hydrographs of rivers, waves, etc.), and structure data which are used for generating a computational grid and specifying boundary conditions of tides and river flows.

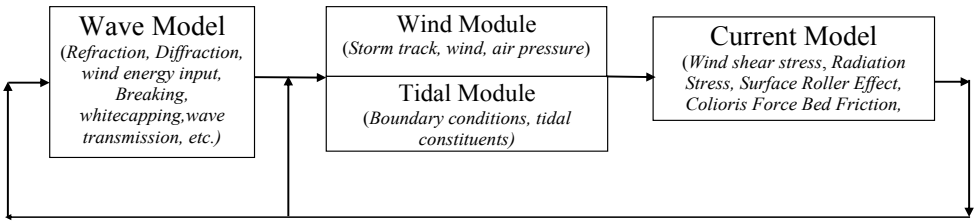

Figure 1 Flow chart of the integrated wind-storm-surge model

The surface wind stress is a major driven force of storm surges, which represents the portion of wind energy input into water columns. Even though the interaction between air and sea water is complex, this wind stress $\vec{\tau}$ can be modeled by the conventional bulk formula (e.g. Large and Pond 1981),

$$\vec{\tau} = \rho C_d |\vec{V}_W| \vec{V}_W$$

where $\vec{V}_W$ = vector of wind velocity at 10 meters above ground, and C_d = drag coefficient (distinct from the nonlinear decay parameter C_D). The hurricane wind velocity is a resultant velocity of the tangential velocity and the hurricane forward velocity given by a hurricane track. Calculation of C_d depends on empirical formulae, for which CCHE2D-Coast provides five options for calculating the drag coefficient proposed by Large and Pond (1981), Powell et al. (2003), and Hwang (2005).

In the wave action model, the energy input by wind forcing is modeled as separated sink and source terms proposed by Lin and Lin (2004a,b).The coefficients in the wind energy input are calibrated by hindcasting Hurricane Gustav (2008) which made landfall at the southern Louisiana coast (see Ding et al. 2013a for the details). For the detailed descriptions of the capabilities of CCHE2D-COAST for forecasting, planning, and investigating coastal disasters due to flooding and inundation induced by tropical cyclones, one may refer to Ding (2013).

2.1.2 A Cyclonic Wind-Pressure Model with Landfall Decay Effect

To predict storm surges induced by tropical cyclonic wind and air pressure depression, spatiotemporal variations of wind and air pressure are needed to calculate wind energy input into ocean and coastal water columns. The widely-used tropical cyclonic wind-pressure model, Holland's wind model (Holland 1980) is a parameterized cyclonic wind-pressure model. This simple model only needs a few parameters for defining hurricane track, size, intensity, and central pressure to determine the air pressure and wind tangential velocity. However, this simple model doesn't include the decay effect of wind after a hurricane makes its landfall.

Hazardous wind and storm surges occur around the coastal area where hurricane makes its landfall and during the period right after its landfall. It is, therefore, important to predict the location and the intensity of storm wind at hurricane landfall. Mainly due to loss of thermal energy input from warm ocean waters, storm wind speed usually decays quickly after landfall. In general, hurricane intensity decay is influenced by a complex combination of physical factors, including the ocean structure prior to landfall, surface heat capacity of water and soil, surface roughness and moistures of soil and vegetation, and variations between day and night (e.g. Marks and Shay 1998, Shen et al. 2002, DeMaria et al. 2006). Kaplan and DeMaria (1995) approximate hurricane maximum velocity decay by a linear differential equation with respect to time after landfall. Their linear decay model only takes into account the decay due to energy loss of heat input from the ocean.

Correlation analyses of various hindcast storms found that the linear decay model was inadequate in simulating the decay process; in particular, sharp drops in wind velocity immediately following landfall of numerous storms suggested that one or more additional

physical factors induce a nonlinear pattern of hurricane decay (Marks and Shay 1998, Shen et al. 2002). Thus, to predict the maximum wind speed and air pressure after hurricane landfall, Ding (2012) developed a new decay model with an additional non-linear decay term to account for increased surface roughness as the storm moves over land.

$$\frac{d(V_{\max}-V_b)}{dt} = -\alpha(V_{\max}-V_b) - \frac{C_D}{h}(V_{\max}-V_b)^2 \quad (1)$$

where t = time after landfall, V_b = background wind velocity, V_{max} = maximum wind velocity, α = parameter of linear decay (1/s), C_D = non-dimensional drag coefficient and h = mean height of the planetary boundary layer (m), the lowest layer of the troposphere in which wind is influenced by land surface friction (Vickery et al. 2000a). Because the last term in Eq. (1) is nonlinear, this equation does not have an analytical solution. A time-marching semi-implicit Euler's scheme is used for computing the maximum wind speed.

The empirical parameters, the decay parameter α and the drag coefficient C_D, have been calibrated by computing the historical post-landfall data of the hurricanes landed in the northern Gulf Coast. The selected hurricanes for calibrations are Andrew (1992), Lili (2002), Ivan (2004), Katrina (2005), Rita (2005), Dennis (2005), and Gustav (2008). Using the calibrated parameter values, Ding (2012) established a statistical database of their optimum parameters. Two regression relations have been developed to predict the two empirical parameter values when a hurricane makes landfall in the Gulf Coast:

$$\frac{\alpha h}{(V_i - V_b)} = 5.1462\times10^{-4} - 1.8312\times10^{-5}\left(\frac{\Delta P}{\frac{1}{2}\rho(V_i - V_b)^2}\right) \quad (2)$$

where V_i = maximum wind velocity at landfall (m/s), ΔP (pascals) is the difference between the central air pressure and ambient pressure at hurricane landfall, ρ = air density (kg/m^3), and

$$C_D \times 10^{-10} = 3.7322\times10^{-8}(V_i - V_b)^{8.8564} \quad (3)$$

Here, h = 1000m. As a result, the decay rate α and the drag coefficient C_D can be directly calculated by using the regression equations, only given the wind velocity and central air pressure at landfall. Ding (2012) also has developed a procedure to reconstruct a two-dimensional wind and atmospheric pressure by combining Holland's hurricane model (Holland 1980) and this nonlinear landfall wind model.

2.1.3 Construction of 2D Wind Field with Decay Effect

Holland's tangential wind field equation (Holland 1980) was used to derive a direct relationship between the decay in maximum velocity and central barometric pressure. This parameterized formula renders hurricane's complex atmospheric processes as a fixed vortex of rotating winds creating a central region of low atmospheric pressure – the eye. Holland's equation is as follows:

This parameterized formula boils a hurricane's complex atmospheric processes down to a fixed vortex of rotating winds that create a central region of low atmospheric pressure – the eye (Mattocks and Forbes 2008).

$$V(r) = \sqrt{(B/\rho)(R/r)^B (P_a - P_c) e^{-(R/r)^B} + \left(\frac{rf}{2}\right)^2} - \left(\frac{rf}{2}\right) \tag{4}$$

where *V(r)* = tangential wind speed (m/s) at a distance of *r* (m) from the center, *R* = radius of the band of maximum sustained winds from the eye's center, P_c = central pressure, P_a = ambient pressure (both in pascals), *B* = empirically determined parameter, $f = 2\Omega sin(latitude)$ is the Coriolis force, and Ω is the rotational frequency of the earth.

An explicit relationship between maximum wind and pressure was derived by setting *R* equal to *r* in Holland's equation (4):

$$V_{\max} = \sqrt{(B/\rho)(P_a - P_c) e^{-1}} \tag{5}$$

Combining Eq. (5) with Eq. (4), thus the tangential wind field at any locations can be expressed as a function of maximum velocity and a position function of *r*.

$$V(r) = \sqrt{V_{\max}^2 (R/r)^B e^{(1-(R/r)^B)} + \left(\frac{rf}{2}\right)^2} - \left(\frac{rf}{2}\right) \tag{6}$$

In order to extend the parametric cyclonic model across an area, a fixed, cylindrical wind field was constructed from the decay curve using Holland's equation and its pressure field analogue *P(r)*, i.e.

$$P(r) = P_c + (P_a - P_c) e^{-(R/r)^B} \tag{7}$$

Before landfall, the wind field is calculated from observed central pressure values using the equation of *P(r)*, and the tangential wind velocity at any location by Eq. (4). After landfall, with

decay effects, V_{max} is calculated from the nonlinear differential equation (1) of the landfall decay model, wind velocity is determined by Eq. (6).

Various methods of calculating the wind field were examined for simulation accuracy. First, the impact of taking decay effects into account after landfall was studied by comparing results from the nonlinear pressure-wind decay model to the results of the basic, non-decay wind field. Second, statistical analysis of the decay model validated the relationship between *B* and the gauge pressure at the eye of the hurricane after landfall, as showing in Eq. (7). In accordance, a similar empirical relation between *B* and a gauge pressure and radius of maximum winds before landfall was utilized (Vickery et al. 2000b):

$$B = 1.34 + 0.00328(P_a - P_c) - 0.00309R \tag{11}$$

In numerous simulation cases, the simulation accuracy of changing *B* with gauge pressure was compared with that of keeping *B* constant.

In Hurricane Sandy, the decay model produced very accurate prediction results for hurricane maximum wind and the central pressure after its landfall (see Figure 2).

(a)

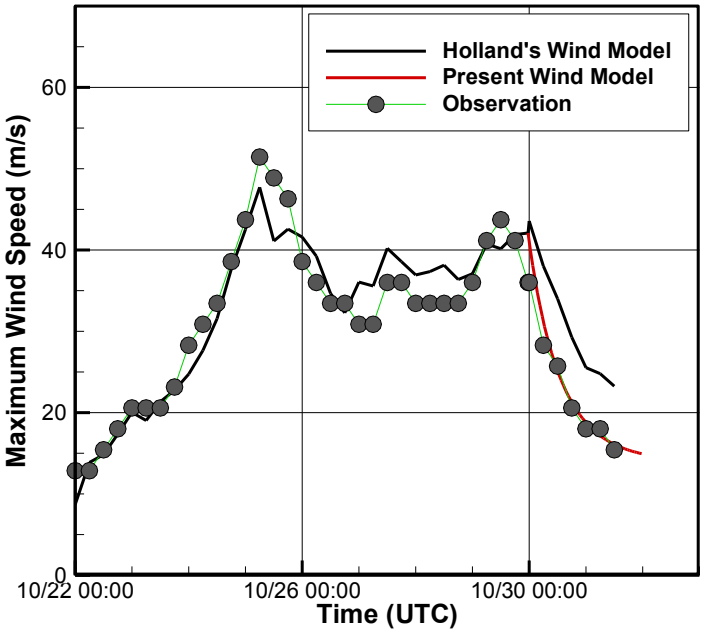

(b)

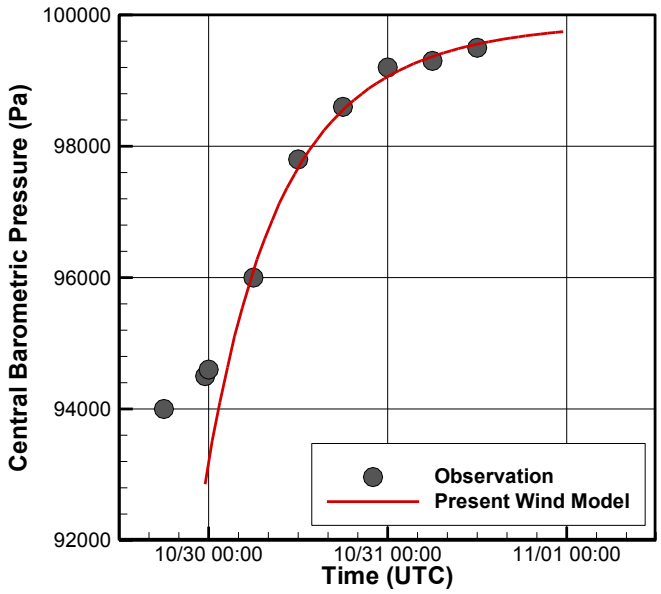

Figure 2 Comparisons of wind speed (a) and central air pressure (b). The observation data are from the best track of Hurricane Sandy (2012) by NOAA.

2.2 Data Gathering

To build and validate the storm-surge model to simulate winds, tides, storm surges, waves, and currents in the track of Hurricane Sandy in the US East Coast, we have collected various types of data such as geospatial data, hurricane track data, and meteorological/oceanographic/hydrological data, from different data sources.

2.2.1 Track of Hurricane Sandy

Hurricane Sandy was formed in the southwestern Caribbean Sea at the late October of 2012, which is a classic late-season hurricane. The cyclone made landfall as a category 1 hurricane in Jamaica, and gained strength to a 100-kt category 3 hurricane in eastern Cuba. Sandy underwent a complex evolution and grew considerably in size while over the Bahamas, and continued to grow despite weakening into a tropical storm north of those islands. The

system restrengthened into a hurricane while it moved northeastward, parallel to the coast of the southeastern United States, and reached a secondary peak intensity of 85 kt while it turned northwestward toward the mid-Atlantic states (see the best track in Figure 3). Although at the landfall of Hurricane Sandy (2012), this cyclone weakened to a post-tropical storm near Brigantine, New Jersey at about 2330 UTC, Oct. 29, 2012, due to its tremendous size (winds grew to about 870 n mi prior to landfall), Sandy drove a catastrophic storm surge into the New Jersey and New York coastlines. The atmospheric structure of Sandy is also very complex. When the cyclone moved up to the high latitude of the east Atlantic Ocean, it merged into the Gulf Stream and encountered the trough of the jet stream from the west of the North American continent. This complex weather system made the surface wind fields around the cyclone being asymmetric, which is different from the symmetrical structure of surface wind of hurricanes in the Gulf of Mexico (Halverson and Rabenhorst 2013).

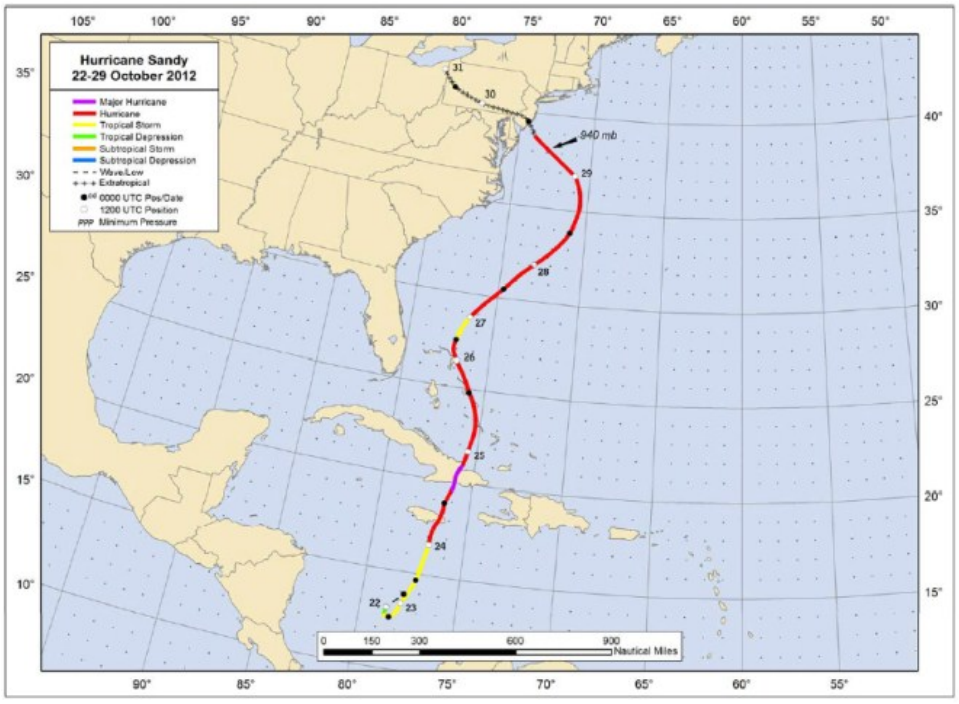

Figure 3 Best track of Hurricane Sandy, Oct. 22-29, 2012 (Blake et al. 2013)

The best track data of tropical storms, also known as HURricane DATabase (HURDAT), provided by NOAA (2014), contain the coordinates of hurricane eye, hurricane central air pressure, hurricane size, maximum sustained wind speed, etc. These parameters of Hurricane

Sandy's best track are used to reconstruct the cyclonic wind and air pressure fields, computed by the above-mentioned parametric hurricane wind model. This wind model has considered the decay effect of Sandy's landfall, in which the maximum wind speed and central air pressure are given in Figure 2.

2.2.2 Geospatial Data

The computational domain for Sandy's storm-surge modeling covers the entire US east coast from Florida to Maine. The bathymetric data of the Atlantic Ocean were prepared using two types of bathymetry data. One is the NOAA geophysical Data Center (NGDC), and USACE-ERDC. The NGDC data is bathymetric topographic data, which includes both topography and bathymetric data at about 100-m resolution. The other one is an existing grid used in the ADCIRC storm-surge simulations, which is a finite elemental mesh data. This ADCIRC depth grid called SL15. It contains 2,137,978 nodes and 4,184,778 triangular elements in total, which covers a very large area including Gulf of Mexico, Caribbean Sea and part of the Atlantic Ocean up to Maine and Nova Scotia.

The topographical data were obtained from three different sources: NGDC, USGS, and NJIT. The NGDC 100 m bathymetric topographic data were used for the coastal areas and the islands in the Atlantic Ocean. The USGS 3-m DEM and the NJIT 1-m Lidar data were used in New York, New Jersey, and the surrounding areas.

2.2.3 Meteorological Data

The best track data of Sandy shows that two peaks of maximum sustained wind speed were found. As show in Figure 2(a), the first peak of the maximum wind speed is 100 kt at 0525 UTC 10/25/2012, when it made landfall at the west of Saniago de Cuba; the second peak of the maximum speed is 85 kt, at 1200 UTC 10/29/2012, right after the landfall of Sandy near Brigantine, NJ.

Accordingly, the air pressure at the hurricane center (eye) reached the first lowest depression, 954mb, at the time when it made its first landfall in Cuba. Then, the air pressure at the Sandy's eye dropped to 940 mb at 1800 UTC 10/29/2012, at the offshore of the New Jersey Coast (Figure 2(b)).

The H*Wind analysis by NOAA's Hurricane Research Division indicates that the hurricane wind after it made landfall in Cuba still preserved a cyclonic wind field, as shown in Figure 4(a). It means that at the low-latitude region, the surface wind is still dominated by this tropical cyclonic rotation and translational movement. However, the surface wind at the offshore of the New Jersey coast, as shown in Figure 4(b), presents a complex wind field: although the cyclone was moving toward the northwest, the maximum sustained wind speed occurred in the lower left corner of the cyclone. Obviously, at this moment, the jet stream has intervened in the structure of the surface wind. As pointed out by Halverson and Rabenhorst (2013), the weather system in the north of the US East Coast made the wind field around Sandy being extremely complex, which is different from the cyclonic structure of hurricanes at the low-latitude area such as the Gulf of Mexico.

(a)

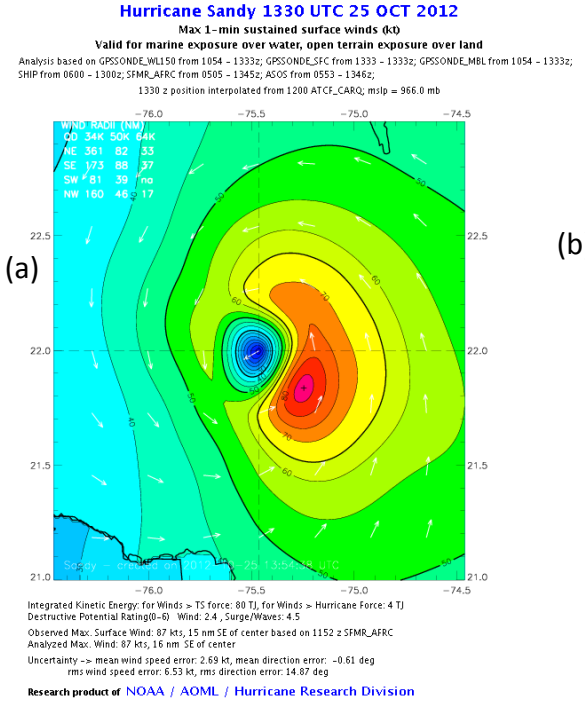

(b)

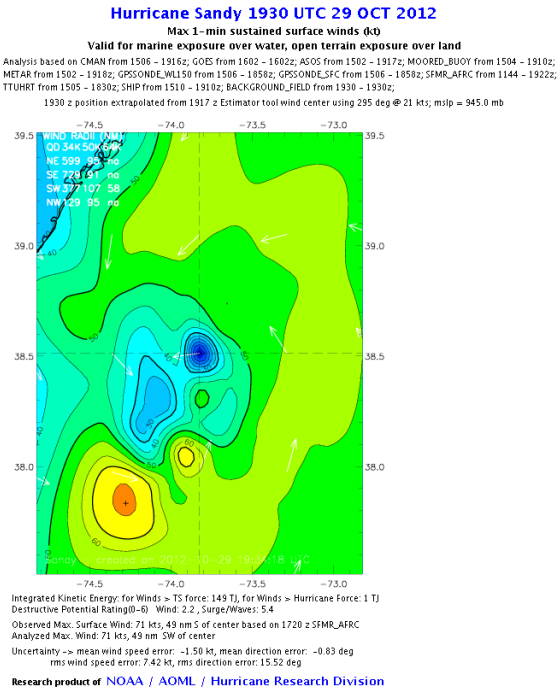

Figure 4 Maximum sustained surface wind (left) at 1330 UTC 10/25/2012 after its first landfall in Cuba, and (b) at 1930 UTC 10/29/2012 before its landfall at the New Jersey Coast

For validation of the hurricane wind model, we have also collected a large amount of ground wind data (wind speed, direction, and air pressure) which are observed by NOAA at the tide gages at the East Coast from South Carolina to Maine.

2.2.4 Hydrological Data (Storm Surges, Tide Levels, Waves, etc)

The strong wind and air depression lift the waters of the entire east coast of the US from Florida to Maine. When Sandy made its landfall, it induced catastrophic storm surges and waves into the New Jersey and New York coastlines which inundated low-lying land areas in the two states. The highest water elevation of storm tide measured by an NOAA-NOS tide gauge at King Point in New York was 14.311 ft (4.362 m) above Mean Lower Low Water (MLLW) at 0206 UTC 10/30/2012. The storm surge at this NOS station was up to 8.54 ft above the normal tide level at this moment. Surveyed high-water marks from the United States Geological Survey (USGS) indicate that the highest water levels in New York occurred on Staten Island. The highest direct measurement of inundation was 7.9 ft above ground level, in the Oakwood neighborhood of Staten Island. Significant flooding due to storm surge (with some contribution from rainfall) occurred in parts of the Hudson River Valley as far north as Albany. In New Jersey, the highest water elevation of storm tide measured at Sandy Hook, NJ was 10.416 ft above NAVD 88, at 2342 UTC 10/29/2012. The surge at this moment reached to 8.567 ft above the normal tide level. After this record, this station failed and stopped reporting the data.

As storm surge from Sandy was pushed into New York city and Raritan Bays, sea water piled up within the Hudson River and the coastal waterways and wetlands of northeastern New Jersey, including Newark Bay, and the Passaic and Hackensack Rivers. Significant inundations occurred along the Hudson River in Weehawken, Hoboken, and Jersey City, where many high-water marks indicated that inundations were between 4 and 6.5 ft above ground level. Inundations of 4 to 6 ft were also measured across Newark Bay in Elizabeth and the area around Newark Liberty International Airport.

The high wind of Sandy generated huge ocean waves along the storm track. The highest significant wave height at NDBC Station No. 44065 was 32.35 ft (9.86 m), recorded at 0050 UTC 10/30/2012. Wave action on the east coast caused beach erosion, damage to coastal structures such as bridge piers and houses near the shores, and highways. Preliminary U.S. damage estimates are near $50 billion, making Sandy the second-costliest cyclone to hit the United States since 1900, In the United States, 72 direct deaths were noted, making Sandy the deadliest U.S. cyclone outside of the southern states since Agnes (1972). (Blake et al. 2013).

For the purpose of validation of CCHE2D-Coast, the water surface elevations during the period of Sandy were acquired from the NOAA's tides-and-currents website at a number of CO-OPS stations (Table 1). The wave parameters (i.e. significant wave heights, mean wave direction, peak wave period, and wave spectral energy distributions) at the Atlantic Ocean were obtained at several NDBC (National Data Buoy Center) stations (Table 2).

The high water mark data was obtained from the USGS website at the USGS Sandy Storm Tide Mapper (USGS 2013).

Table 1 List of NOAA's Tide Gages

No.	Station Name	CO-OPS Station ID	Datum	Conversion to NAVD88 (m)
1	Montauk, NY	8510560	NAVD 88	
2	New Haven, CT	8465705	MLLW	
3	The Battery, NY	8518750	NAVD88	
4	Bergen Point West Reach, NY	8519483	MLLW	-0.89916
5	Sandy Hook, NJ	8531680	NAVD88	
6	Atlantic City, NJ	8534720	NAVD88	
7	Ocean City Inlet, MD	8570283	NAVD88	
8	Bishops Head, MD	8571421	NAVD88	
9	Solomons Island, MD	8577330	NAVD88	
10	Lewes, DE	8557380	NAVD88	
11	Wrightsville Beach, NC	8658163	NAVD88	
12	Kiptopeke, VA	8632200	NAVD88	
13	Chesapeake Bay Bridge Tunnel, VA	8638863	MLLW	

Table 2 List of NDBC Buoys

No.	Station Name	NDBC ID
1	LONG ISLAND - 30 NM South of Islip, NY	44025
2	New York Harbor Entrance - 15 NM SE of Breezy Point , NY	44065
3	DELAWARE BAY 26 NM Southeast of Cape May, NJ	44009
4	EAST HATTERAS - 150 NM East of Cape Hatteras	41001
5	SOUTH HATTERAS - 225 South of Cape Hatteras	41002

2.3 Hindcasting Storm Surges and Waves in Hurricane Sandy in the US East Coast

For validation of the coastal model, CCHE2D-Coast, simulations of hydrodynamic processes during the period of Hurricane Sandy were performed by two steps: the first one is to compute wind, storm surges, and waves in a regional scale domain covering the entire US East Coast; the second is to simulate flood and inundation in the low-lying area in the northeast New Jersey for assessing the flooding impact of Sandy .

2.3.1 Computational Domain and Mesh Generation

As the first step of the storm-surge simulation, the regional scale domain, as shown in Figure 5, consists of the US East coast from Florida to Maine and Nova Scotia and the part of the North Atlantic Ocean. The east boundary of the domain goes through Bermuda along the northeast direction. This computational area includes the North Atlantic Ocean from 30^{O}N to 45^{O}N.

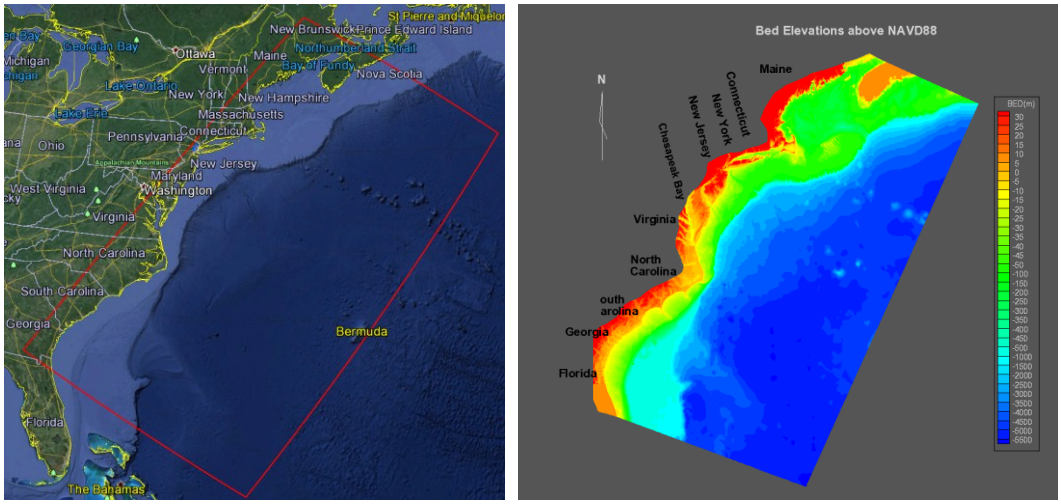

Figure 5 Computational domain and Bathymetry and Topography of the US East Coast

A non-orthogonal structural grid was generated by using CCHE2D-Mesh (Zhang and Jia 2009). It consists of 1,008,018 nodes (1679×594) with spatially-varying resolutions: high resolution in coastal regions and low-lying land in New Jersey, lower resolution at deepwater of the ocean. Figure 6 shows the computational grid only covering the coastal regions of New York and New Jersey, including the Hudson River and the wetland in northeast New Jersey.

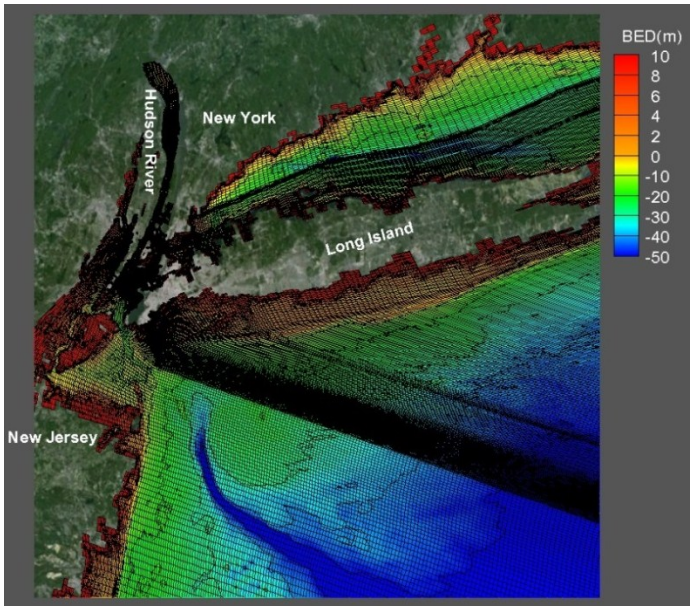

Figure 6 Computational grid in the New York and New Jersey Coasts

2.3.2 Computational Conditions

The bottom roughness coefficients, i.e. Manning's *n* values, are obtained by interpolating the values from the SL15 mesh data. The values in the SL15 have considered the sea bottom roughness, coastal structures (i.e. dikes, roads, sea walls etc.), and vegetation at wetland. The roughness values are set as 0.02 in the water area and 0.03 in inland area, respectively.

Storm Tracks

The best track of Sandy (Figure 3) provided by NOAA's National Hurricane Center (NHC) is used as the storm track. The information of the storm track includes the coordinates of the cyclone centers at different recorded time, the central air pressure, and the radii of the cyclone.

Tides

Based on the observations of tides at NOAA's tide gages in the Atlantic Ocean (http://tidesandcurrents.noaa.gov/gmap3/), the tidal elevations at Bermuda is used as the tidal boundary condition at the deepwater open boundary of the Atlantic Ocean.

Waves

Wave set-up induced by storm winds can cause an additional increase in water surface elevation and increases the extent of inundation area and depth. By using the wave model in CCHE2D-Coast, the wind-induced wave fields are computed over the entire computational domain as shown in Figure 5. In the simulations of storm surge by coupling the wave model with the hydrodynamic model, the wave field was recomputed every one hour based on the latest flow results.

On the offshore boundary, wave parameters as the wave boundary conditions are computed by a deep water wave model, Young's hurricane wave model (Young 1988, Young and Burchell 1996). The model assumed that the JONSWAP (Hasselmann et al, 1973, 1976) relationship, originally developed for fetch limited conditions, could also be applied in hurricane wind fields with the specification of a suitable 'equivalent fetch'. Therefore, the significant wave height (*Hs*) and peak period (T_p) are computed by the JONSWAP spectrum. As long as the wave parameters are computed on the offshore boundary, the multidirectional wave spectral density at every offshore boundary node is calculated based on the given hurricane wind directions and the Bretschneider-Mitsuyasu (B-M) spectrum (Mitsuyasu 1970).

Model Spin-up and Initial Conditions

Before a storm surge simulation starts, the model has to be initialized, or spun up, so that a well-developed sea state is created for flow dynamic simulations driven by tides and storm winds. This model was spun up by simulating the tidal flows over the US east coast for 10 days, i.e. from 0000 UTC 10/15/2012 to 0000 UTC 10/25/2012. The time-step size is 120 seconds. An eddy-viscosity model was used for calculating the eddy viscosity in the flow model. During the spin-up period of the simulation, the effect of surface wind was neglected.

2.3.3 Simulation results of cyclonic wind fields, surge tides, and waves

The simulation of storm surges and waves started at 0000 UTC 10/25/2012, 5 days before Hurricane Sandy made landfall at the New Jersey coast. It was carried out till 0000 UTC 11/01/2012, for a week.

The surface wind fields of Hurricane Sandy were reconstructed by using the Holland's wind model. However, after the cyclone made it landfall in New Jersey, the decay of landfall was considered by modifying the maximum wind speed and the central air pressure based on Eq. (1) and Eq. (5) of the nonlinear surface wind model developed by Ding (2012). α and C_D decay parameter regressions, i.e. Eqs. (2) and (3) were used to estimate Sandy's decay process from forecasted maximum winds and minimum pressure at landfall (see Figure 2). The cyclonic wind fields were represented by the modified Holland's wind model with a variable hurricane strength parameter (B); rotational velocities were scaled by 0.7 to match surface wind speeds. After comparing a few formulations for calculating the drag coefficient C_D in Eq. (12), Large and Pond (1981) was used to calculate the drag coefficients for surface wind stress.

The frequency of wave-current interaction was two hours, namely, the wave field driven by the cyclone wind was updated every 2 hours during the storm-surge simulation. In the computation of wave-action equation of the spectral wave energy, the total 21 frequency bins and 25 wave directions were used to discretize the wave spectra for computations of irregular wind-induced waves. The effect of wave breaking in shallow waters and the whitecapping in deepwaters were included. The unsteady wave action was performed.

In the simulation of surge tide, the wave-induced radiation stresses, surface wind stresses, and the bottom friction stresses were considered. A strongly implicit scheme was used for solving the time-dependent flow equations. The time-step size for computing flows is 120 seconds. Using this computationally-efficient model, one-week storm surge simulation (without wave-current interaction) took 3 hours on a single CPU of Intel(R) Core (TM) i7 CPU@2.22GHz; fully-coupled wave-current simulation took 8 hours on the single CPU on a laptop computer. All the computed results of wind, wave, current, and water elevations can be visualized by applying CCHE2D-GUI. The animations of these physical variables can be generated by this user interface.

As two examples, Figure 7 presents comparisons of wind speed at four NOAA gages at Ocean City Inlet, MD, Bergen Point, NY, NDBC 44025, and NDBC44065. The first two stations record the wind parameters every 6 minutes; the last two NDBC stations provide hourly wind data. This parametric wind model produced a good result of wind at the Ocean City Inlet, but an

overestimated wind speed at the Bergen Point, NY. Due to the "hybrid storm" structure of Sandy (Halverson and Rabenhorst 2013), to obtain better prediction of wind, a meso-scale numerical weather model such as the weather research and forecasting (WRF) Model is needed. Nevertheless, the wind fields generated by the present parametric wind model have produced good results of waves and storm surges, as discussed below.

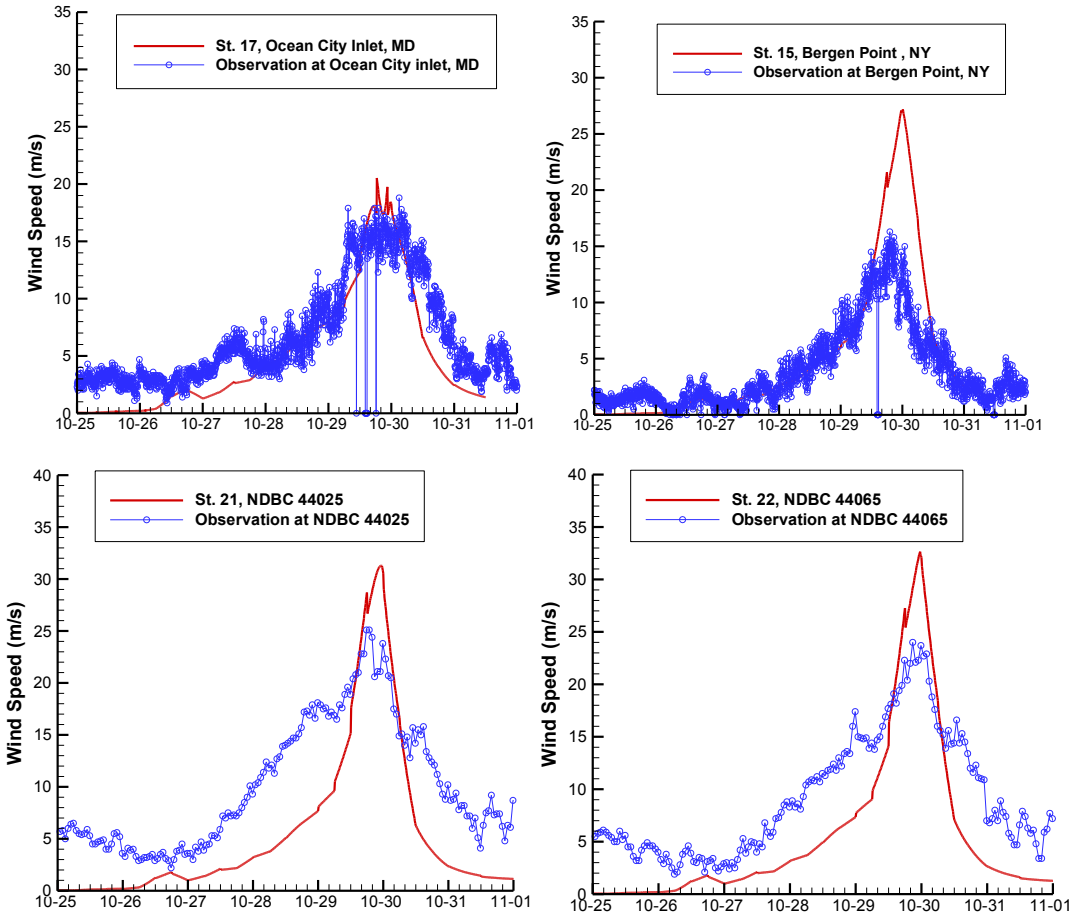

Figure 7 Comparison of wind speed at four NOAA gages

When the hurricane were approaching the US East Coast, storm surges induced by wind and air pressure depression were taking a ride with the astronomical tides in the Atlantic Ocean, and then it formed the surge tides at a wide area of the East Coast from Massachusetts to North Carolina. The surge tides reached up to the peaks around the coasts near the place of the landfall of Sandy. Four snapshots of the water levels and the wind fields before and after Sandy's landfall are presented in Figure 8. Before Sandy's landfall, at 2000 UTC 10/29/2014, the storm started to gather the sea waters and created a huge amount of storm water envelope

from Long Island Sound to Delaware Bay. At the hurricane landfall, 0000UTC 10/30/2012, the peaks of storm surges arrived at the coasts of New York, New Jersey, Maryland, and Virginia. As shown in Figure 8(d), the storm was pushing the surge waters to the East Coast till 0400 UTC 10/30/2014.The storm surge tide won't leave the coasts of New York and New Jersey until 0800 UTC 10/30/2014.

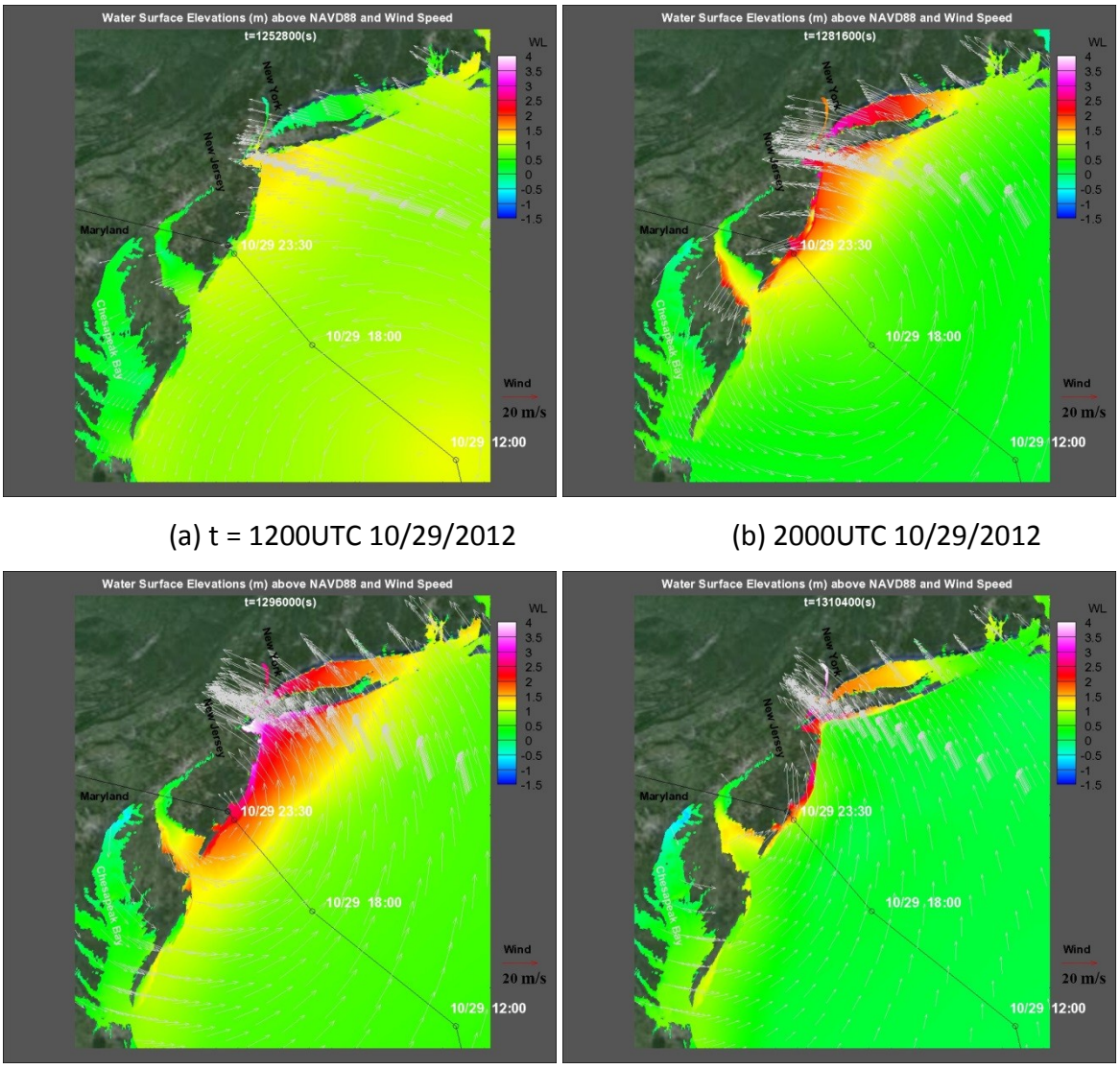

(a) t = 1200UTC 10/29/2012 (b) 2000UTC 10/29/2012

(c) t = 0000UTC 10/30/2012 (d) t = 0400UTC 10/30/2012

Figure 8 Snapshots of water levels and wind fields around the landfall of Sandy (the black solid line indicates the best track of Sandy)

In the computed results of storm surges, the spatial distribution of the maximum water surface elevations in the period of a storm can represent the extent of flood and inundation in

coasts and inland areas. Figure 9 presents the maximum water levels above NAVD88 over the entire computational domain. In two areas the highest levels of the storm tides due to Sandy are found: one is in the Raritan Bay, NJ; another is the Bay of Fundy, Nova Scotia. The water levels in the Raritan Bay were induced by the storm. But the high waters in the Bay of Fundy were driven by the high tide of the Atlantic Ocean waters. By further zooming in the maximum water level map, the maximum surge levels in the region from North Carolina to Massachusetts are shown Figure 10. It indicates that the storm has lifted the coastal waters up to 1.5 m at the Delaware Bay and the Cape Cod Bay, higher than 2.0m in almost all the coasts of New York and New Jersey. By close-up view at the areas of NY and NJ coasts, as shown in Figure 11, the New Jersey coast, the Hudson River, and the south beach of Long Island received most storm surge waters. The maximum water elevation, up to 5 m above NAVD88 was computed at the west of the Raritan Bay, NJ.

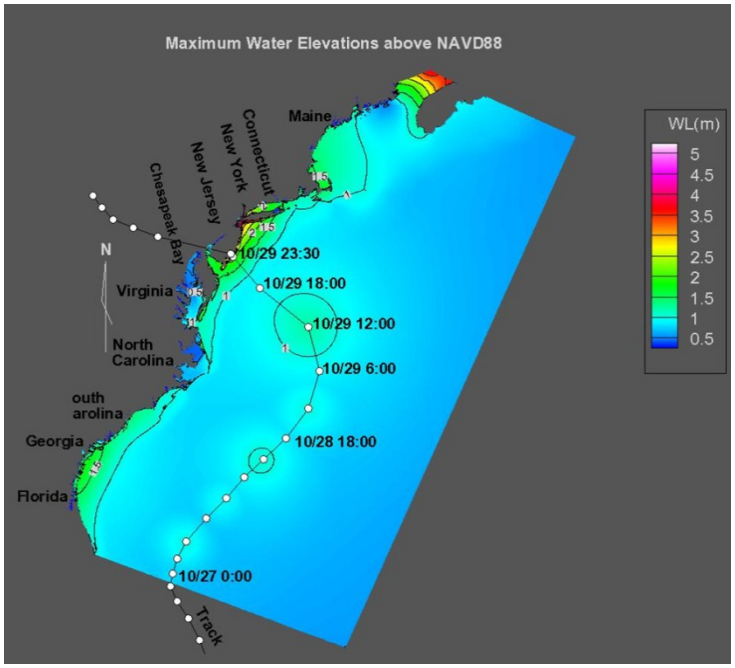

Figure 9 Computed maximum water surface elevations above NAVD88 over the entire computational domain.

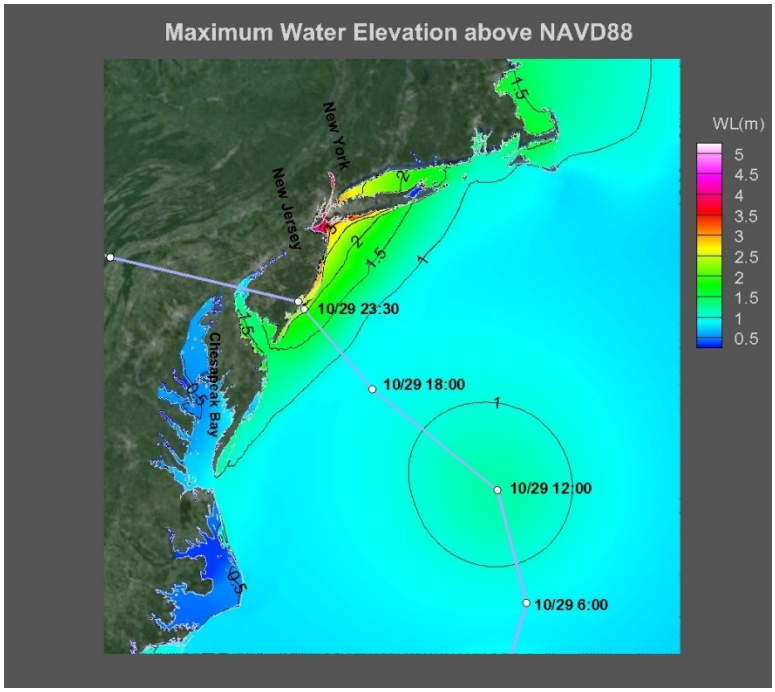

Figure 10 Close-up view of the computed maximum water levels in a region from North Carolina to Massachusetts

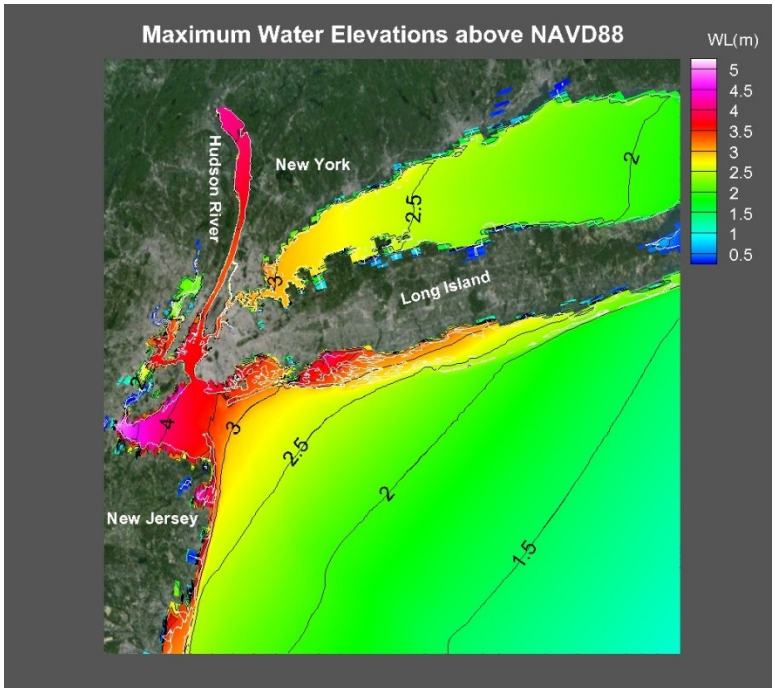

Figure 11 Maximum water elevations in the coasts of New York and New Jersey

The computed peak storm tide levels at the NOAA tide gages (permanent stations) located in the U.S. East Coast were extracted from the simulation results of Hurricane Sandy. The locations of the tide gages are shown in Figure 12, which are obtained from the USGS

Hurricane Sandy Storm Tide Mapper (USGS 2013). Table 3 listed the values of the Sandy peak storm tides from the observation stations and the computational model (CCHE2D-Coast). It shows that most of computed peak storm tides are close to the observations at NOAA's gages. But at a few stations in the inland the model couldn't catch the flood water, because the bathymetrical data won't be able to identify river courses and low-lying land in these places. Therefore, to have a better computational result in a wider range of the coast, the basic data including topography and bathymetry have to be improved. By removed those problematic inland stations, the comparisons of the peak storm levels are presented in Figure 13, and the computational peak tide levels are in good agreement with the observations.

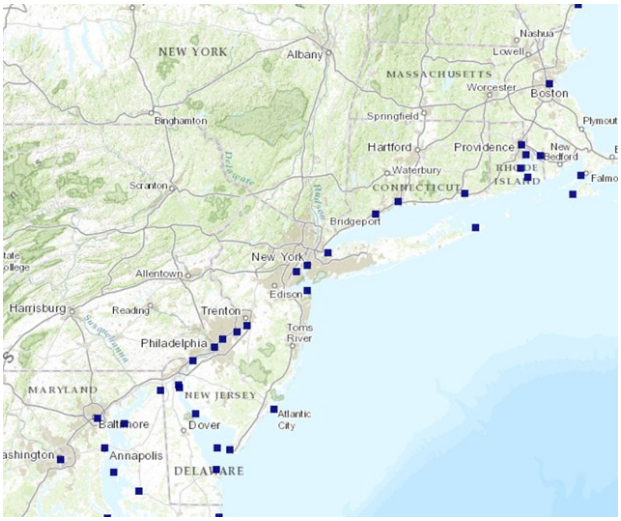

Figure 12 Locations of tide gages in the U.S. East Coast monitored by NOAA-CO-OPS

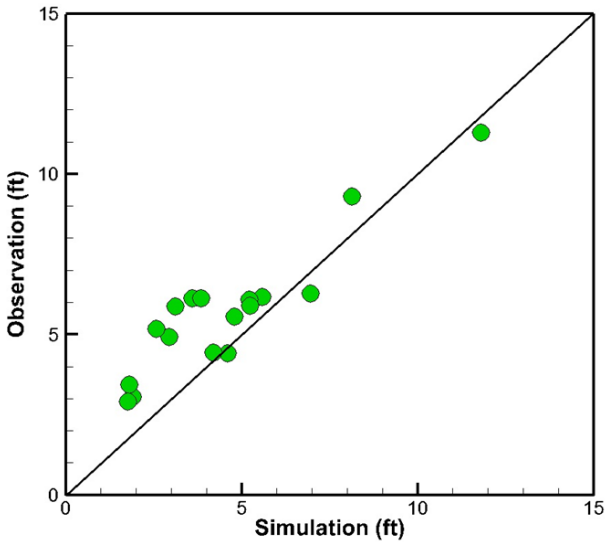

Figure 13 Comparisons of Hurricane Sandy peak storm-tide data recorded at NOAA tide gages

Table 3 Peak storm tide levels at NOAA permanent monitoring stations

NOAA #	Location	Long (deg)	Lat (deg)	Observed (ft)	Computed (ft)	Note
8461490	New London, CT	-72.1644	41.1523	6.160	5.586	
8467150	Bridgeport, CT	-73.2792	41.0007	9.300	8.143	
8551910	Reedy Point, DE	-75.6600	39.4075	6.130	3.590	inland river
8557380	Lewes, DE	-75.2067	38.6309	6.080	5.220	
8570283	Ocean City Inlet, MD	-75.1783	38.1775	4.420	4.594	
8571421	Bishops Head, MD	-76.1250	38.0692	3.050	1.904	
8571892	Cambridge, MD	-76.1550	38.4225	3.440	1.800	
8574680	Baltimore, MD	-76.6650	39.1159	3.830	-999	dry
8575512	Annapolis, MD	-76.5667	38.8325	3.110	-999	dry
8443970	Boston, MA	-71.1400	42.2025	7.420	3.722	
8447435	Chatham, MA	-70.0367	41.5375	5.870	3.107	
8447930	Woods Hole, MA	-70.7583	41.3725	4.440	4.193	
8423898	Fort Point, NH	-70.7983	42.9209	6.410	-999	dry
8534720	Atlantic City, NJ	-74.5050	39.2042	6.280	6.954	
8536110	Cape May, NJ	-75.0467	38.8175	5.900	5.235	
8510560	Montauk, NY	-72.0438	40.9219	5.550	4.803	
8518750	The Battery, NY	-74.1000	40.5492	11.280	11.798	
8545240	Philadelphia, PA	-75.2283	39.7825	7.520	-999	dry
8452660	Newport, RI	-71.4133	41.3542	6.130	3.842	
8454000	Providence, RI	-71.4867	41.6559	6.890	-999	dry
8632200	Kiptopeke, VA	-76.0750	37.0142	4.920	2.945	
8635750	Lewisetta, VA	-76.5500	37.8442	2.920	1.756	
8638610	Sewells Point, VA	-76.4167	36.7959	5.170	2.572	

The computed results of storm surges can also compare with the high water marker (HWM) data surveyed by USGS (2013): Prior to the arrival of Hurricane Sandy to the East Coast, the U.S. Geology Survey (USGS) deployed non-transmitting storm tide sensors and wave height sensors along with real-time deployment streamgages (RDGs) along the Northeast coast (Figure 14). Prior to, during, and following the storm, these sensors and gages provided real-time situational awareness of storm surge flooding. For the details of the survey of storm tide and flooding from Hurricane Sandy by USGS, one may refer to McCallum et al. (2014).

In comparison with the USGS-observed high water marks (HWMs) in the coasts of New York and New Jersey (USGS 2013), the value of R^2 of the maximum water elevations is 0.7293 (Figure 15). Considering the resolution of the grid and the accuracy of the DEM data, the computed water elevations are acceptable.

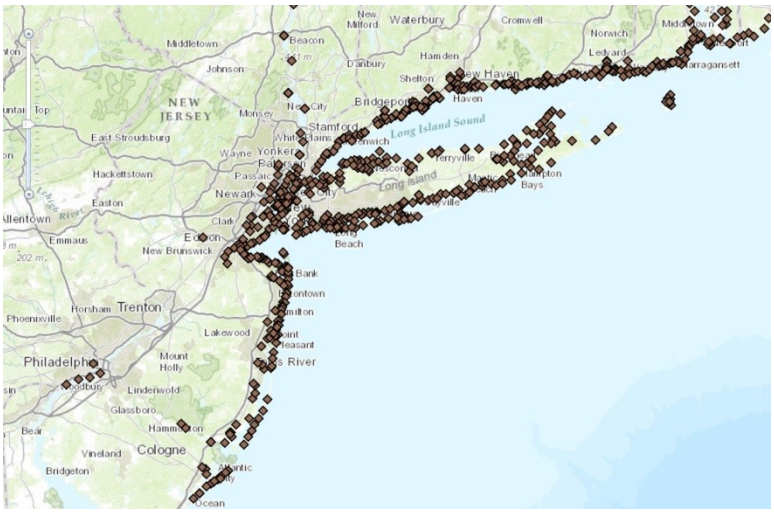

Figure 14 Locations of high water mark data collected and surveyed by U.S. Geological Survey following the passage of Hurricane Sandy (USGS 2013)

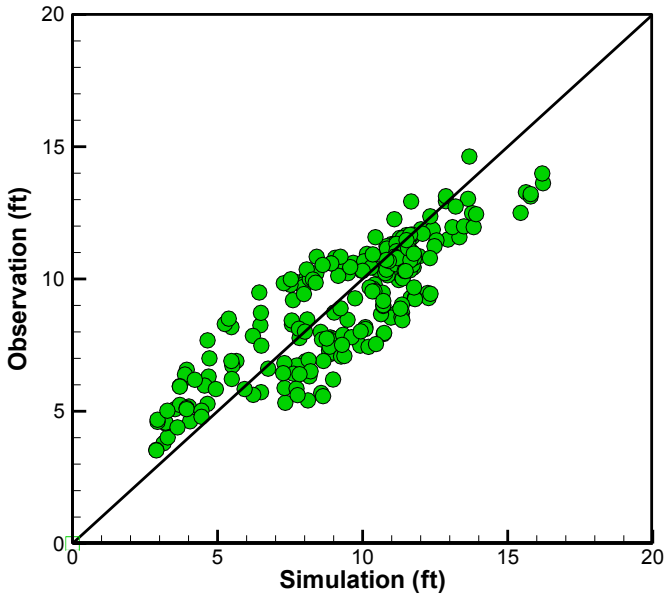

Figure 15 Comparisons of high water marks in the coasts of New York and New Jersey above NAVD88 observed by USGS (R^2 = 0.7293)

Figure 16 further presents the comparison of time series of water elevations between computation and NOAA's Observations at eight selected NOAA tide gages. These stations are located from the coasts of New York to Virginia. The histories of water levels at these stations show that 1.5-m peak of surge tides due to Sandy reached to Montauk, NY, 3.5-m peak at Sandy Hook, NJ, 2.0 m at Atlantic City, NJ, and 1.2 m at Ocean City Inlet, MD. The computed water surface elevations captured the storm surge tides from NY to VA in a large regional East

Coast area. The storm-surge model reproduced the dynamic variations of surface water elevations at the US east coast.

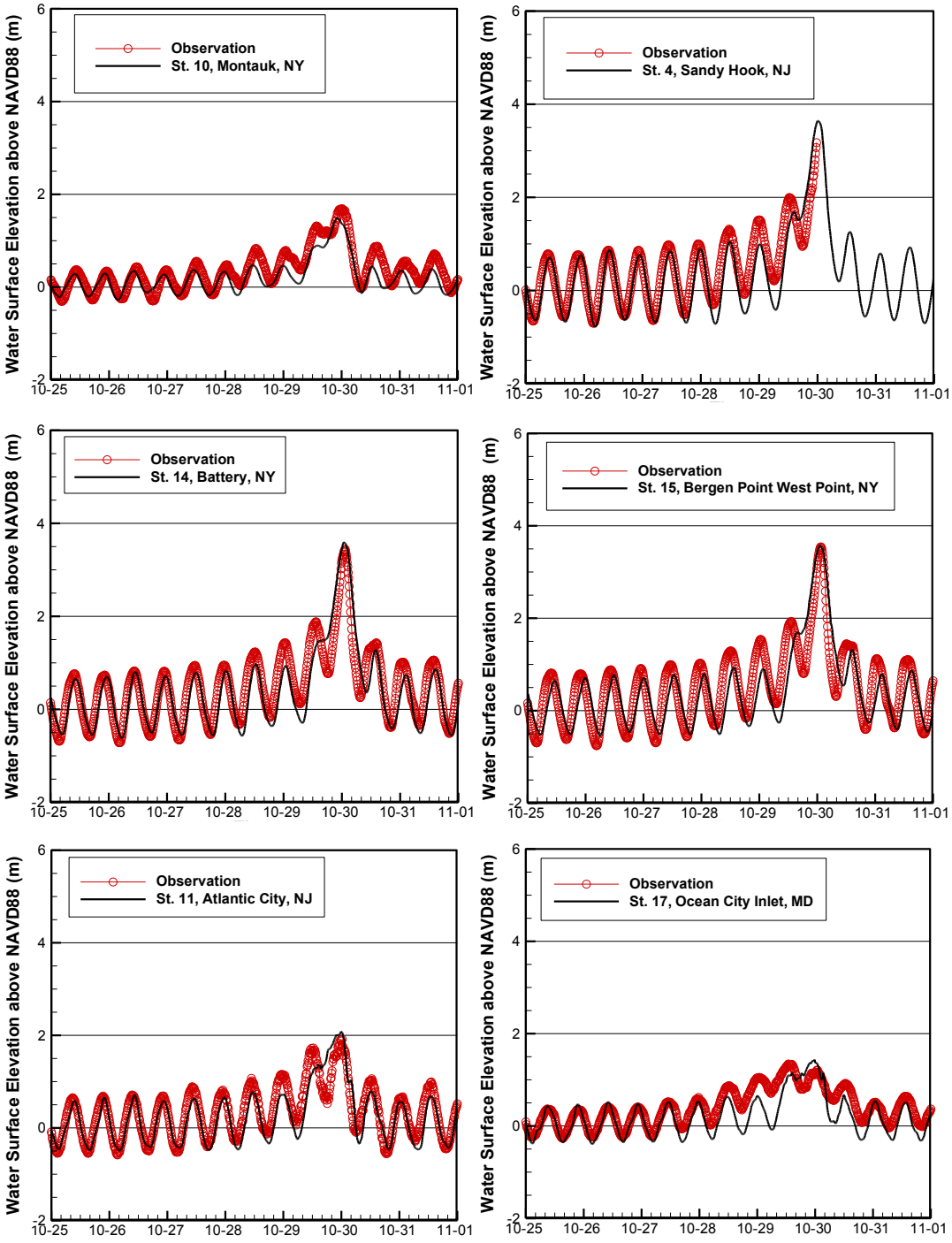

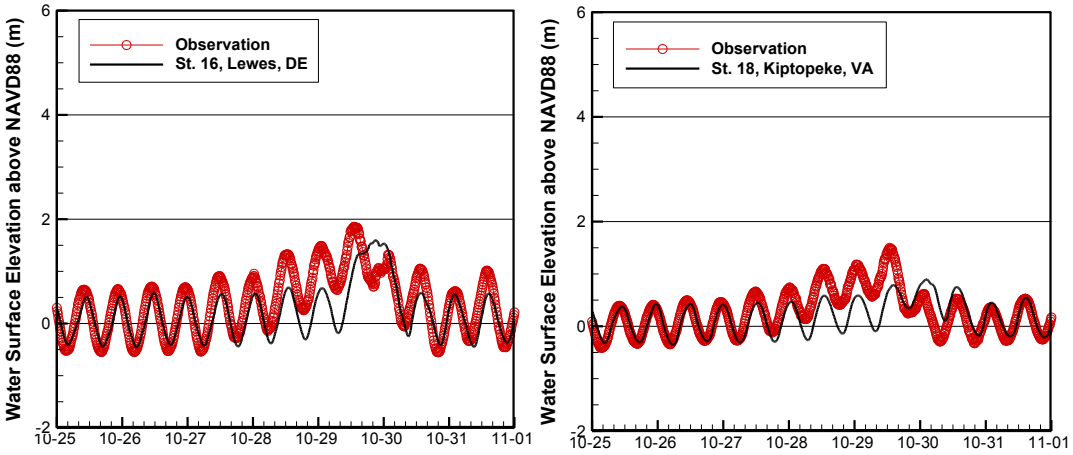

Figure 16 Comparisons of water elevations at eight selected NOAA tide gages

The wave energy spectral fields (containing wave heights, periods, and directions) induced by the cyclonic wind of Hurricane Sandy were computed along with the simulations of storm surges every two hours from 10/25 to 11/01/2012. As shown in Figure 17, when the cyclone was approaching to the east coast along with the storm track, high waves driven by high wind traveled from the deep ocean to the seashores of New York and New Jersey. The figure presents the high wave packet existing at the right hand side was moving with the cyclone. At the moment of the hurricane landfall, 0002 UTC 10/30/2012, the highest wave was growing in the continental shelf at the offshore of Long Island, NY, and at the same time, it was quickly breaking in the shallow water in front of the barrier islands from the Long Island coast to the coasts of Delaware. Even though the surface wind didn't include the wind of jet stream at the high latitude region, the computed wave fields are reasonable for quantitatively representing the wave dynamic processes for growing, decay, breaking, and shoaling.

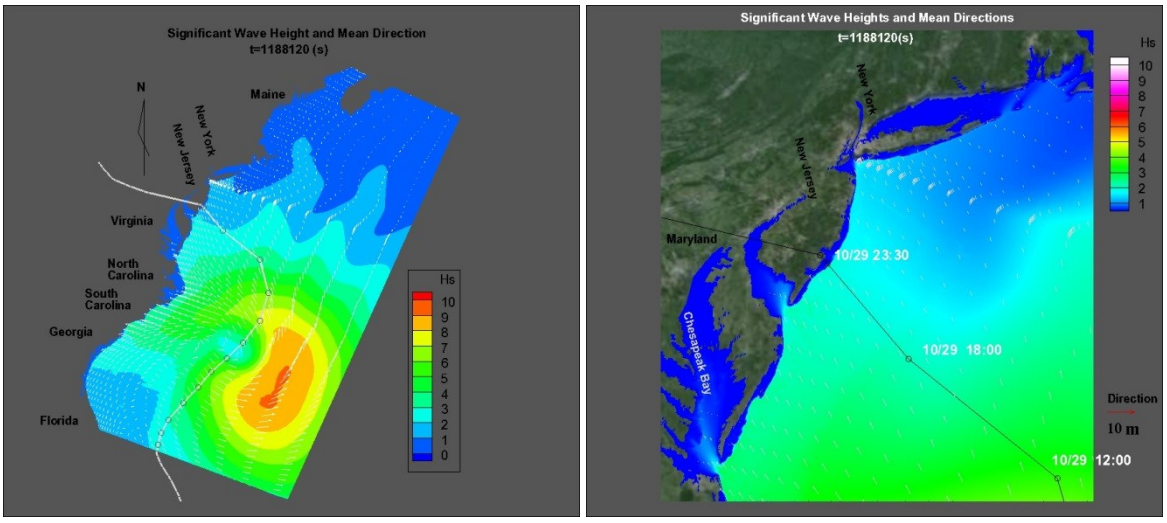

(a) 1802 UTC 10/28/2012

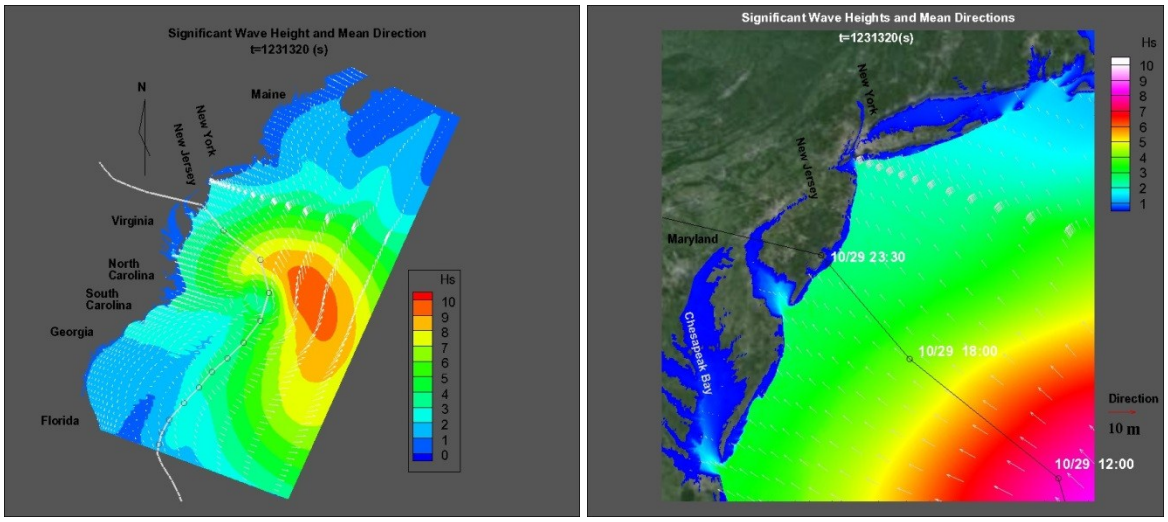

(b) 0602 UTC 10/29/2012

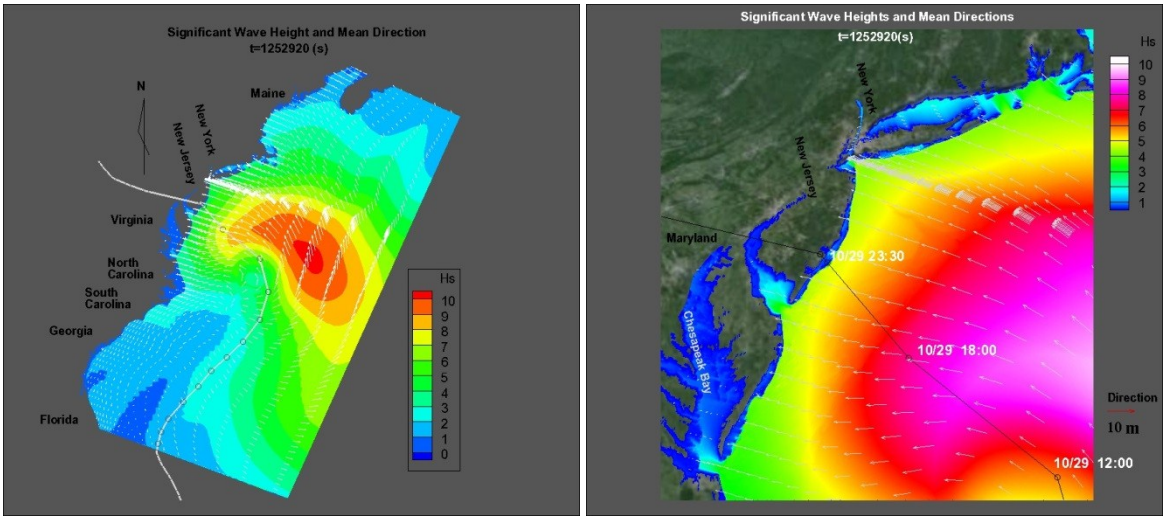

(c) 1202 UTC 10/29/2012

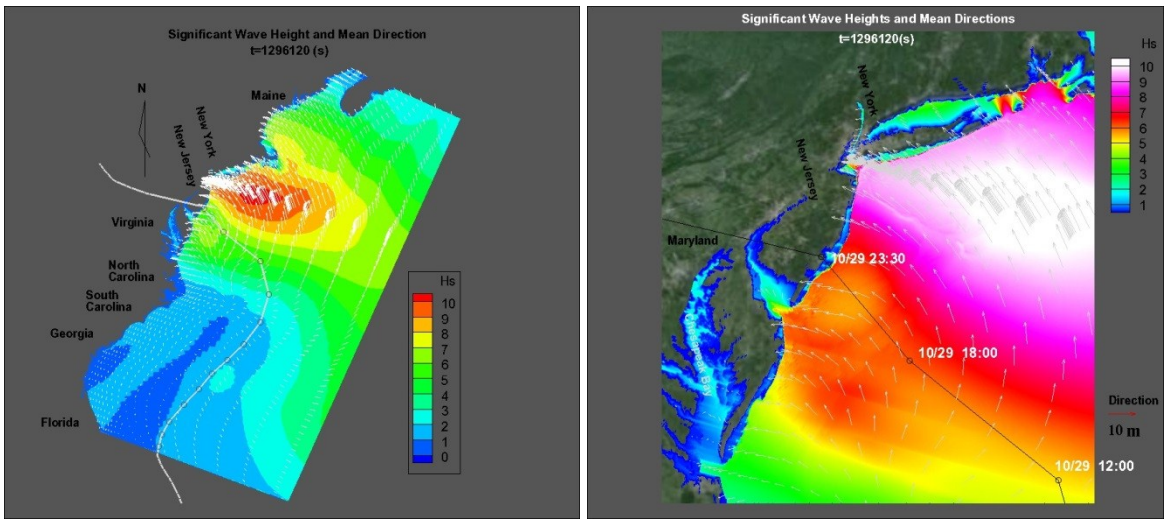

(d) 0002 UTC 12/30/2012

Figure 17 Computed significant wave heights and mean directions in the Atlantic Ocean and the East Coast

Figure 18 presents the computed maximum significant wave heights in the entire East Coast. The waves give a clear picture of swath of the cyclone in the Atlantic Ocean and the East Coast. Figure 19 gives a closer view of the significant wave heights in the East Coast from Massachusetts to North Carolina. The wave heights varied from 5 meter at the coast of Delaware to 9 meter at the shore of Long Island NY. By further zooming in the area of the NY and NJ coasts, as shown in Figure 20, it is found that the offshore significant wave height wave at this area reached 10 meter. Figure 21 presents an example of comparisons of wave heights and peak periods at the NOAA's NDBC buoy No. 44065, which is located at the offshore of the south beach of Long Island, NY. The simulation of wave actions has caught well the variation of the wave features in the ocean. Figure 22 shows the comparison of the spectral wave energy at the NDBC # 44009, which is located in the offshore of the Delaware Bay. It indicates that the computed wave spectrum is very close to that of the NOAA's observation.

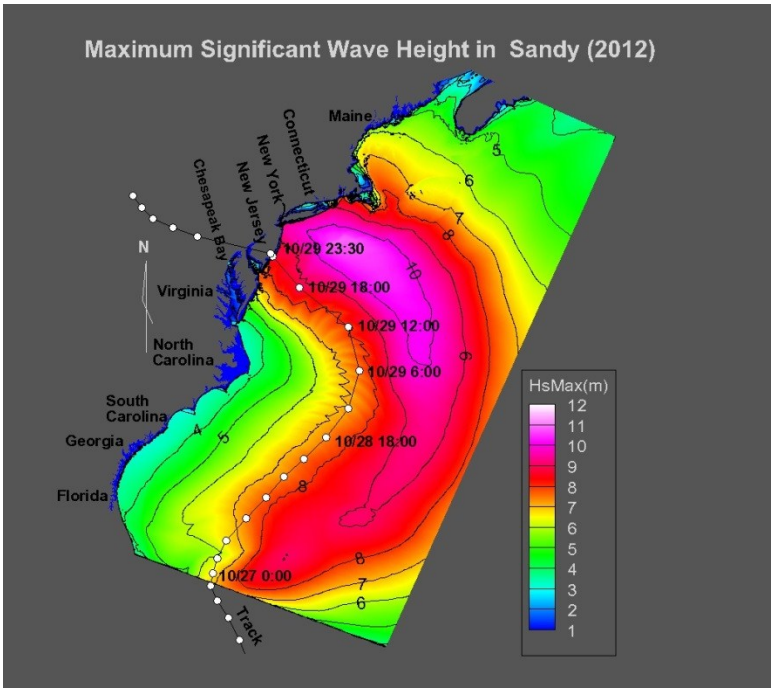

Figure 18 Computed maximum significant wave height in the US East Coast

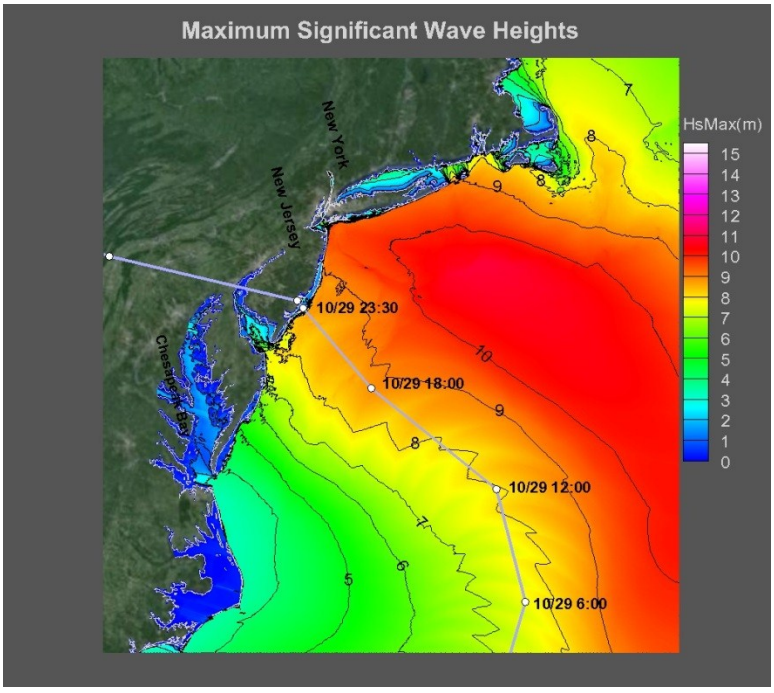

Figure 19 Maximum significant wave height in the East Coast from Massachusetts to North Carolina

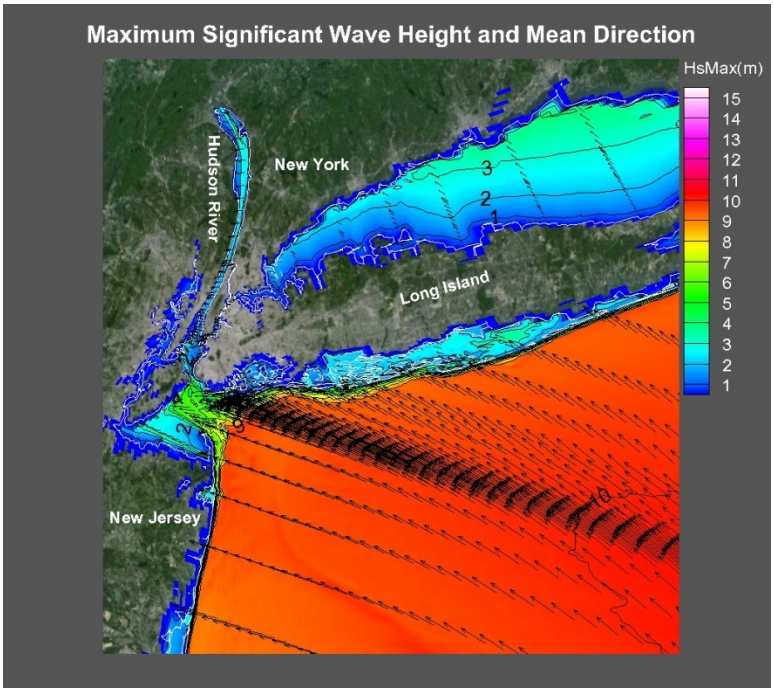

(a) Maximum significant wave height and mean direction

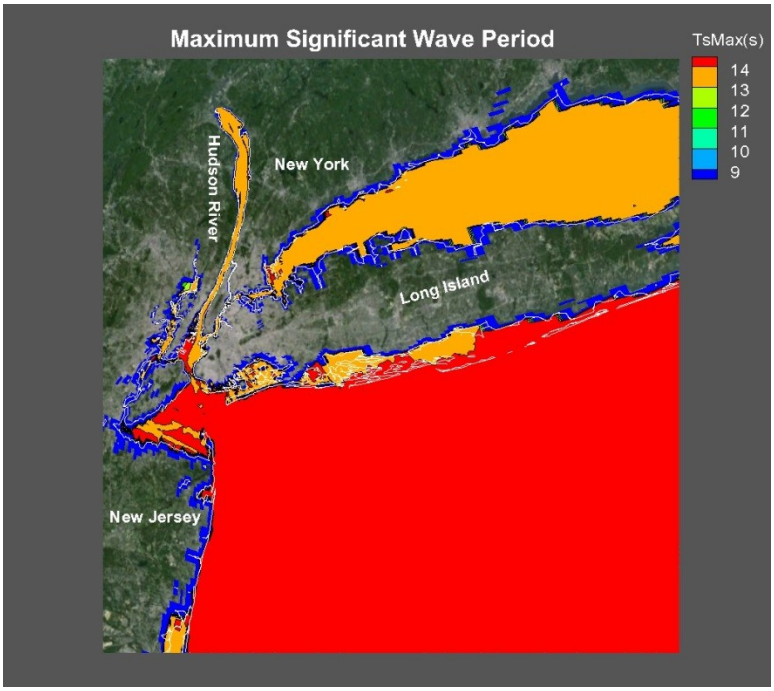

(b) Maximum significant wave period

Figure 20 (a) Maximum significant wave height and mean direction, (b) maximum significant wave period in the coasts of New York and New Jersey

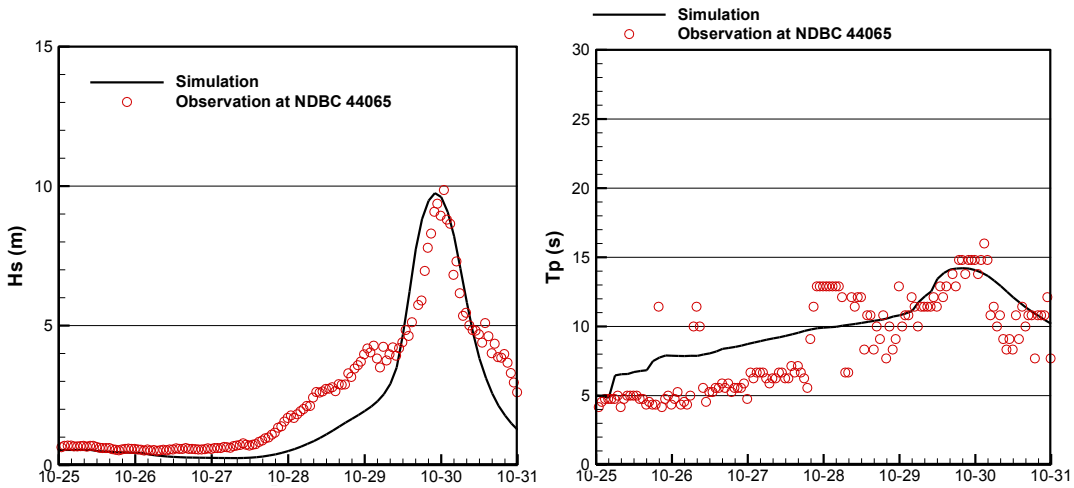

Figure 21 Comparisons of significant wave heights and peak periods at the NOAA's NDBC 44065 buoy.

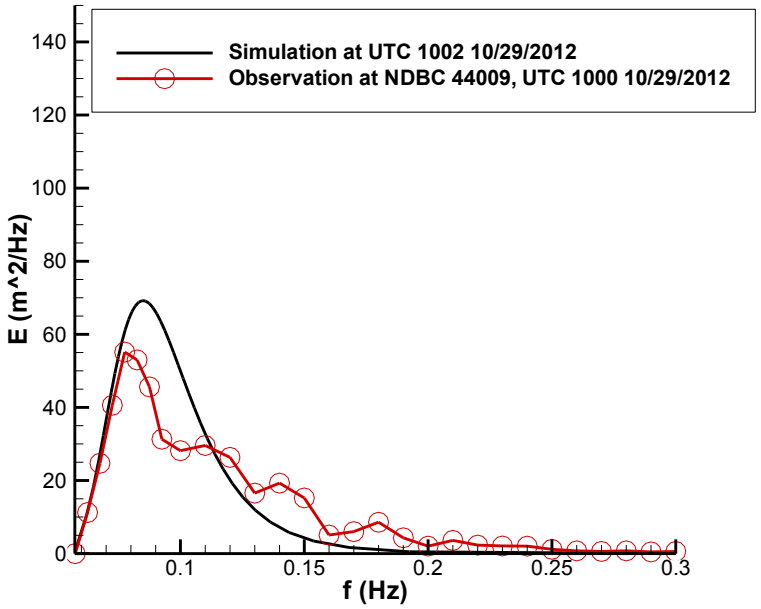

Figure 22 Comparison of wave spectral energy at NDBC 44009 at 1000 UTC 20/29/2012

Remarks

In the study, the storm surges and waves driven by Hurricane Sandy (2012) were computed by using an integrated coast-ocean process model, CCHE2D-Coast. The surface wind and air pressure fields of the cyclone were reconstructed by a parametrical cyclonic wind model, which was developed to include the decay effect of hurricane landfall. The simulated wind, wave, and water elevations were compared with the observation data by NOAA and USGS. This preliminary numerical result indicates that this coast-ocean model reproduced well the storm

surge tides and waves in the entire east coast of the US. To further improve the accuracy of the hindcast results of wind and wave, a mesoscale numerical weather model may be needed to take into account the hybrid system of this late-season hurricane interacting with the Gulf Stream and cold storm as pointed out by Halverson and Rabenhorst (2013).

2.4 Hindcasting Flood and Inundation in Sandy in the Local Areas of Hackensack

2.4.1 Computational Domain, geospatial data, and Mesh Generation

For simulations of flood and inundation induced by Sandy in the Hackensack area in the northeast New Jersey, the computational domain is defined as shown in Figure 23. This domain contains two rivers in the area, i.e. Hackensack and Passaic Rivers. The south boundary stretches to the estuary in the south, covers the Newark Bay. It also has considered the installations of flood mitigation measures (dikes and barriers). The domain size is approximately 15km x 33km.

Figure 23 Computational domain covering the Hackensack area in the northeast New Jersey

The obtained geospatial data as described in section 2.2.2 were processed to generate the mesh for the computational domain. The topography of the model domain was generated by merging USGS 3-m DEM and NJIT 1-m Lidar data. The major water bodies (e.g. Newark Bay, Hackensack River, Passaic River, swamp areas, tidal rivers, etc.) included in the model domain were mapped using the existing hydrologic shape files. The topographic DEM included in the water bodies were extracted using the hydrologic shape files and were replaced by the ADCIRC bathymetry data. The resultant topographic-bathymetry data was resampled at 5-m spatial resolution and processed to generate the mesh for the computational domain. Figure 24 and Figure 25 show the processed topographic-bathymetry data used for mesh generation, in which the dot points indicate the bathymetric data obtained from the ADCIRC depth grid.

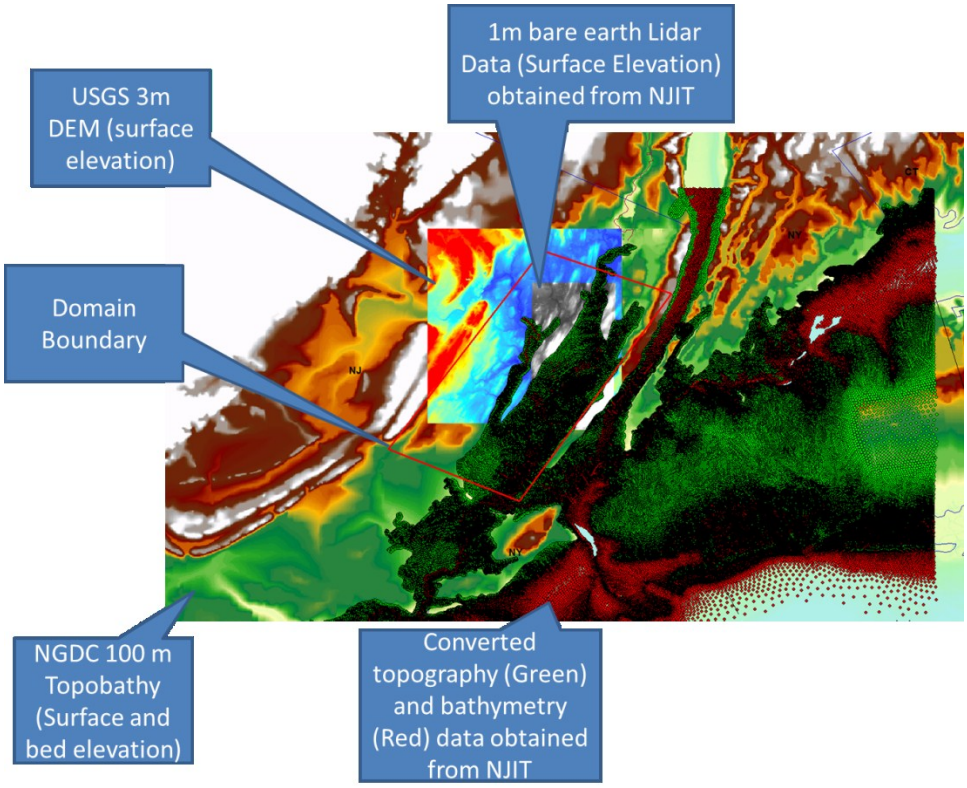

Figure 24 Processed topographic-bathymetry data used for mesh generation

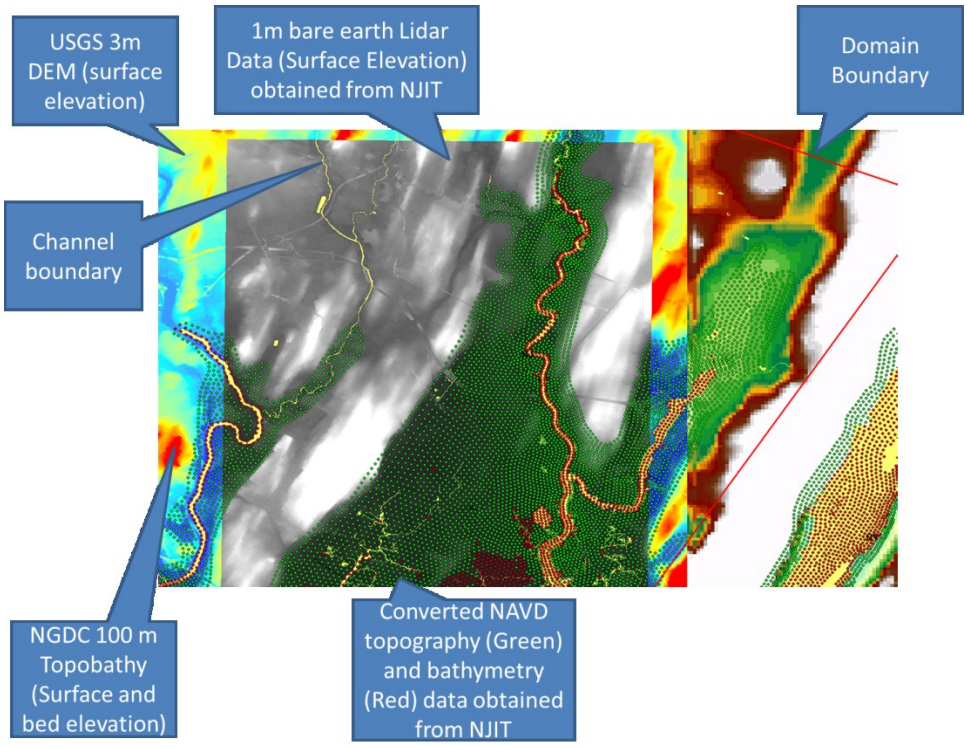

Figure 25 Detailed view of the processed topographic-bathymetry data used for mesh generation. The dots are the bathymatrical data points in the ADCIRC depth grid

The coordinate system of the CCHE2D computational mesh is the X and Y coordinates based on the UTM ZONE 18N. Namely, the DEM data and the bathymetrical data in the ADCIRC depth grid which are based on the longitudinal-latitudinal coordinates were projected onto this UTM zone. The computational mesh of the non-orthogonal grid for the CCHE2D-Coast model was generated by using the CCHE-MESH, a mesh generator for the CCHE2D models (Zhang et al. 2009). As presented in Figure 26, the final computational grid for the current geographic conditions is shown in the CCHE2D-MESH GUI. The local domain includes almost all the low-lying land in the northeast New Jersey from the Hackensack area down to Newark Bay, two tidal rivers (the Hackensack and Passaic rivers). This non-orthogonal grid is a structured mesh, of which the domain is 2071×1104, containing a total of 2,286,384 nodes. The spatially-varying resolution in the grid enables to have an accurate representation of the complex boundaries of river courses, buildings, and roads. Figure 27 presents a close-up view of the computational grid around the Moonachie area, in which the highest resolution of this structured non-orthogonal mesh is around 0.7 m, the coarsest resolution at the south of Newark bay is up to 20 meter.

Because of using the bare earth ground data, bridges and buildings have been removed from the bed elevation data.

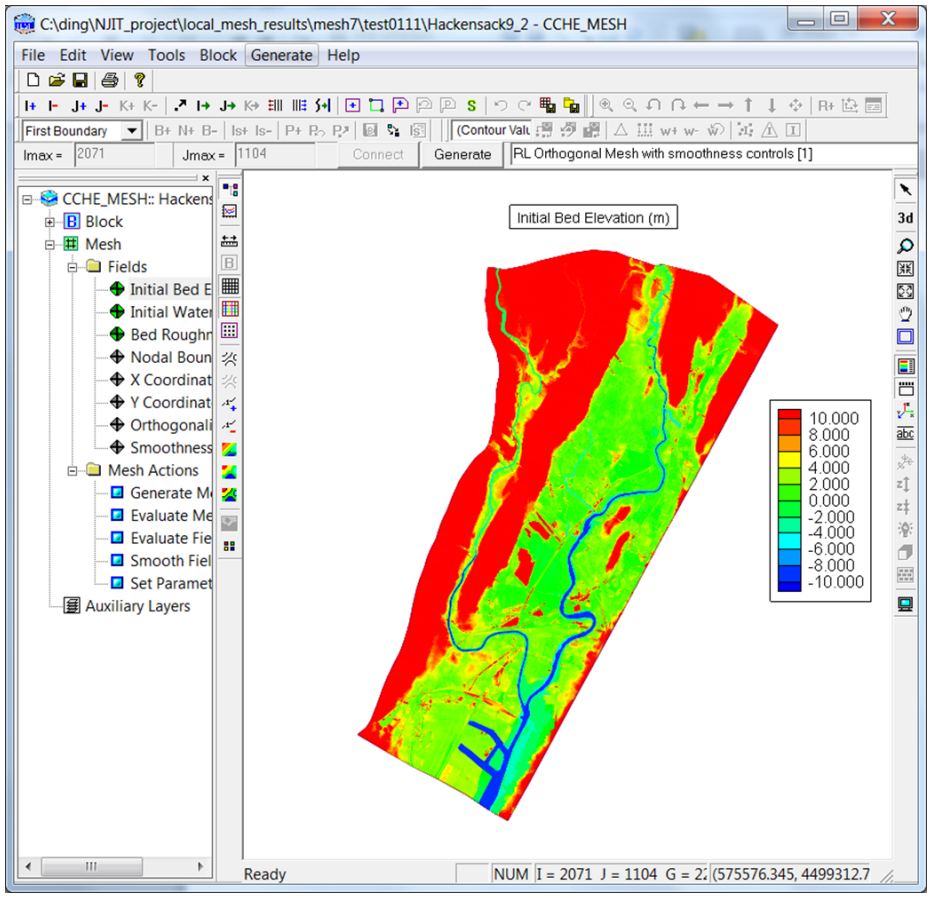

Figure 26 Bed elevations above NAVD88 in the generated mesh shown in the CCHE-MESH GUI (Mesh Size= 2071×1104=2,286,384)

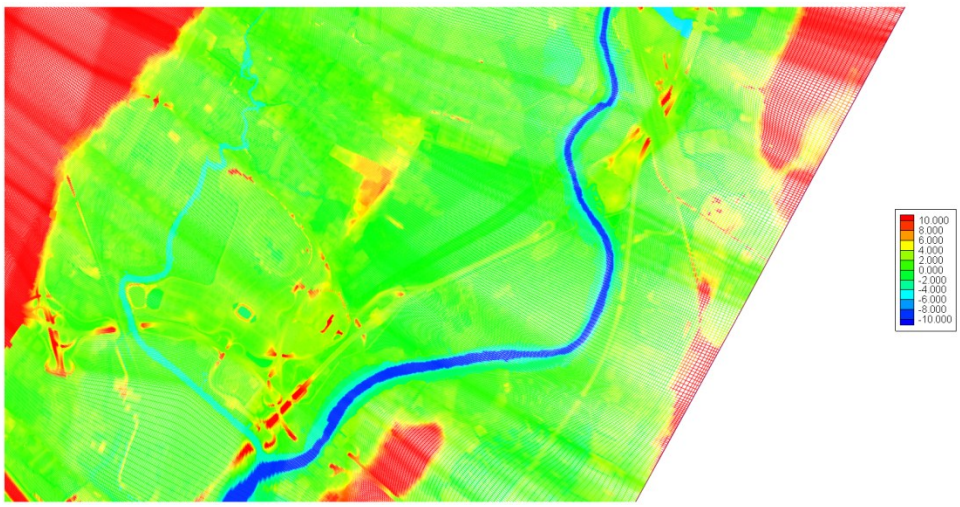

Figure 27 Close-up view of the computational grid around the Moonachie area: Non-orthogonal mesh with spatially-varying resolution: highest resolution < 1.0m

2.4.2 Computational Conditions

Water Surface Elevations as the Boundary Conditions

In the simulations of flood and inundation in the local domain, the water surface elevations observed surge tide levels at the NOAA tide gage No. 8519483 at Bergen Point West Reach, NY were specified directly at the south boundary located at the south of the Newark Bay. Figure 28 is the plot of the water levels from Oct. 15 to Nov. 5, 2012. The datum of the NAVD88 at this station is +0.0532 m (0.1744 ft) above MSL.

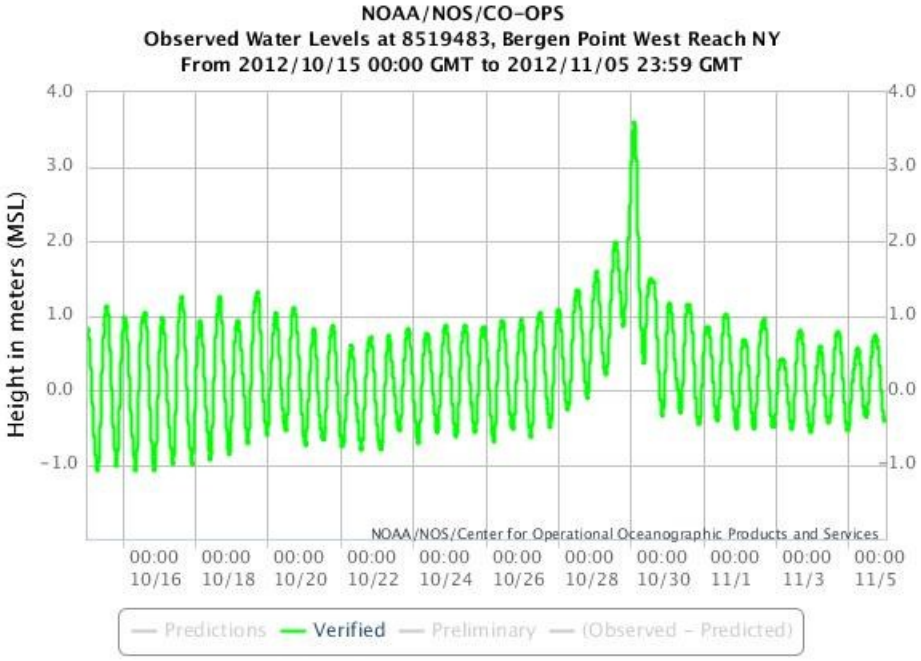

Figure 28 Water surface elevations above MSL during the period of Hurricane Sandy at the NOAA tide gage no. 8519483 at Begen Point Waest Reach, NY

Conditions of Wind, Waves, and Atmospheric Pressure

The wind parameters (speed and direction) in the area were given by the observation data measured at the same NOAA station at Bergen Point, NY. The time series of the wind speed and direction are shown in Figure 29. The drag coefficient for calculation of surface wind stresses was assigned to a constant value, 0.0015, which is corresponding to the estimated values by Large and Bond (1981) at the 15-m/s wind speed.

Based on the previous simulation of the waves in the entire US East Coast, the hurricane-wind-induced wave heights at the local area of the northeast New Jersey are small (less than one meter in the main channels of the two rivers and the Newark Bay area, as shown in Figure 20(a)). By also considering the local low-lying areas covered by vegetation, the effect of wave setup in the local domain is negligible.

After a test simulation with the air pressure given by the parametric cyclonic wind model, it was found that the differences in water levels induced by the surface atmospheric pressure gradient can be neglected in the area.

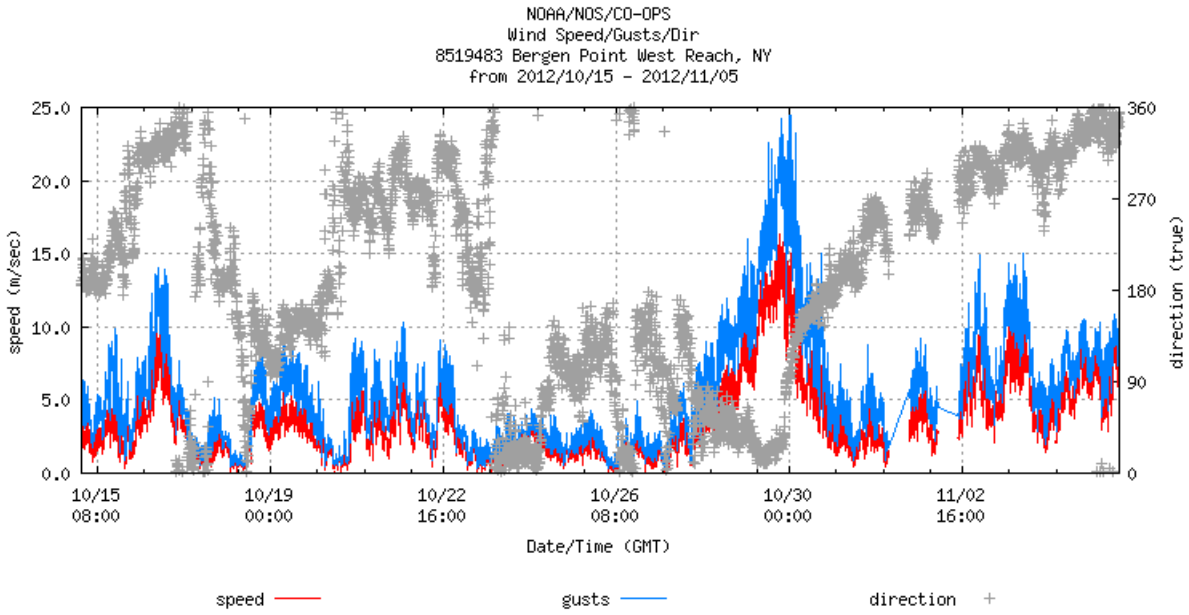

Figure 29 Wind speed and directions observed at the NOAA station Bergen Point, NY

River Discharge

The time series of discharges (hydrographs) at the upstream of the two rivers were given by the two USGS hydrologic stations: the hydrograph at the Hackensack River upstream was provided by the USGS observations at the USGS 01378500 Hackensack River gage at New Milford NJ; the one at the upstream of the Passaic River was specified by using the measured discharges at USGS 01389500 Passaic River at Little Falls NJ. The two hydrographs during the period of Hurricane Sandy (2012) are shown in Figure 30. It indicates that after Sandy made its landfall, the peak discharge of 1020 cfs (28.9 cms) occurred at 1:00am 10/30/2012, at the

upstream of the Hackensack River. But in the Passaic River, the peak discharge of 1,650 cfs (46.7 cms) came to its upstream on Oct. 27, 2012, before the landfall of Sandy.

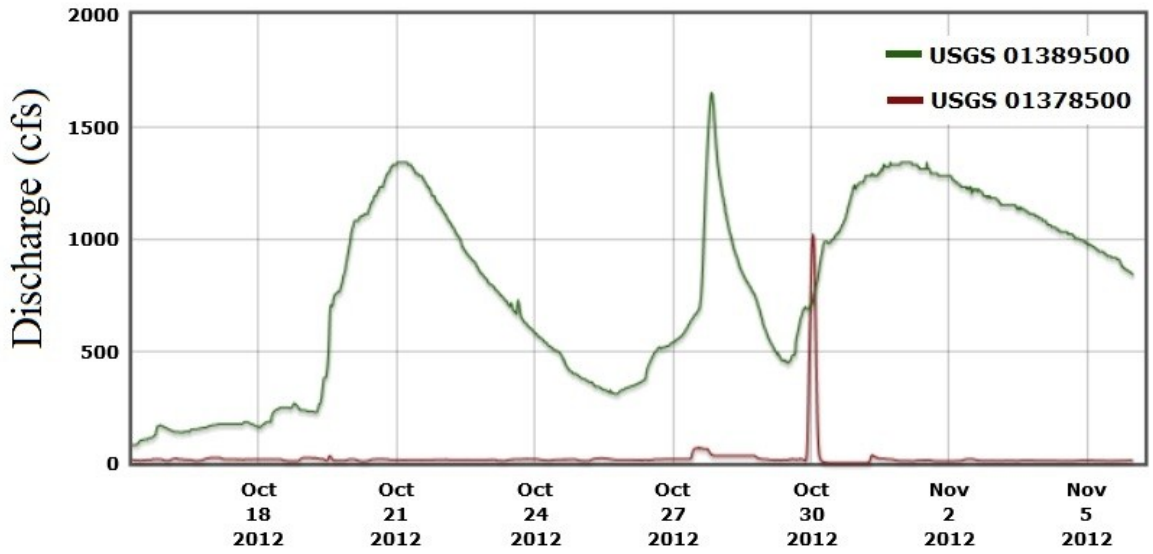

Figure 30 Hydrographs at USGS 01389500 Passaic River at Little Falls NJ and USGS 01378500 Hackensack River at New Milford NJ.

Bed Roughness

The bed roughness coefficient, i.e. Manning's n, was assigned to the spatially-varying values based on the local still water depth by the following equation:

$$n = \begin{cases} 0.02 + 0.01/h & \text{if } h \geq 0.5m \\ 0.04 & \text{if } h < 0.5m \end{cases}$$

It gives an *n* value close to 0.02 in the navigation channel with the depth more than 10 m, and a value of 0.04 to the flood plain and most land areas. The computed results given below will show that this assumption for the spatially-varying n value is quite reasonable.

Model Spin-up and Initial Conditions

Before introducing the surge tides of Sandy to the computational domain, the simulation model, CCHE2D-Coast, was spun up from 0000 UTC 10/15/2012 to 0000UTC 10/29/2015, by only simulating the tidal flows in the local area. The tidal levels at the NOAA gage at Bergen Point, NY were used as the boundary conditions of the water surface elevations

at the south of Newark Bay. The time step in the spin-up period was set to 30 seconds. An depth averaged parabolic eddy-viscosity model (Jia et al. 2013) was used for calculating the eddy viscosity in the flow model. During the spin-up period of the simulation, the wind fields were considered as uniform, of which the speed and direction were given by the observation data at the NOAA gage at Bergen Point, NY (see the time series of wind in Figure 29).

2.4.3 Hindcasting Simulation Results

To examine the model's capability and accuracy in predicting the flood and inundation in the Hackensack area of the northeast New Jersey, the hindcasting simulation of storm surge propagations and tidal flows during the period of Sandy in the local domain was carried out for three days, from 0000 UTC 10/29/2012, ended at 0000UTC 11/1/2012. To have better simulation for the dynamic propagation of storm surges in the local area with complex geometries and infrastructure, the time step was set up a shorter value, 15 second. For the three-days surge tide simulation, it took 18.3 hours on a PC with a single CPU of Intel(R) Xeon® CPU E5-2687W 0 CPU@3.10GHz.

The simulation of the storm surges in Sandy provided a detailed dynamic process of flood and inundation in the Hackensack area. Figure 31 presents a series of snapshots of the water level distribution showing the dynamic propagation of storm surges from Newark Bay to the upstream of the two rivers. As the results shown, at 1100UTC 10/29/2012, before the peak of storm surge tide, the tidal flows were travelling mostly within the river channels. At 0100UTC 10/30/2012, almost one hour after the hurricane made its landfall, the storm surge peak arrived at the bay area, some low-lying area near the west bank of Hackensack River in Moonachie already was inundated. Three-hour after Sandy's landfall at 0300 UTC 10/30/2012, the storm surge peak arrived at most of areas from Hackensack, Little Ferry, Moonachie, and Newark Bay. At 0500 UTC 10/30/2012, the storm surge tide started to retreat from Newark Bay, but the surge waters still were moving into the upstream of the Hackensack River, and entering in the Overpeck Creek. At 0700 UTC, even though the peak surge waters have gone back to the ocean, the flooding waters still kept flowing into some areas in the northwest corner of Moonachie. After that, from 2100UTC 10/30/2012, the astronomical tides were again

dominated in the local area, however, the flood waters stayed in the inundated low-lying areas in the northeast New Jersey.

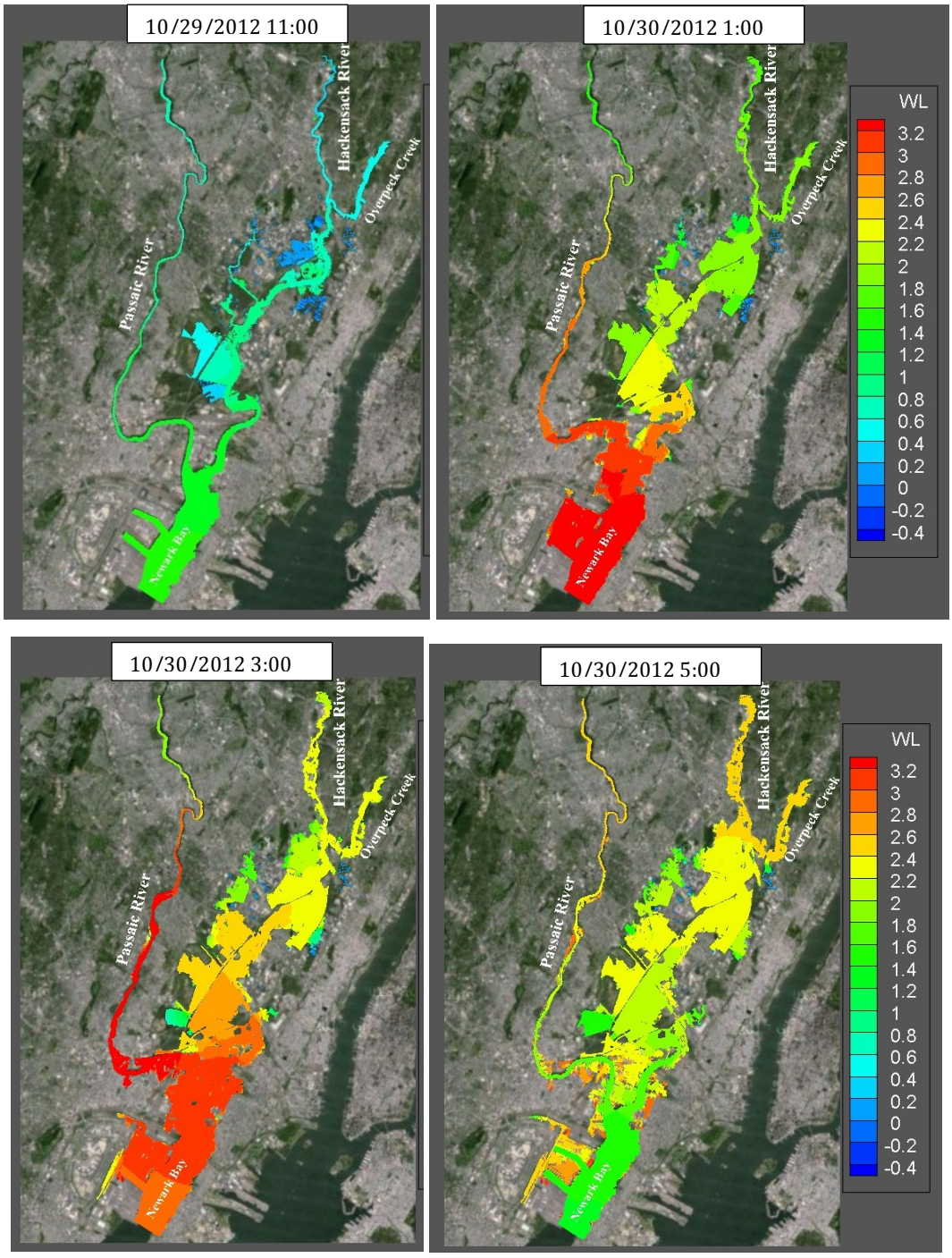

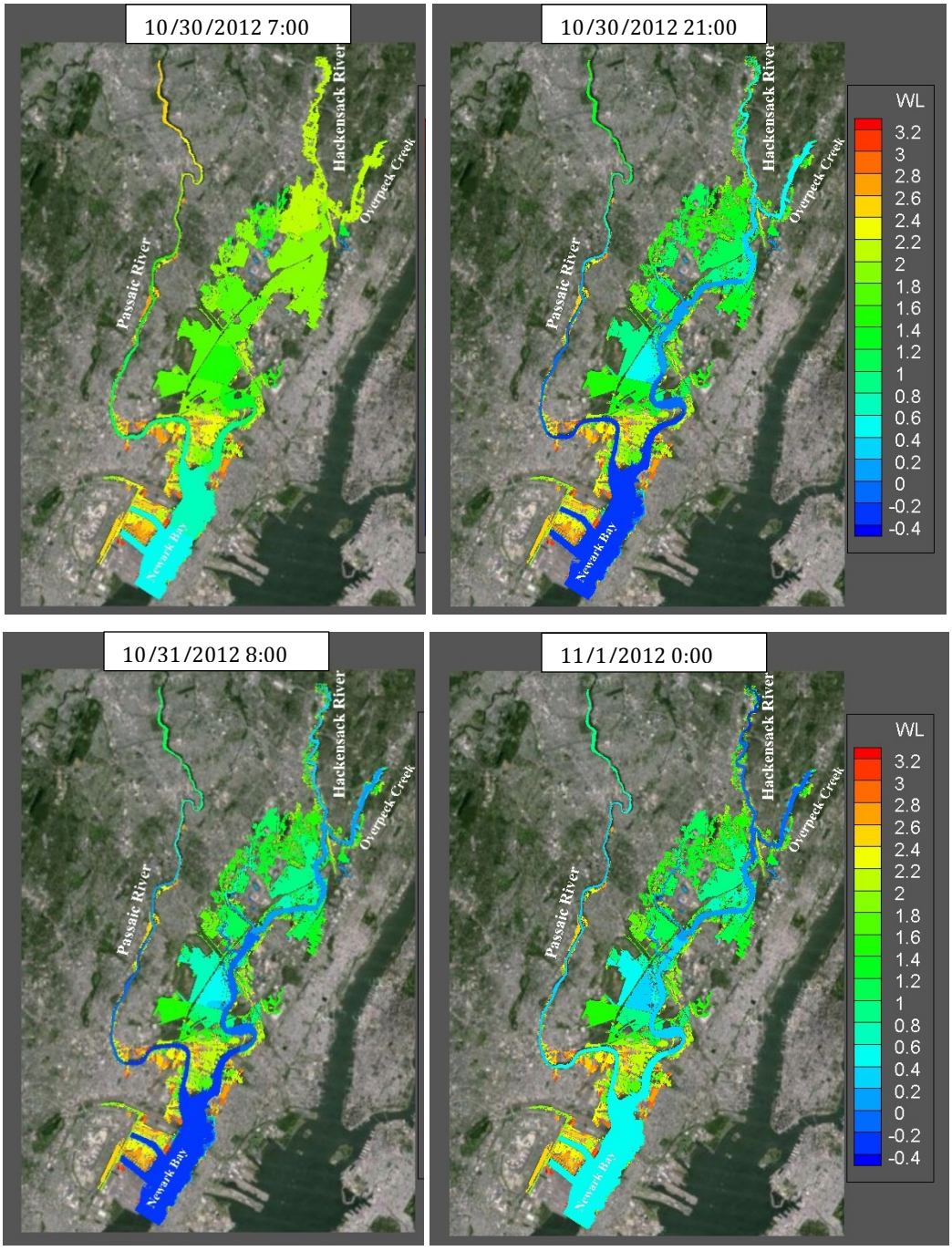

Figure 31 Time-dependent water level distribution in Sandy in the Hackensack area of New Jersey

There are a number of available observation data of water surface elevations in the local computational domain: The New Jersey Meadowlands Commission (NJMC) has operated a total of 11 real-time tide gates to monitoring water level changes in the Hackensack area (NJMC 2014). It provides one observed water level every one hour. Most of the tide gates are located in the branch tidal rivers (or streams) of the Hackensack River. The USGS deployed a storm tide

sensor (No. SSS-NJ-HUD-002WL) in the Hackensack River at NJ Route 3, near Lyndhurst, NJ. During the storm (USGS 2013). This sensor measured the water levels from 10/28 to 10/31, one data every 30 seconds.

Three NJMC tide gate data at Rutherford, Franks Creek, and Moonachie, and the USGS storm tide data are used for comparing with the simulated water surface elevations. For the NJMC tide gates, only the water levels measured at the upstream of tide gates are used for the comparisons, because the simulation didn't consider the operation of tide gates. Figure 32 shows the comparison of water levels (above NAVD88) at Rutherford, NJ, which is located in the Berrys Creek Canal. The simulated surge tides matched well the observed levels at the upstream of the tide gate.

The simulated water levels at Moonachie, NJ are compared with the NJMC's observations. As shown in Figure 33, the simulations are underestimated to some degree. The reason is probably that the tide gate is located in a small tide river called the Moonachie Creek, the bathymetric data obtained may not be accurate, and the local refinement of the depth grid may be needed.

The tide gate at the Franks Creek is installed in the north bank of the Passaic River close to Newark Bay. It should be more sensible than the other gates in the Moonachie area. Figure 35 presents the comparison of water levels at this station. It indicates that almost all the computed levels are in good agreement with the observations, but only the surge tide peaks were mismatched. The peak storm tide observed at this station was 2.225 m above NAVD88. However, the measured peak storm tide at Moonachie was 2.899 m above this datum. By comparing with the other observed tidal levels at the surge peak, it is clear that the observation at the storm peak at the Franks Creek might have some problems during the time of the storm tide peak.

Figure 35 gives the comparison of water levels at the USGS storm-tide No. SSS-NJ-HUD-002WL in the Hackensack River at NJ Route 3, near Lyndhurst, NJ. The dash line is the lowest recordable water level (=0.5273 m above NAVD88) by the storm-tide sensor, so the sensor gave the same data of water level when the surge tide elevations are lower than the location of the

sensor. The simulated water levels above the location of this sensor matched well with the observation data at this USGS storm-tide observation station.

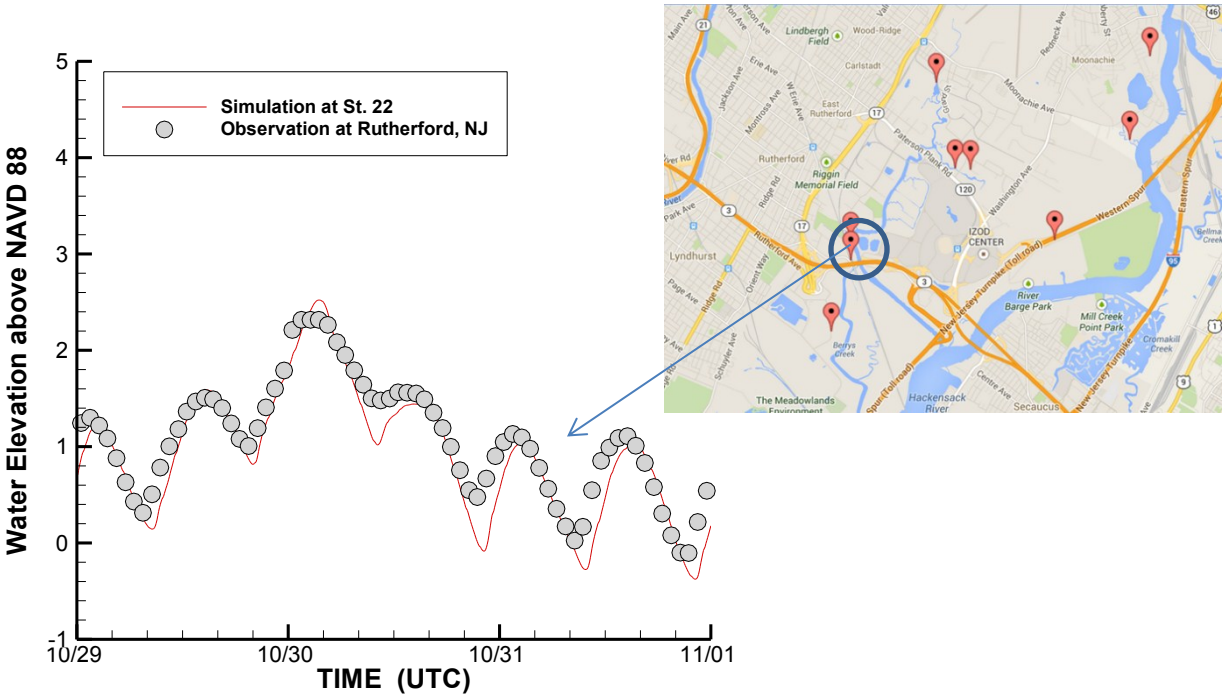

Figure 32 Comparison of water levels in the NJMC real-time tide gate at Rutherford

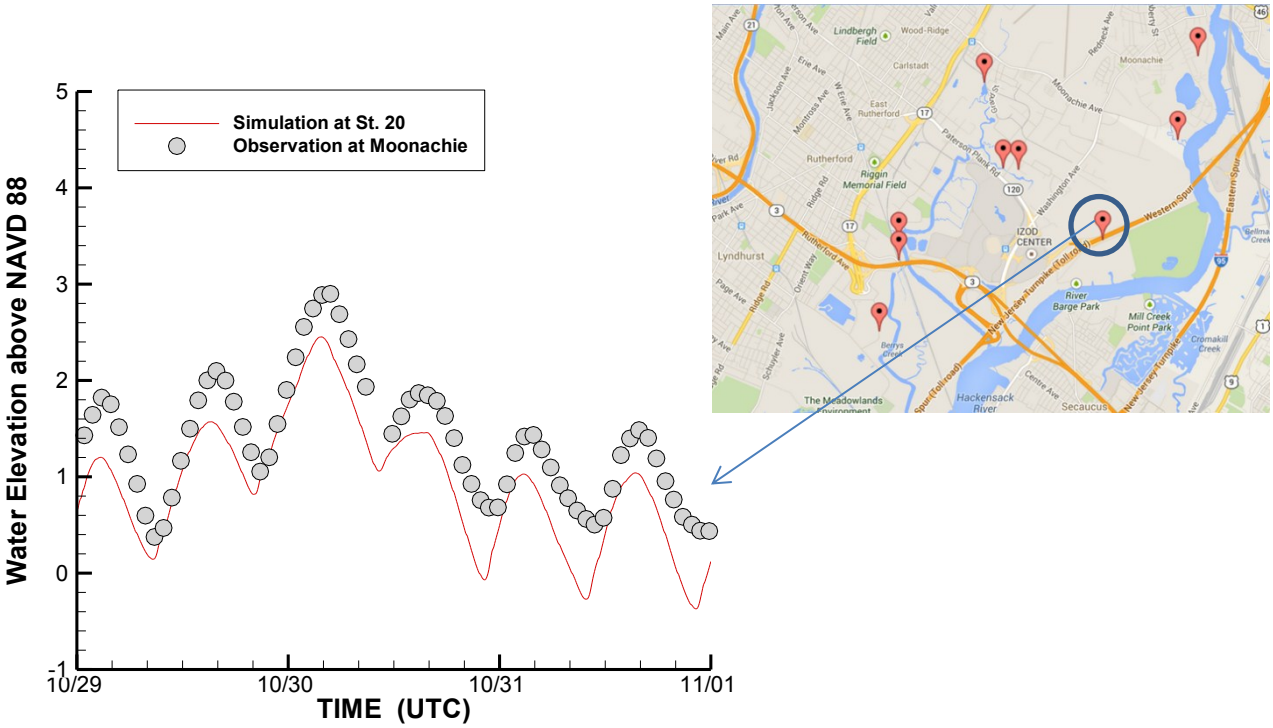

Figure 33 Comparison of water levels at the NJMC real-time tide gate at Moonachie

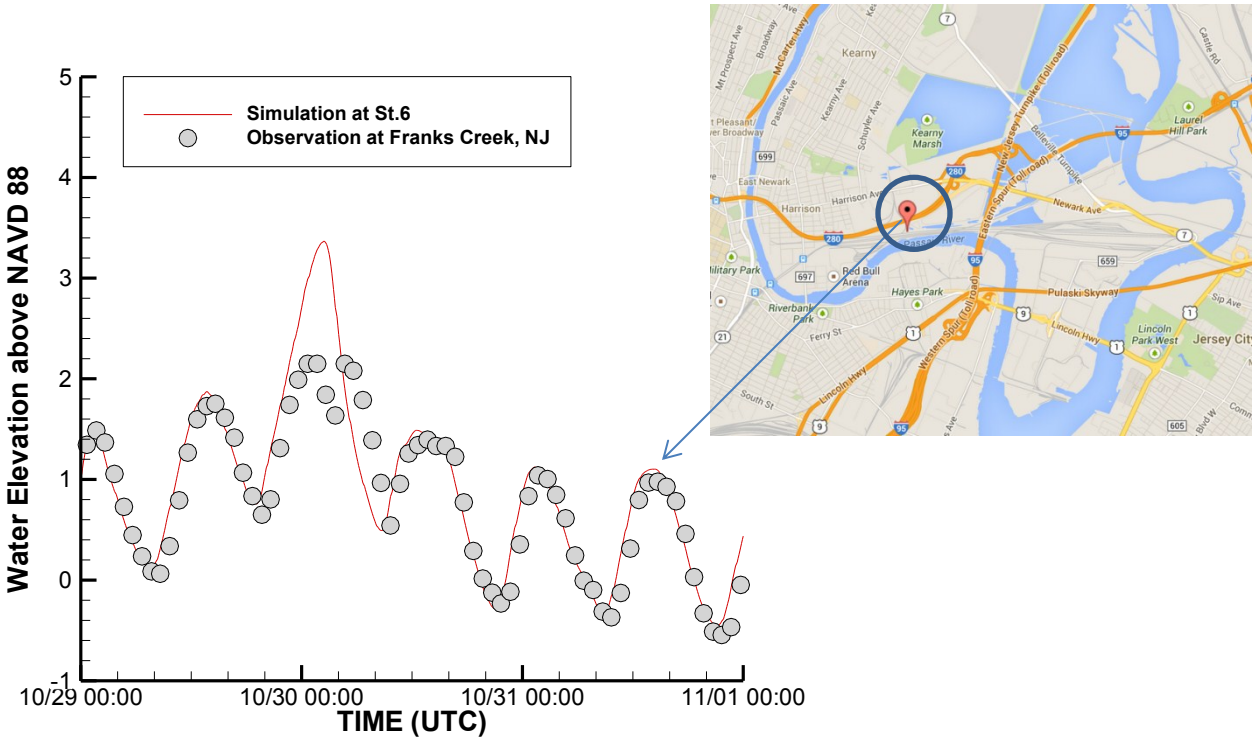

Figure 34 Comparison of water level at the NJMC tide gate at Franks Creek

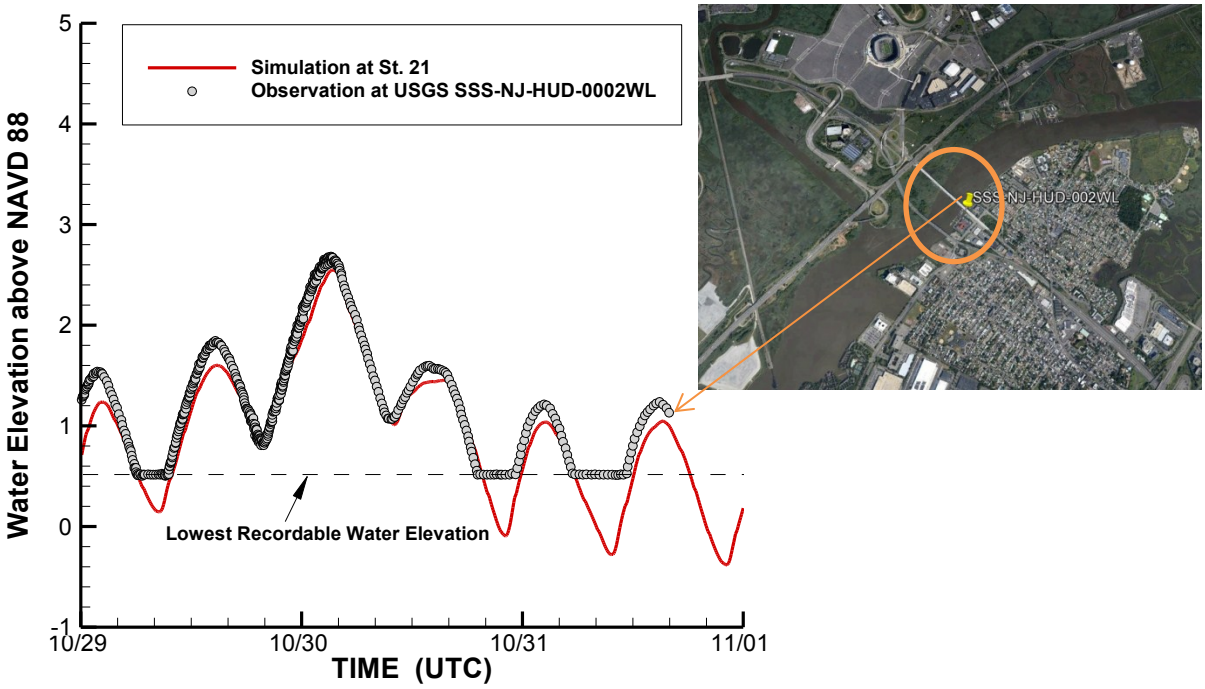

Figure 35 Comparison of water levels at the USGS storm-tide No. SSS-NJ-HUD-002WL in the Hackensack River at NJ Route 3, near Lyndhurst, NJ. The dash line is the lowest recordable water level (=0.5273 m above NAVD88) by the storm-tide sensor.

CCHE2D-Coast can identify the maximum water surface elevations at every computational nodal point in storm-surge simulations, which can be used to find out the flooding water extents through a hurricane. Figure 36(a) presents the spatial distribution of the maximum water levels above NAVD88 over the entire computational domain. By comparing with the surge boundary map observed by FEMA in Figure 36(b), the computed flooding extent map is very close to the FEMA's flood map. In some place such like in the town of Secaucus, no flooding water was computed, it is most likely because of the inaccurate DEM data and building/street information.

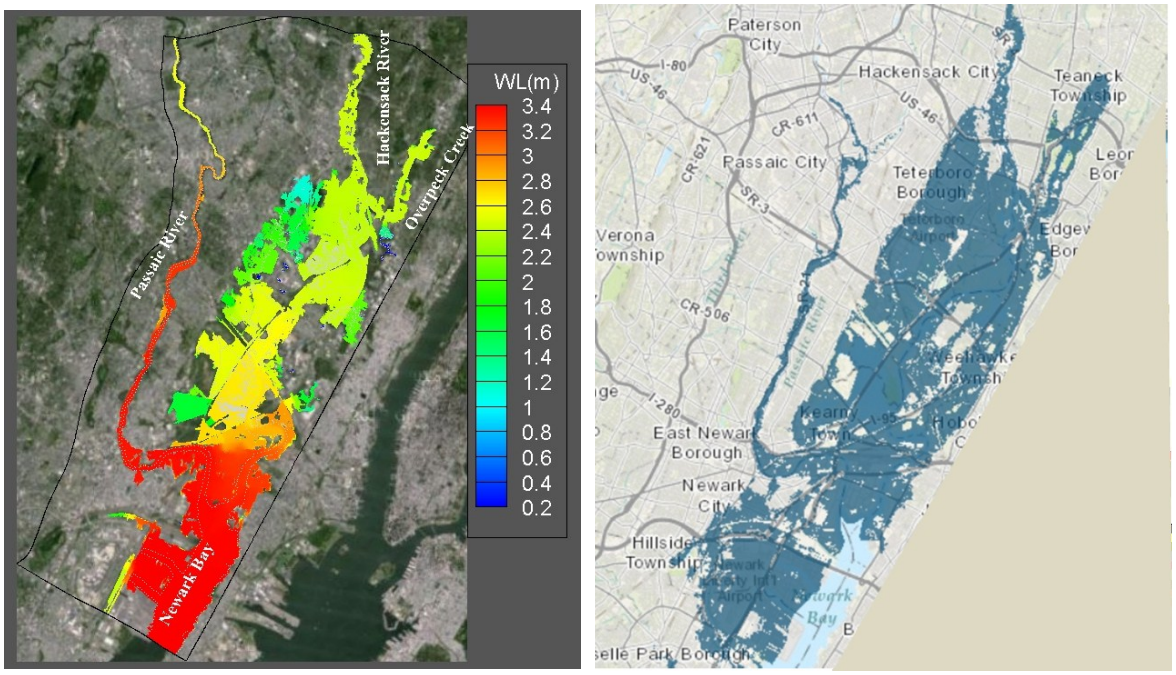

(a) (b)

Figure 36 Comparison of flooding extent maps: (a) Maximum water surface elevations in Sandy computed by CCHE2D-Coast; (b) FEMA SurgeBoundaries Final 0214

Through comparing the water level changes and the flooding water extent maps with observation data measured by USGS and the local institute, it is found that this storm-surge model is capable of reproducing the hydrodynamic processes of storm surge waters and the areas of flooding and inundation induced by Hurricane Sandy. Therefore, this validated storm-surge model is further applied to evaluate the performance of flood mitigation solutions (protection structures).

3 Impact Assessment of Structure Measures

In this section, by using the validated CCHE2D-Coast model, the performance of structure measures is assessed by simulating the flood and inundation with the conditions of a Sandy-like storm and several sea level rise scenarios.

3.1 Structure Measures for Flood Prevention in the Hackensack Area

Five structure measures (mitigation solutions) for flood prevention from storm surges in the Hackensack area have been proposed. They are named as follows:

- **Arc Wall**: a levee (approximately 5.6-mile long) to protect the areas including south Hackensack, Little Ferry, Moonachie,
- **Kearny Wall**: a 2.0-mile-long wall (barrier) with tide gates to protect almost all the two river basin areas,
- **Wall 78**: a 1.5-mile-long wall with a tide gate to cross Newark bay,
- **Wall Middle**: a 4.2-mile-long levee with a tide gate installed, which follows Highway #3 crossing the Hackensack River,
- **Wall North**: a 5.5-mile-long levee with installation of a tide gate crossing the Hackensack River to protect most areas of Moonachie, Little Ferry, Hackensack.

The layouts of the five mitigation measures are shown in Figure 37. In the following simulations with the installation of the protection measures, with no specific mention, the crest height of the structures is 12.000 ft above MSL (i.e. 12.190 ft above NAVD88, or 3.716 m above NAVD88) for all the five mitigation solutions.

For the cases with the structures crossing the rivers or Newark bay, it is assumed that the tide gates will be closed at 0000 UTC 10/29/2012, before the surge peak comes to the domain, until 0000UTC 11/1/2012, when the surge waters completely retreat.

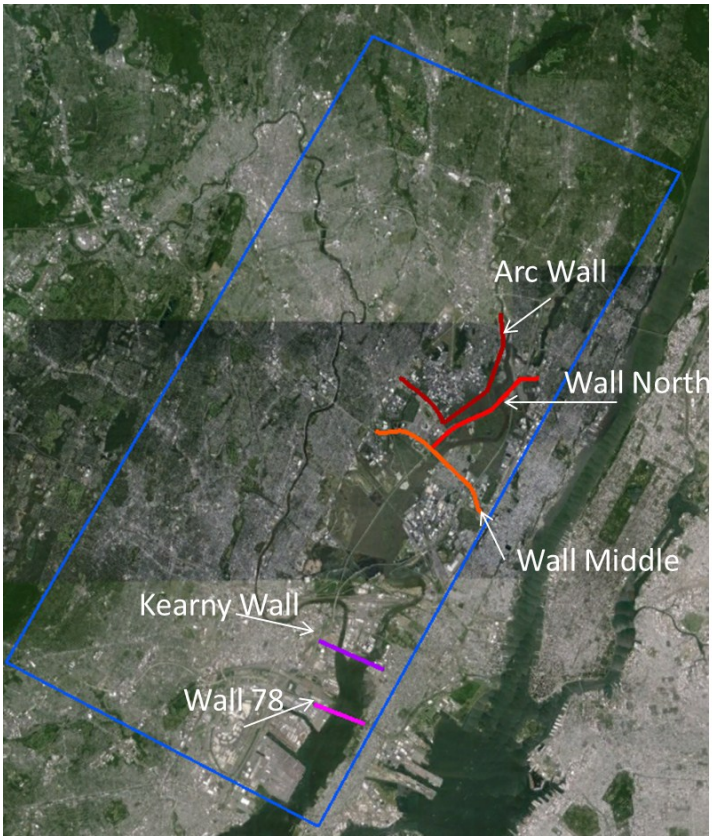

Figure 37 Five solutions for flood protection from storm surges in Hackensack area

3.2 Conditions of Extreme Storm and Sea Level Rise

Since Hurricane Sandy was the deadliest and most destructive tropical cyclone of the 2012 Atlantic hurricane season, as well as the second-costliest hurricane in United States history, the meteorological and hydrological conditions in Sandy are used as the driving forcing conditions of the extreme storm to assess flood and inundation in the computational domain of northeast New Jersey.

To determine the future sea level scenarios, after having reviewed a variety of literature on the global and local (the East Coast) sea level rise (SLR) (e.g. Frumhoof et al. 2007; Cooper et al. 2005), and we decided to assume two possible future SLR scenarios based on Frumhoff et al (2007) (Figure 38) to model the sea level in 2100, i.e.

(1) SLR = 9.6 inches (24.4 cm), and

(2) SLR = 37.6 inches (95.5 cm).

The first one is corresponding to the mid-range of the most recent IPCC projections under the lower-emissions scenario, the second is related to the mid- range of a more recent set of projections under the higher-emissions scenario. In all the simulations with the structure measures and the sea level rise conditions, the hydrographs of the discharge (Figure 30) in the upstream of the two rivers (Passaic and Hackensack) are also applied.

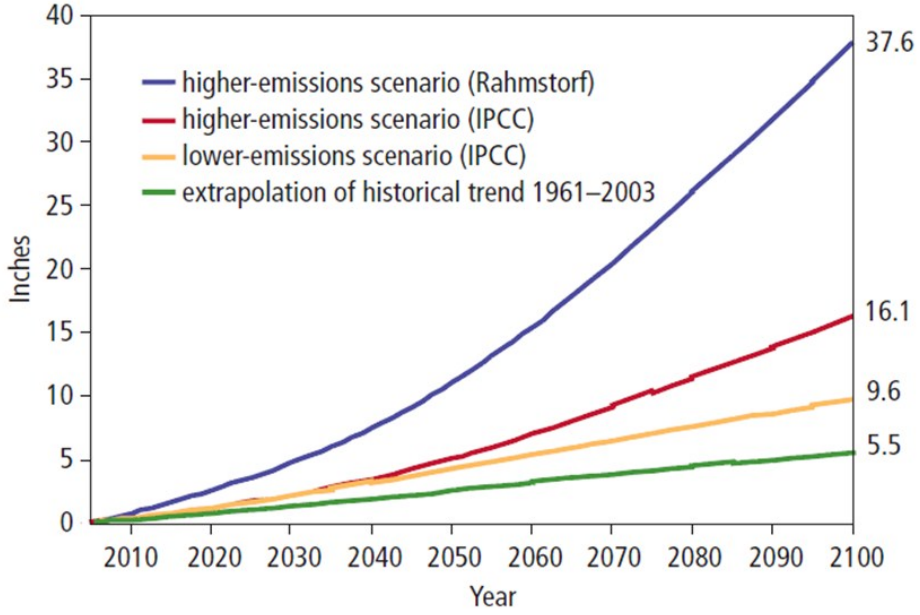

Figure 38 Projected rise in global sea level relative to 2005 (from Frumhoof et al. 2007): This graph depicts the average or mid-range of a number of different sea-level rise (SLR) simulations: a continuation of recent observed SLR rates (green line), the mid-range of the most recent IPCC projections under the lower-emissions scenario (yellow line), the mid-range of the recent IPCC projections under the higher-emissions scenario (red line), and the midrange of a more recent set of projections under the higher-emissions scenario (blue line).

For the cases with the future sea level rise, the simulations for creating a well-developed sea have been performed by spinning up the storm surge model for two weeks from 10/15/2012 to 10/29/2012. After all the initial conditions of flow fields at 0000 UTC 10/29/2012 were prepared by the “spin-up” process, the structures, then, were placed in their locations, and the simulations of storm surges were carried out for three days from 10/29/2012 to 11/1/2012 to complete the assessment of flooding and inundation due to the storm and SLR.

3.3 Results

3.3.1 With the current sea level (SLR = 0.0)

Computational simulations for all the cases with the installation of structures and the selected SLR scenarios have generated a huge amount of numerical results. They include the spatiotemporal variations of water surface elevations, water depths, and flow velocities at all the nodal points inside the computational domain outputted by the model at a certain interval (mostly 2 hours). Visualization and plots of the flow fields need great efforts. In the following section, we neglect the analysis of detailed hydrodynamic processes through the given storm, but more attentions are paid to the questions on how much flooding water will extend and what if the structures can hold the surge waters or overtopping may happen. To do so, we will have an important overall picture for each case to assess the scale and dimension of flood and inundation under the Sandy-like extreme storm and the given SLR scenarios.

Under the current sea level (*status quo*), the maximum water surface elevations (MWSEs) and water depths (MWDs) for all the cases with the five structure measures and one baseline case (i.e. no structures at all for flood mitigation) have been obtained by the simulations of CCHE2D-Coast. From Figure 39 to Figure 44, six figures give the computed MWSEs and MWDs for the six cases with one no structure (baseline case) and the other five installations of Arc Wall, Kearny Wall, Wall 78, Wall Middle, and Wall North, respectively. As shown in Figure 40, the storm surge waters won't be able to invade the area behind the Arc Wall, and no overtopping happens over the flooding water propagation process. The computed results show that the Arc Wall works for protection of the area of Moonachie and Little Ferry. For other four structures installed, similar performance of flood protection by the mitigation measures can be concluded: no overtopping happens to any protection walls; and the structures (Kearny Wall, Wall 78, Wall Middle, and Wall North) are expected to prevent the lands behind the structures from being invaded by the storm surge waters.

As a summary, Figure 45 depicts the maximum water levels at front of structures and their crest heights (i.e. 12.192 ft above NAVD88). It indicates that the highest flooding waters are lower than the structure crest, no overtopping happens, indeed. However, for the cases of

Kearny Wall and Wall 78, the computed results show that only a little amount of freeboard may be left at front of the two structures. Table 4 further provides the computed values of the freeboards for al l the five solutions. It concludes that the Arc Wall will preserve the most sufficient freeboard, up to 3.643 ft, following that, it is the Wall North. And the Kearny Wall will have the least freeboard (0.423ft or 5.076in), which apparently won't be able to prevent overtopping if the future sea level is higher that its freeboard. Meanwhile, ***it is found that the structure which is placed in the north is expected to preserve more freeboard at front of the structure. That means the structures installed close to the bay will have higher risk to be overflowed by the surge waters.***

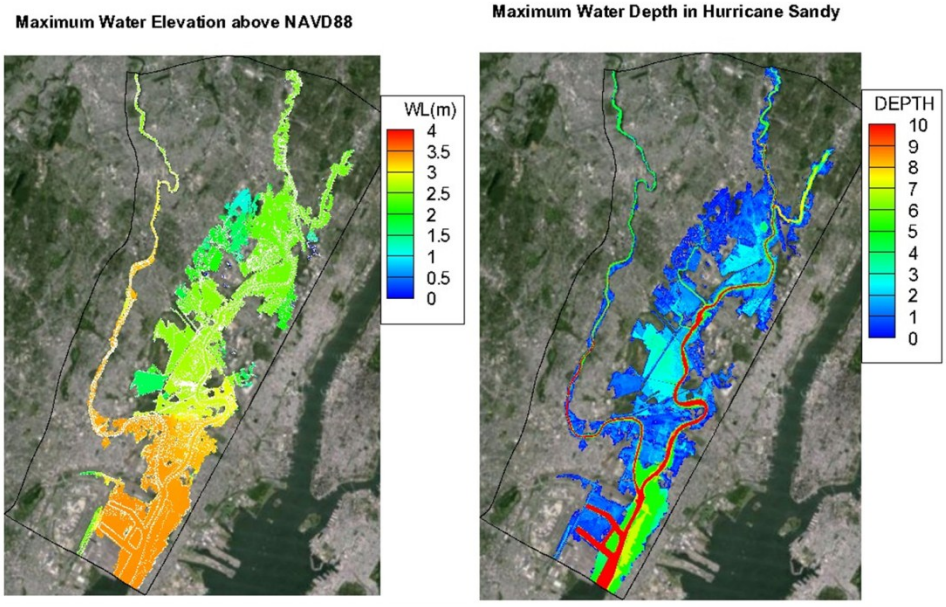

Figure 39 Maximum water surface elevations and depths in the baseline case (no mitigation structures installed) (SLR=0.0in)

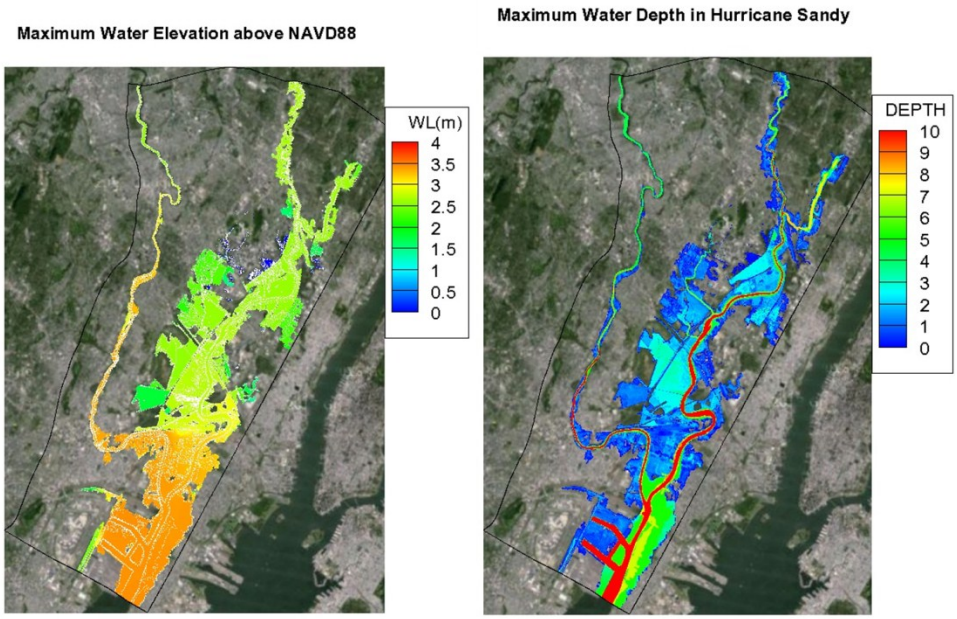

Figure 40 Maximum water surface elevations and depths with the Arc Wall installed (SLR=0.0in)

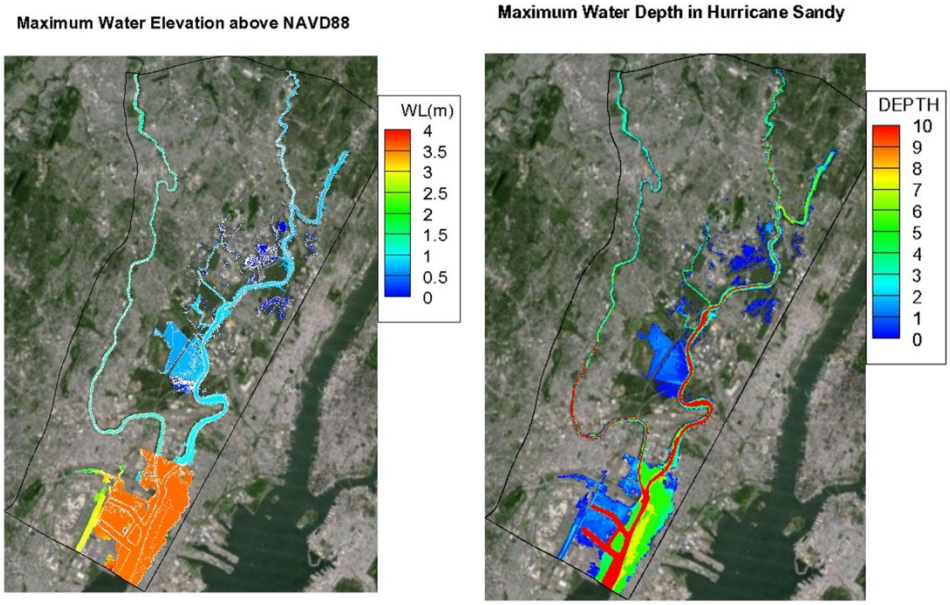

Figure 41 Maximum water surface elevations and depths with the Kearny Wall installed (SLR=0.0in)

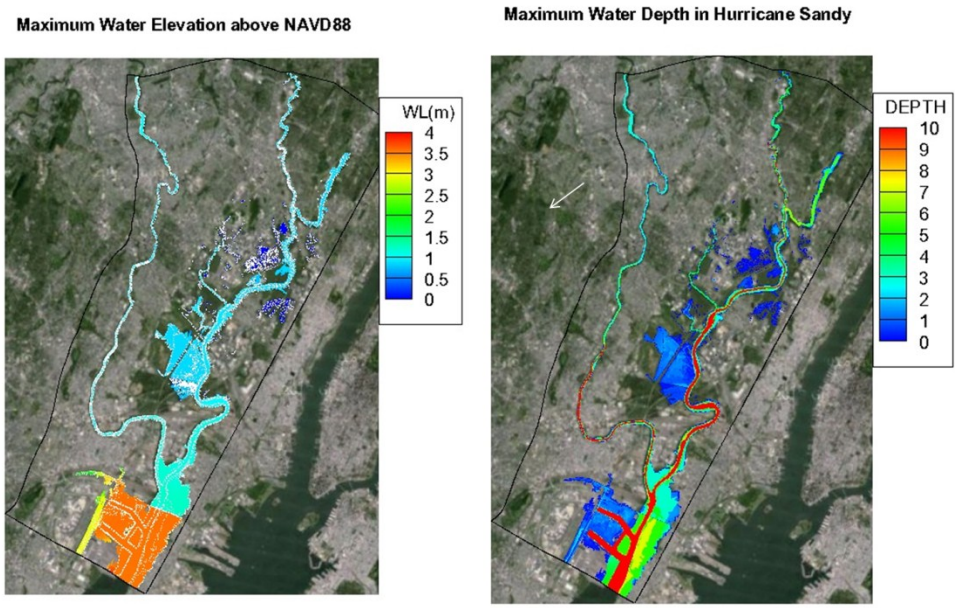

Figure 42 Maximum water surface elevations and depths with the Wall 78 installed (SLR=0.0in)

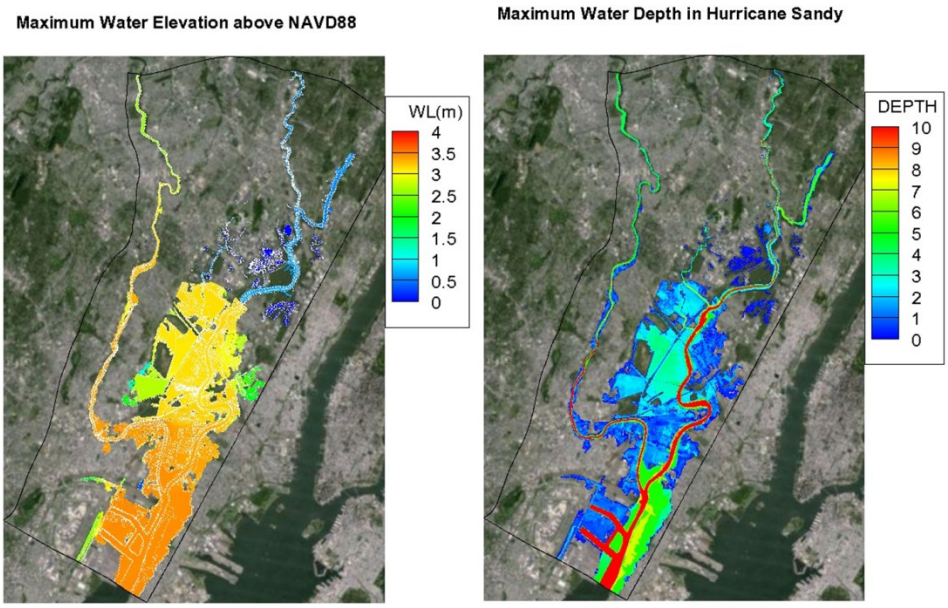

Figure 43 Maximum water surface elevations and depths with the Wall Middle installed (SLR=0.0in)

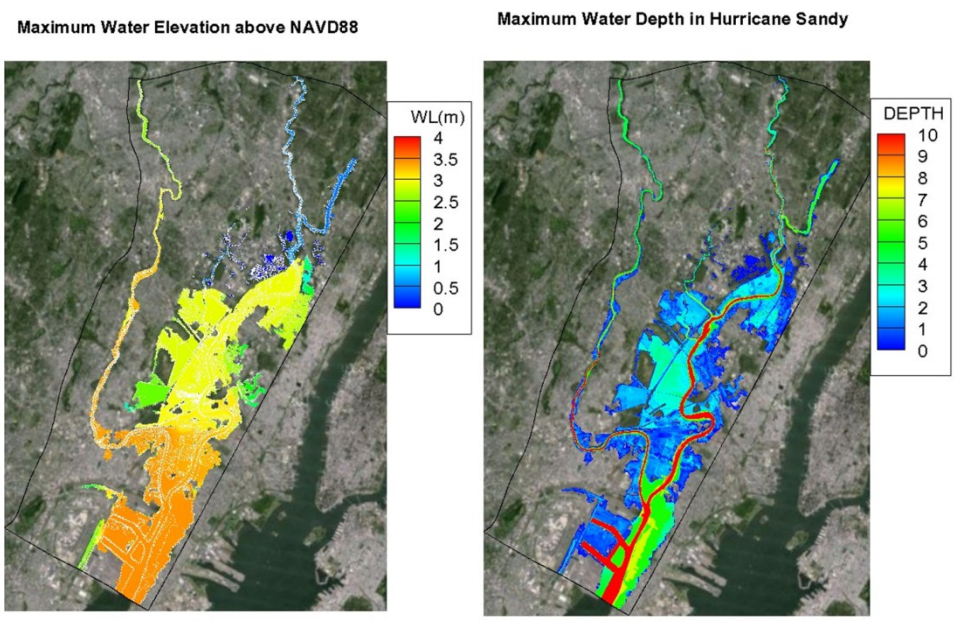

Figure 44 Maximum water surface elevations and depths with the Wall North installed (SLR=0.0in)

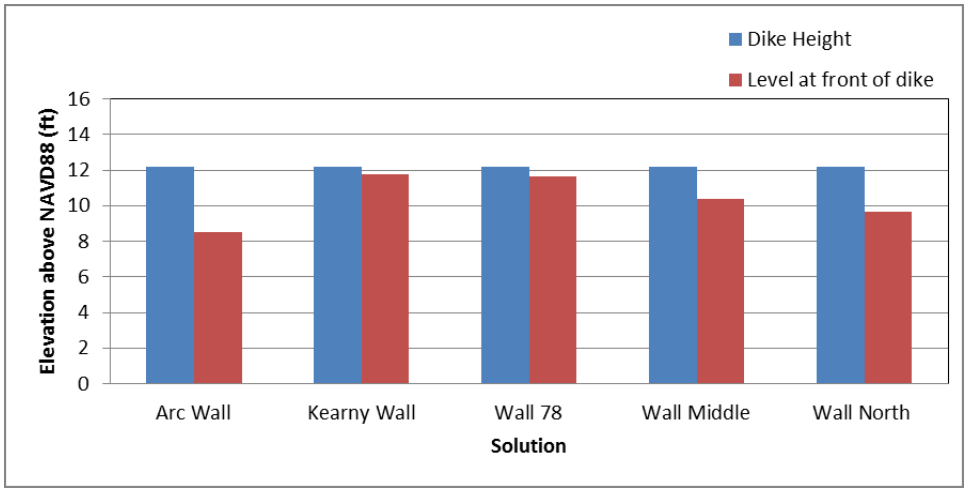

Figure 45 Maximum Water Surface Elevations at Front of Structures (SLR = 0.0in)

Table 4 Maximum water levels (WLmax) at front of structures and freeboard (the structure crest height=12.192 ft above NAVD88): SLR = 0.0in (the current MSL)

Case No	Solution	WLmax (ft)	Freeboard (ft)
1	Arc Wall	8.548	3.643
2	Kearny Wall	11.768	0.423
3	Wall 78	11.677	0.515
4	Wall Middle	10.364	1.827
5	Wall North	9.652	2.539

3.3.2 SLR = 9.6 inches

As the first scenario of sea level rise in this study, the sea level is corresponding to the mid-range of the most recent IPCC projections under the lower-emissions scenario. With the same condition of Sandy, the storm surge waters are expected to flood and inundate a wider inland of the Hackensack area. In comparison with the flooding extent map under the current sea level shown in Figure 39, after the sea level rises up to 9.6 in, the flooding map plotted in Figure 46 has predicted more low-lying areas in Hackensack and Little Ferry will be flooded by the storm surge waters. The surges may reach the central area of the town of Hackensack. It may result in more property damages in the city and the residential areas. At the same time, the flooding water depth will increase in response of the sea level rise.

As shown in Figure 47, under this SLR scenario, the Arc Wall measure may still enable to protect the areas behind the structure. But some flooding waters may invade the south of Hackensack (which is mostly the residential area) through the north tip of the wall. It implies that the Arc Wall may need to extend itself to farther north to get the residential properties protected. As presented in Table 5 and Figure 52, with this SLR, there will be 2.789 ft freeboard reserved in front of the structures, and no overflow or overtopping may happen on the top of the wall.

From Figure 48, it is found that the Kearny Wall may still be able to stop most of surge waters flowing into the north of the area. But after calculation of the freeboard on the basis of the maximum water levels at front of the structure, the results in Table 5 show that overtopping and overflow may occur over a short period when the surge peak is higher than the crest of the structure. Even though there won't very much flooding water inundating the area behind the structure, the overtopping and overflow will put the structure in danger.

The Wall 78 measure may have the similar risk to its stability during the peak of storm surges due to overtopping and overflow over the structure.

The Wall Middle may be able to stop most of flooding waters due to the storm surge. But the freeboard is only 0.692 ft left, if the wind is strong and the induced wave could be high enough to overtop the structures. It may also threaten the structure's stability.

The Wall North may be able to protect all the areas in Hackensack, and play a similar role in flooding protection as the Arc Wall can provide. 1.752-ft freeboard in front of the wall may just enable to prevent wind-induced waves from being overtopping. The less freeboard may result in a less resilient protection, because the risk to the structure's stability is still high.

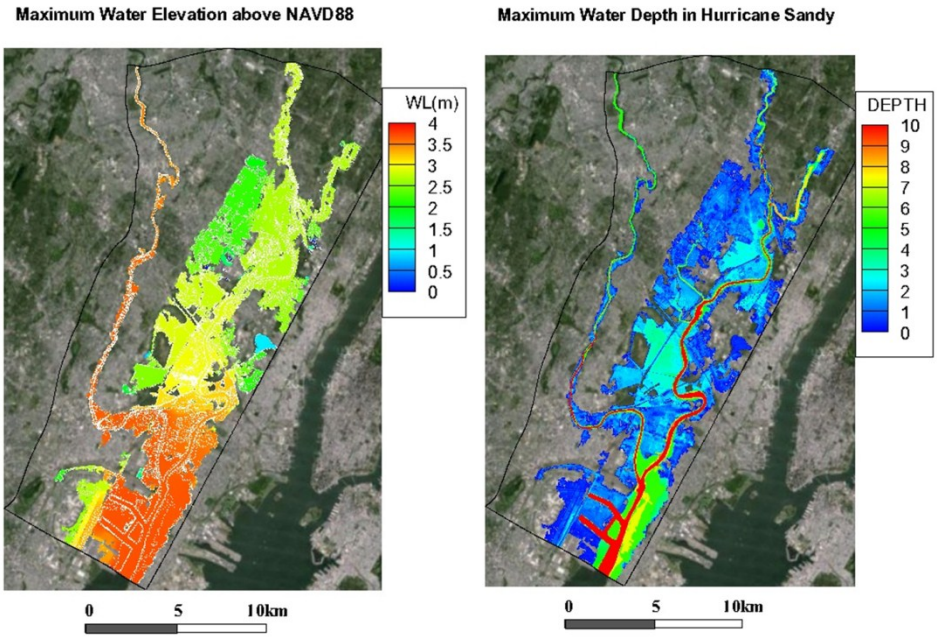

Figure 46 Maximum water surface elevations with no mitigation structures installed (SLR=9.6in)

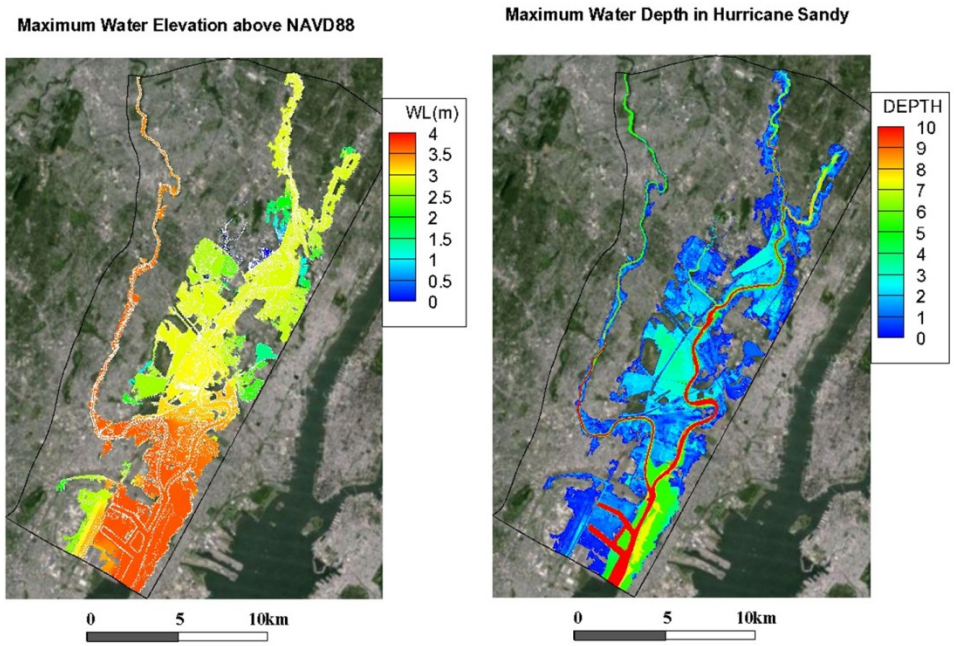

Figure 47 Maximum water surface elevations with the Arc Wall installed (SLR=9.6in)

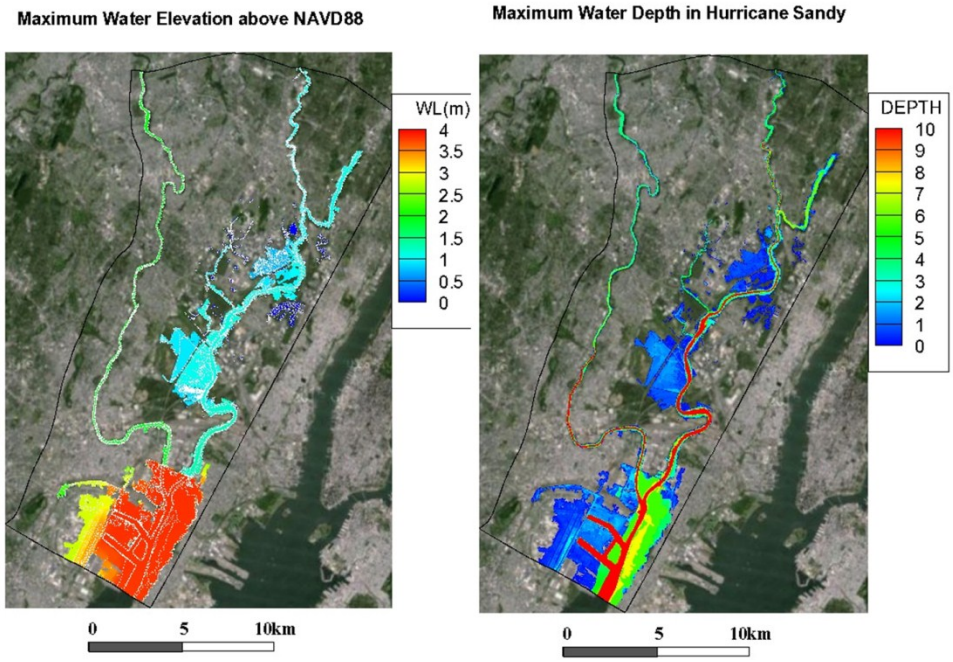

Figure 48 Maximum water surface elevations with the Kearny Wall installed (SLR=9.6in)

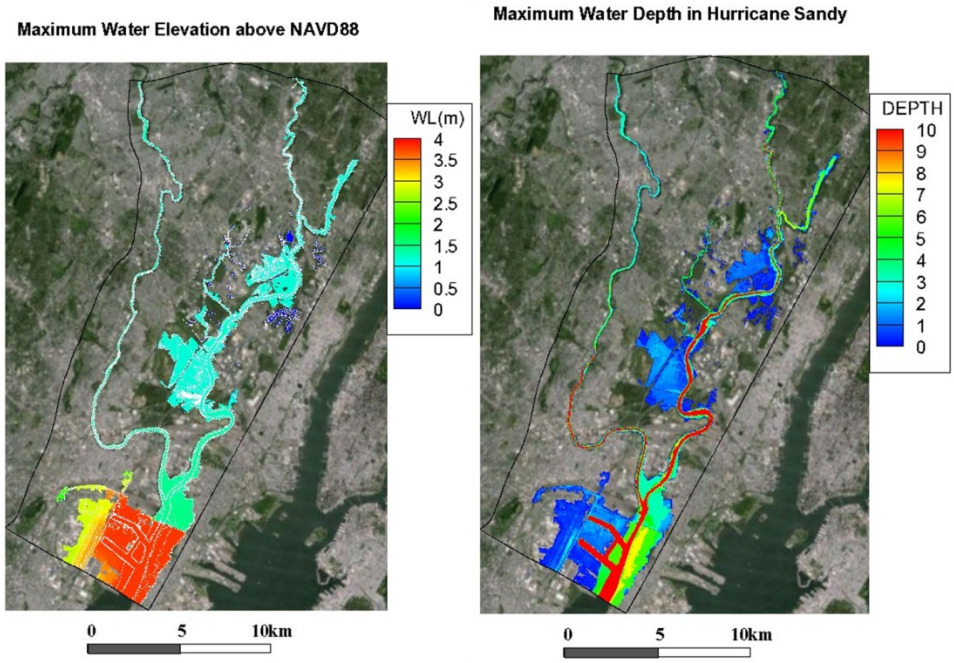

Figure 49 Maximum water surface elevations with the Wall 78 installed (SLR=9.6in)

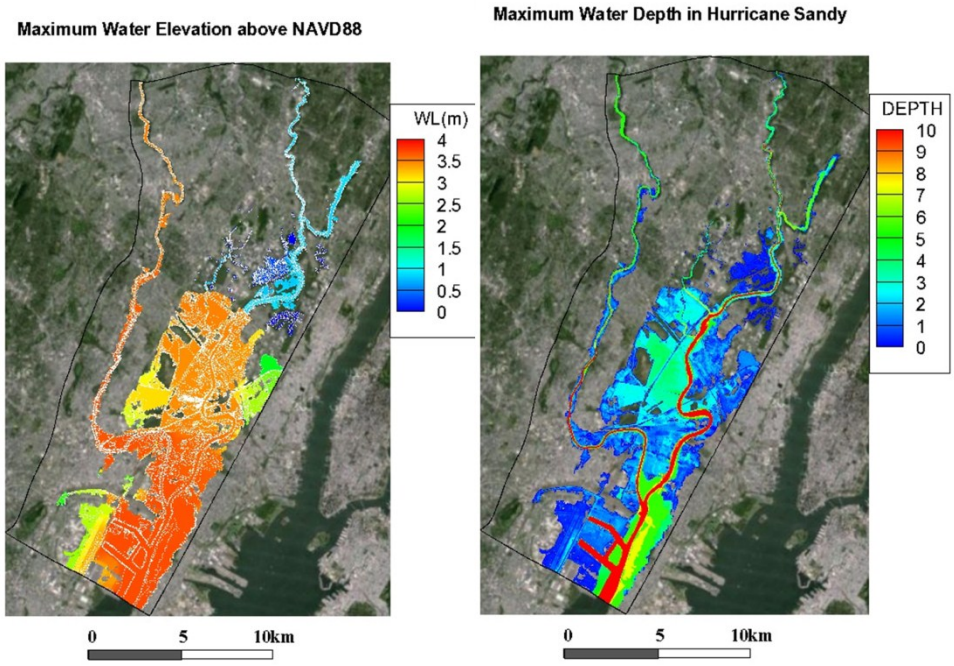

Figure 50 Maximum water surface elevations with the Wall Middle installed (SLR=9.6 in)

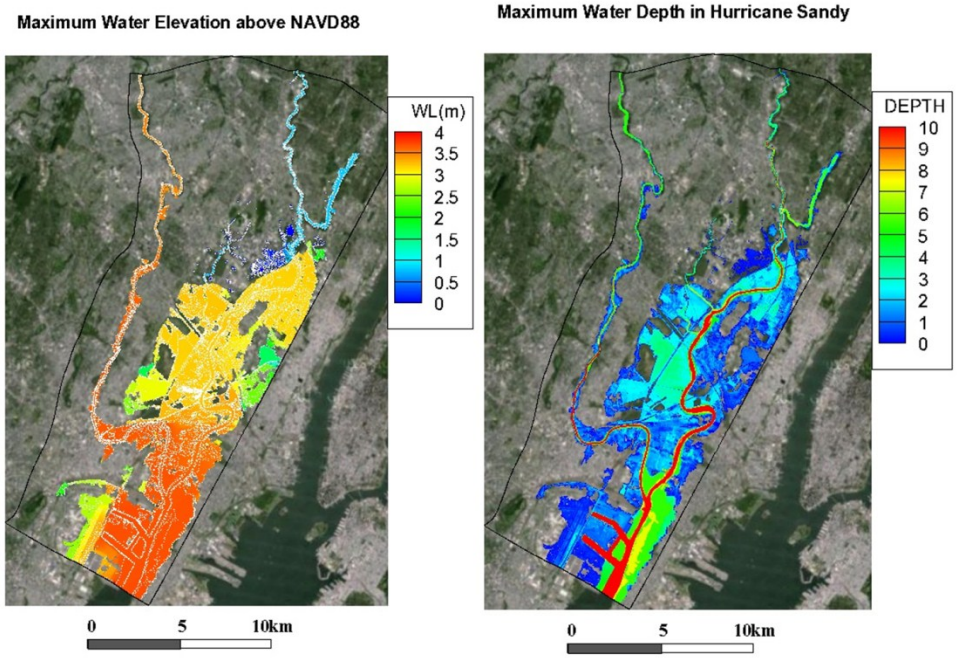

Figure 51 Maximum water surface elevations with the Wall North installed (SLR=9.6 in)

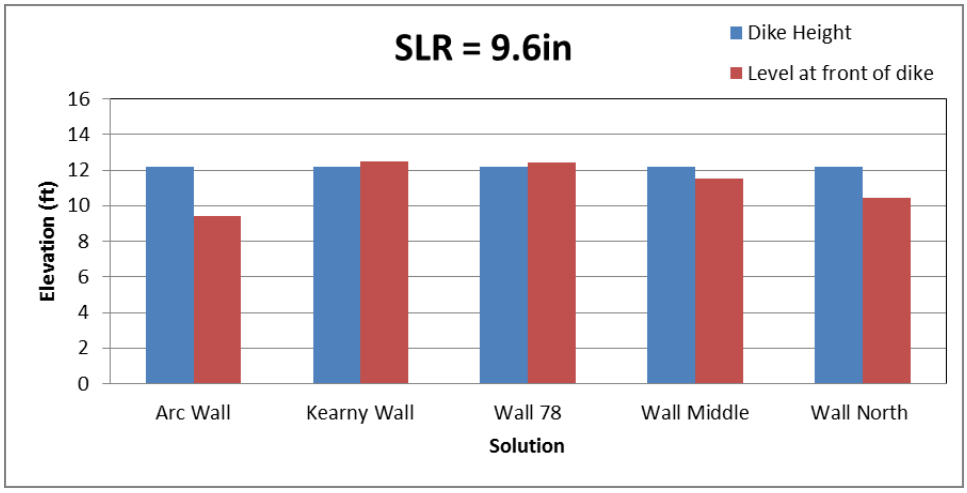

Figure 52 Maximum Water Surface Elevations at Front of Structures (SLR = 9.6in)

Table 5 Maximum water levels (WLmax) at front of structures and freeboard (the structure crest height=12.192 ft above NAVD88): SLR = 9.6 in

Case No	Solution	WLmax (ft)	Freeboard (ft)	Note
1	Arc Wall	9.403	2.789	
2	Kearny Wall	12.516	-0.325	overflow
3	Wall 78	12.441	-0.249	overflow
4	Wall Middle	11.499	0.692	
5	Wall North	10.440	1.752	

3.3.3 SLR = 37.6 inches

With further SLR to 37.6 in, as shown in Figure 53, the model has predicted that almost all the cities and residential areas in Hackensack, Little Ferry, Moonachie, etc. will be flooded by the storm surge waters, and the maximum flooding water depth in the south of Hackensack may be deeper than 2 meter (> 6 ft). Therefore, without any mitigation measures, A Sandy-like hurricane will complete inundate this region, and induce even worse scenario than Hurricane Sandy in 2012 due to potential property damage and loss of life.

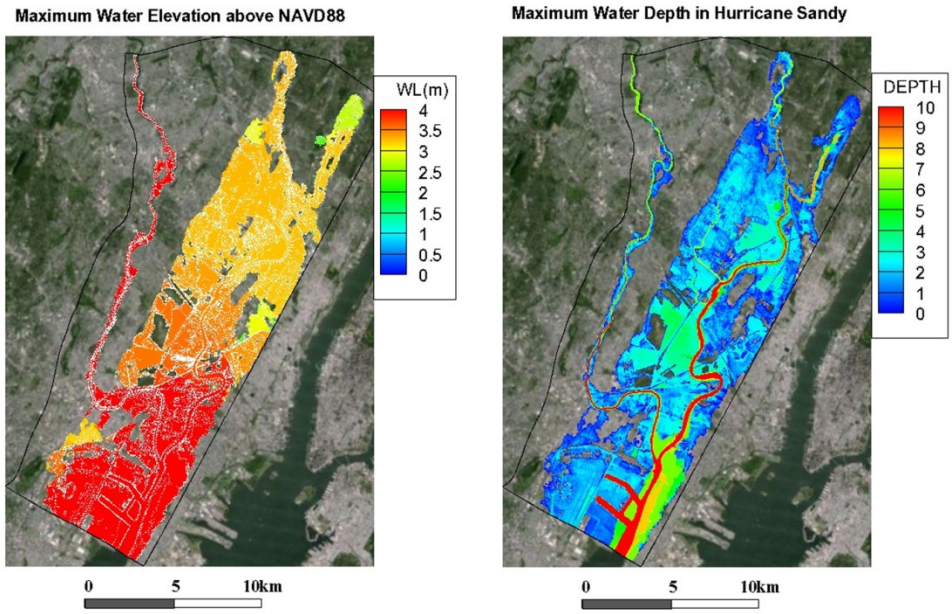

Figure 53 Maximum water surface elevations with no mitigation structures installed (SLR=9.6in)

Based on the simulation results of the cases with the five flood protection structures installed, the maximum water levels in Figure 54, in comparison with the crest heights, give a quick assessment of the performance of the measures. The water levels indicate that four structures (Kearny Wall, Wall 78, Wall Middle, and Wall North) may encounter severe overflow and overtopping, and less than half of foot freeboard will be left in the Arc Wall which won't be able to prevent surge waters from being overtopping the structure crest. More details on the freeboards and the water levels are given in Table 6. As a result, all the five structures may face a high risk to be destabilized by the high waters from the storm surges if the sea level rises up to 37.6 in.

The flood water extent maps and maximum water depths with the five mitigation measures are given in Figure 55 to Figure 59, respectively. These simulated results of flood waters can be used for further assessing the risk of flooding and inundation under this worst SLR scenario.

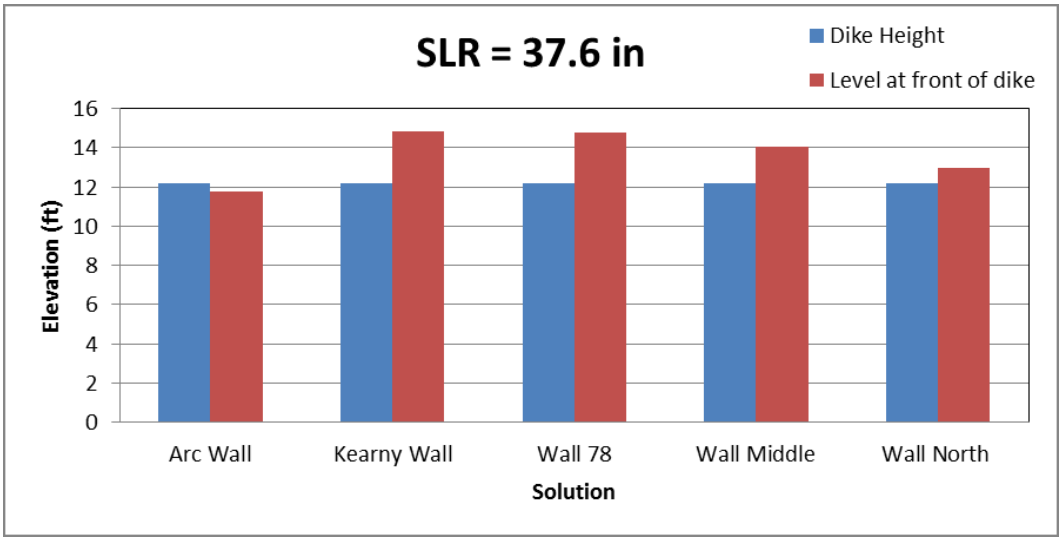

Figure 54 Maximum Water Surface Elevations at Front of Structures (SLR = 37.6in)

Table 6 Maximum water levels (WLmax) at front of structures and freeboard (the structure crest height=12.192 ft above NAVD88): SLR = 37.6 in

Case No	Solution	WLmax (ft)	Freeboard (ft)	Note
1	Arc Wall	11.778	0.413	
2	Kearny Wall	14.810	-2.618	overflow
3	Wall 78	14.757	-2.566	overflow
4	Wall Middle	14.068	-1.877	overflow
5	Wall North	12.969	-0.778	overflow

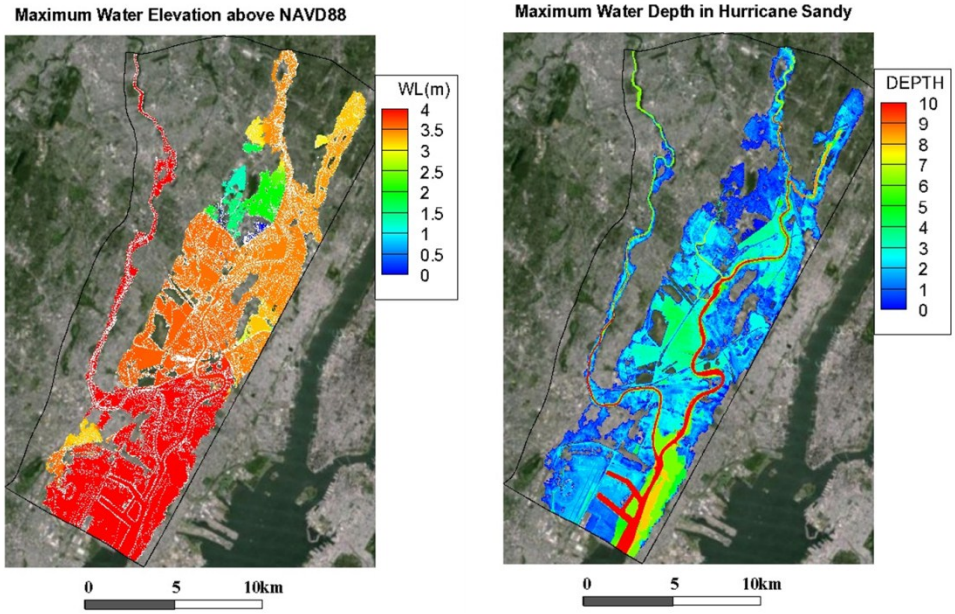

Figure 55 Maximum water surface elevations with the Arc Wall installed (SLR=37.6in)

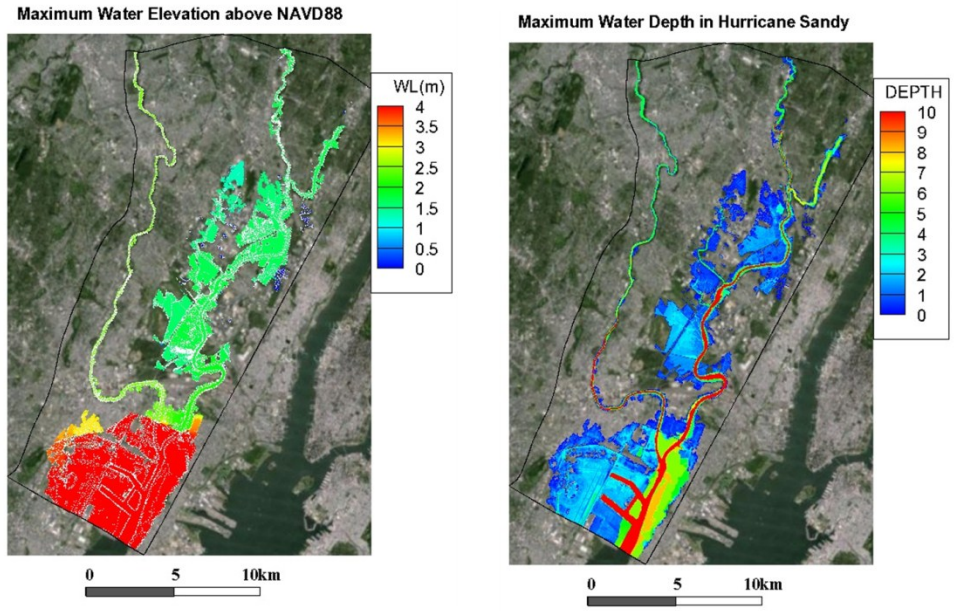

Figure 56 Maximum water surface elevations with the Kearny Wall installed (SLR=37.6in)

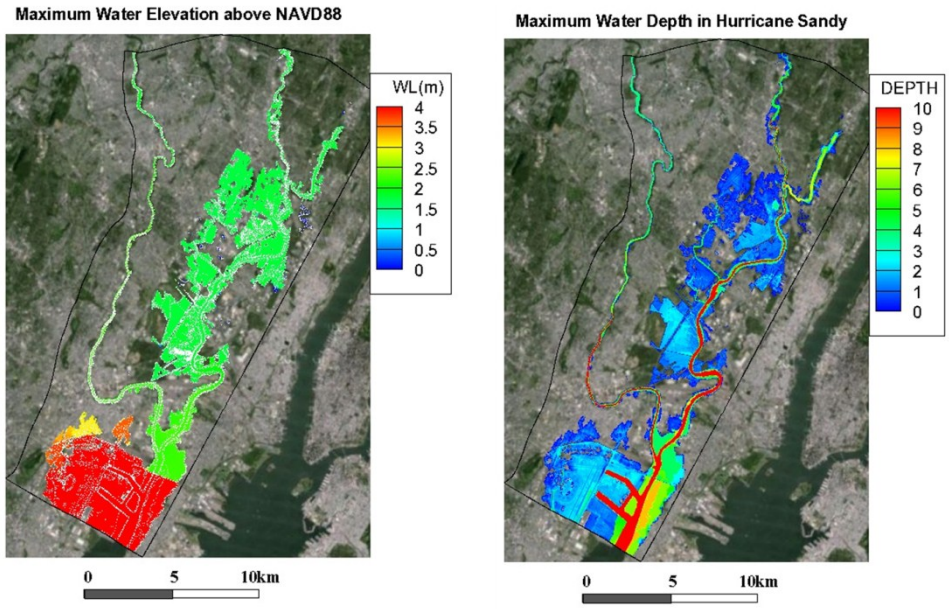

Figure 57 Maximum water surface elevations with the Wall 78 installed (SLR=37.6in)

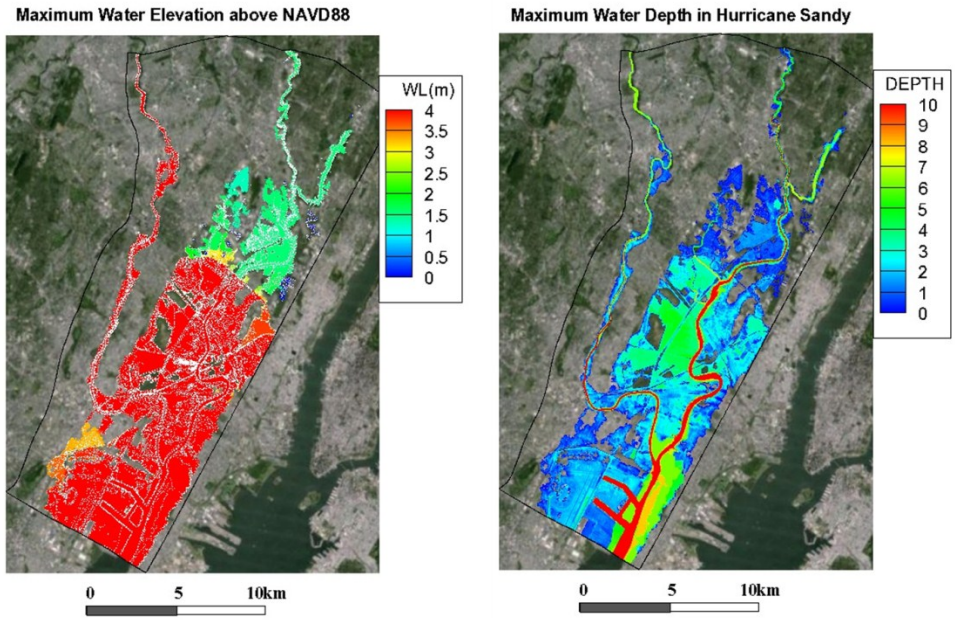

Figure 58 Maximum water surface elevations with the Wall Middle installed (SLR=37.6 in)

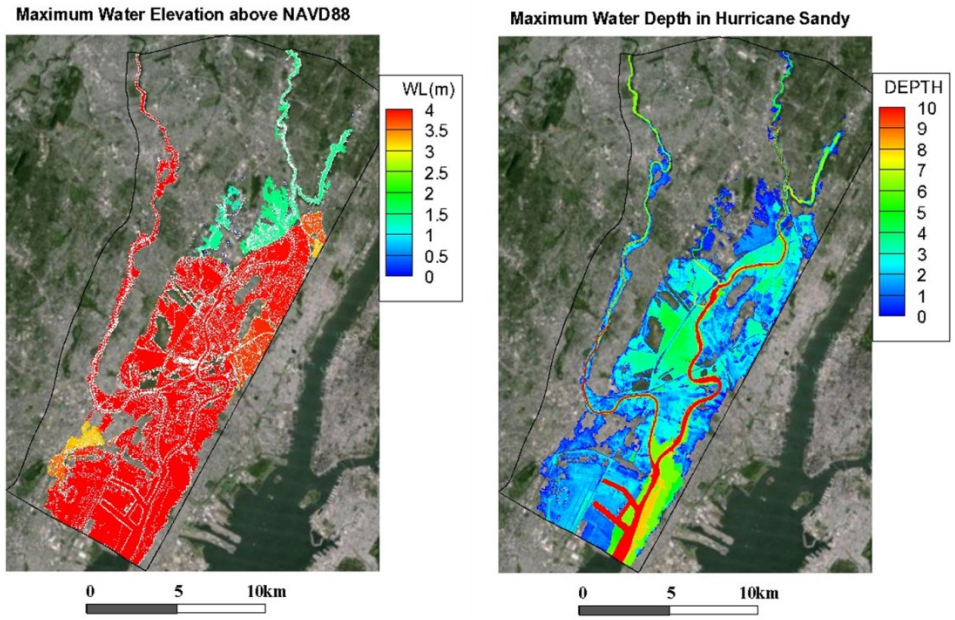

Figure 59 Maximum water surface elevations with the Wall North installed (SLR=37.6 in)

3.4 Remarks

Through the analysis of the simulation results (18 runs in total) for the five flood protection structures under the combined conditions of a Sandy-like storm and two future sea level scenarios, we can summarize major findings into the following remarks:

- Without mitigation measures, the Hackensack area will be severely flooded by the storm surge waters under the rising sea level. With both SLR scenarios, potential risk of property damage and possible casualties will be much worse than those by Sandy in 2012. In other words, the urban area of northeast New Jersey is very vulnerable to hurricane and sea level rise.
- The freeboard in flood protection structures is used as an indicator to examine if overtopping or/and overflow occur on the top of the mitigation measures. As shown Figure 60, after the sea level rises to 9.6 in (the first scenarios of this study), the Kearny Wall and Wall 78 may encounter overtopping and overflow. If it further rises up to 37.6 in, all the four mitigation measures, except the Arc Wall, will have the surge waters flowing over the structures.
- The flood protection structures which are placed in the north are expected to preserve more freeboard at front of the structures than those in the south. That means the structures installed close to the bay will have higher risk to be overflowed by the surge waters. Therefore, the Arc Wall, which is placed in the most northern of the Hackensack River, will receive the least pressure of the storm surge waters from the Newark Bay. However, this solution is able to protect only the areas of Hackensack, Little Ferry, and Moonachie. And if the sea level is lift up to 37.6 in, the Arc Wall, with a small freeboard preserved, may face the risk of overtopping.

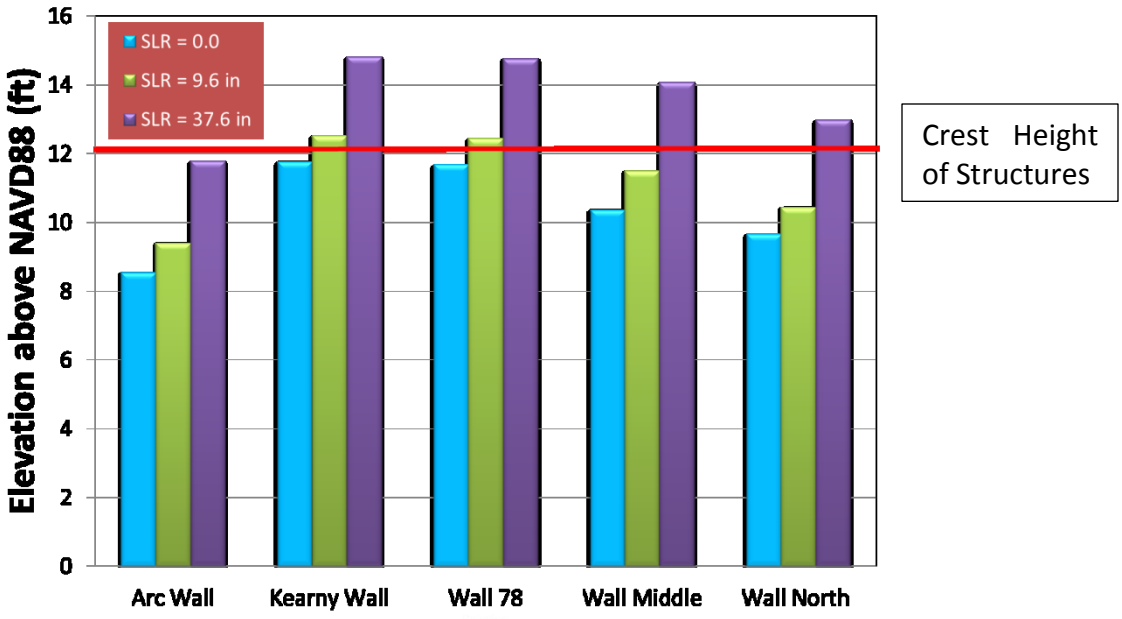

Figure 60 Maximum water surface elevations at front of structures for all the SLR scenarios

- In order to find a better design height of the Arc Wall, two more cases for the Arc Wall are proposed: (1) the crest level of the structure = 8 ft above MSL, and (2) the crest level = 10 ft above MSL. By simulating the storm surges under the current sea level (i.e. no sea level changes), the results of the maximum water levels at front of the Arc Wall are obtained and plotted in Figure 61. It indicates that the 8-ft crest height is insufficient to prevent overflow and overtopping, the 10-ft and 12-ft crest heights may be safer to provide flooding protection for the Hackensack area. However, by checking with the water levels in Figure 60, the Arc Wall with 10-ft high crest won't be safe if the SLR is up to 37.6 in. More details on the flood water extent maps with the 8-ft high Arc Wall are shown in Figure 62, and those of flooding and inundation with 10-ft crest height are then given in Figure 63. By comparing with the flood maps for the Arc Wall of 12-ft crest height, no significant difference behind the structure can be found.

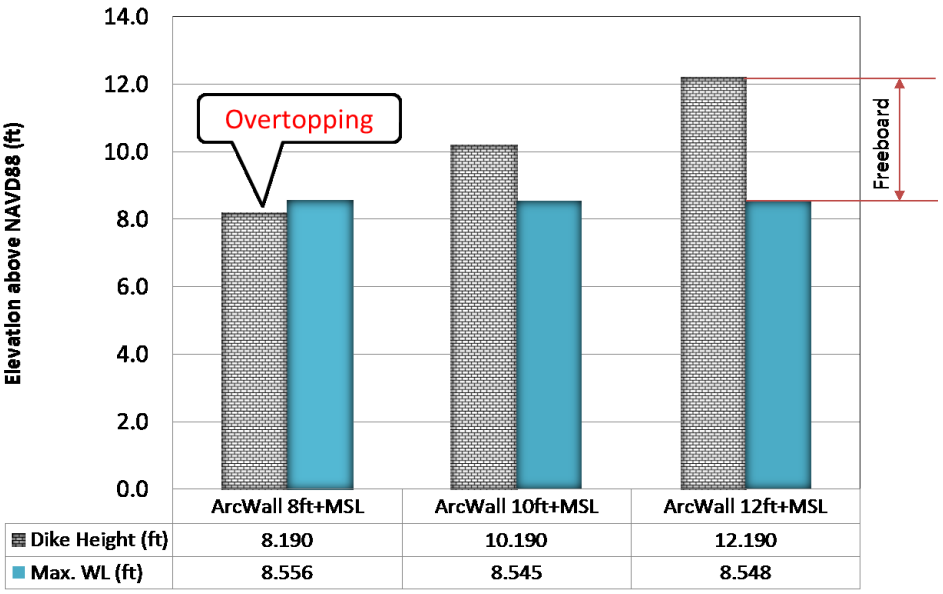

Figure 61 Maximum water elevations at front of the Arc Wall under the current sea level (i.e. SLR = 0.0)

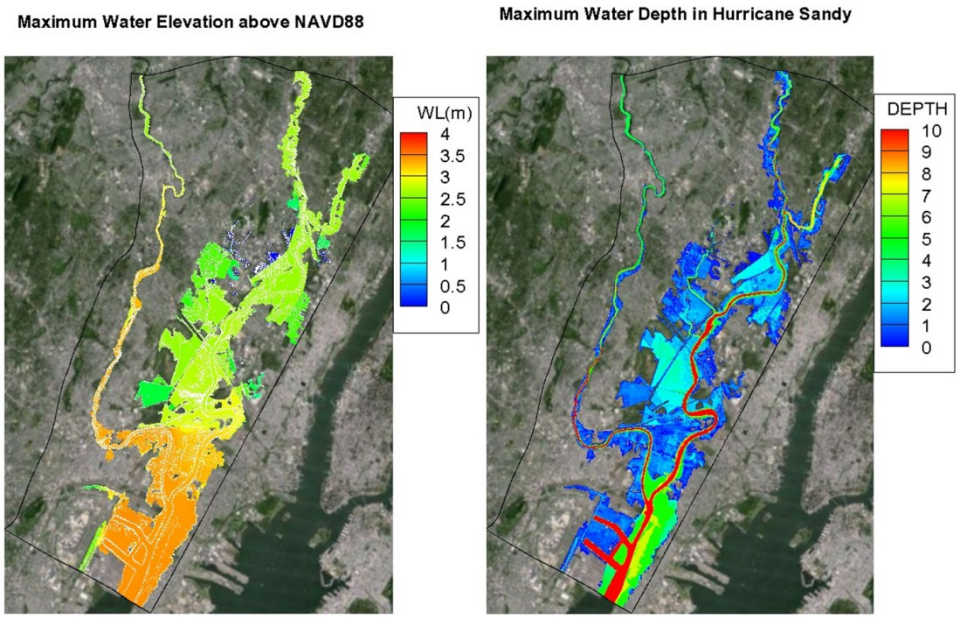

Figure 62 Maximum water elevations and depths with the 8-ft-high Arc Wall under the current sea level (SLR=0.0)

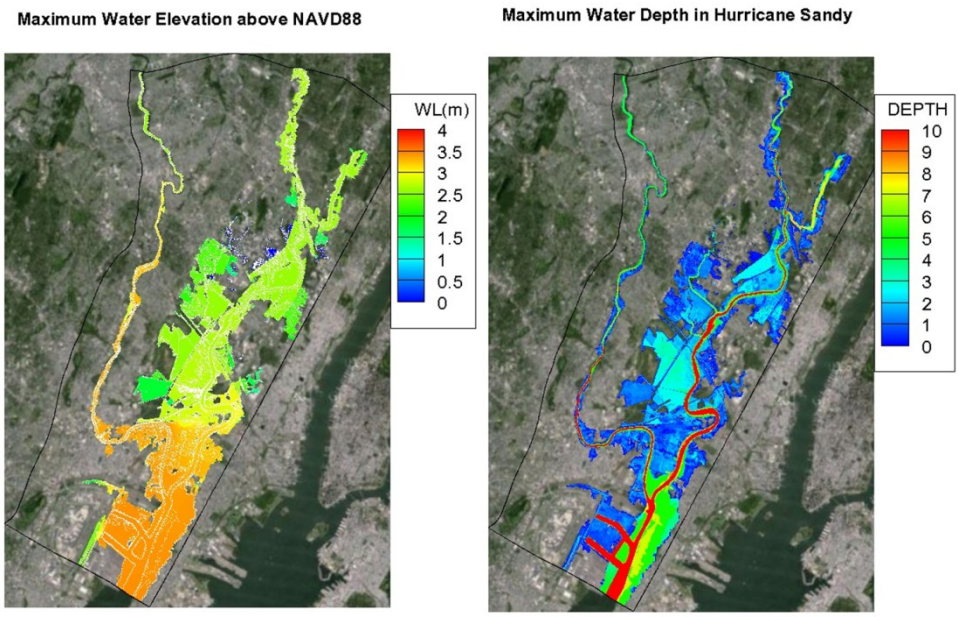

Figure 63 Maximum water levels and depths with the 10-ft high Arc Wall under the current sea level (SLR=0.0)

- Future research topics: (1) Based on the simulation results of flood and inundation under the combined hydrological conditions of an extreme storm conditions and the SLR scenarios, the risk of flooding and protection structures can be further quantified. (2) The variation of hurricane intensity in the future due to global warming may need to be taken into account. (3) The wind-induced waves may need to be computed to examine how overtopping of waves occurs if a freeboard at front of a structure is not sufficient.

4 Simulation of Contaminant Leaching during Hurricane Sandy

This study is to apply CCHE2D-Chem, an integrated model developed in the NCCHE (e.g. Jia et al. 2013), to simulate pollutant leaching in two hypothetical scenarios. The contaminants are assumed to be released in the site of the Kearny freshwater marsh when the storm surge waters of Hurricane Sandy inundate this area. In the two cases, one is assumed with high leaching rate and the other with slow leaching rate. The flow fields of storm surges induced by Sandy (2012) computed by CCHE2D-Coast are used as input flow conditions for simulation of contaminant leaching. The simulation conditions and results are briefly discussed below.

4.1 Leaching Site

At a site in the Kearny freshwater marsh (Figure 64), elevated concentrations of arsenic (As), cadmium (Cd), chromium (Cr), lead (Pb), and mercury (Hg) that exceeded the Ontario Aquatic Sediment Quality Lower Effect Levels were found in the sediments. The heavy metal concentrations range from 10 ppb to 1 ppm.

The leaching site as shown in Figure 65 was chosen for demonstrating the potential heavy metal leaching from marshland to flood water. The mobility of heavy metals are affected by many factors including the chemical forms and properties, soil organic content, the quantity and type of soil binding sites, soil ion strength, pH, temperature, the concentration of complexing anions (organic and inorganic), and competing cations in soil solution (McLaren and Crawford 1973, Tyler and McBride 1982, Kuo et al. 1985, Elliott et al. 1986)

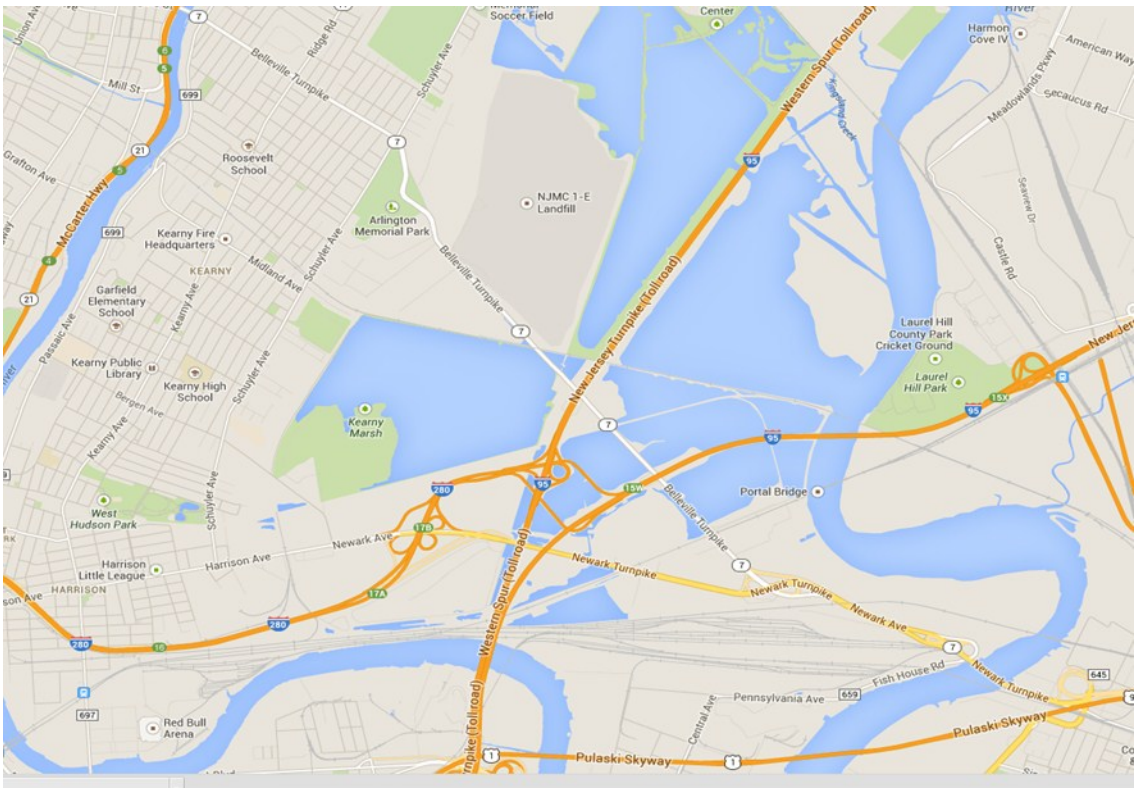

Figure 64 Map of the Kearny freshwater marsh site

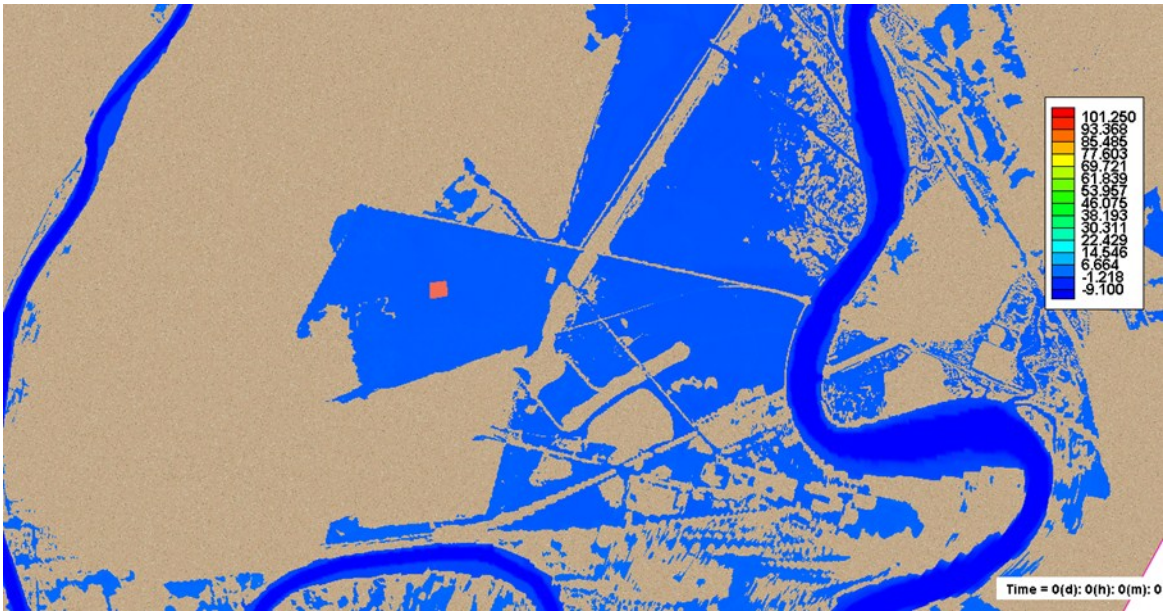

Figure 65 Leaching location in the numerical mesh

4.2 Computational Conditions

All these factors are site specific and need extensive investigations to find out. An approximation was used to estimate the range of the leaching rate of As from the marshland to the floodwater. There were studies (Solomon et al. 1990, Smedley and Kinniburgh 2002, USEPA 2005, Dubey et al. 2007, Zhu et al. 2011) showing Arsenic leaching from CCA-treated woody debris to the floodwater and sediments after Hurricane Katrina. Measured As concentration in sediment right after Hurricane Katrina ranged from 1-100 ppm (µg/kg). For that specific case, the leaching rate was estimated at 0.1 mg/s from soil to the overlying floodwater during the inundation period.

The contaminant is assumed to leach through flood waters due to rising of surge tide in Hurricane Sandy in 2012. Two scenarios of the leaching were simulated: one with high leaching rate of 0.1 mg/s (Scenario 1) and the other with slow leaching rate of 0.001 mg/s (Scenario 2). For the short period of inundation, chemical decay is assumed negligible.

4.3 Results

The simulations were calculated using CCHE2D-Chem model (Zhu, et al. 2012, Jia et al. 2013). It is a two-dimensional depth-averaged model to simulate chemical fate and transport with the input of simulated flow fields. Based on mass balance and fate processes, the model solves the transport equations of contaminant in water, within bed sediments and the interaction between water and sediments through adsorption partition. Users can specify single or multiple pollution sources/sinks. The general fate processes include volatilization, photolysis, hydrolysis, and biodegradation.

For the simulation of contaminant release, the flow fields of the surge tide were already computed and stored into a dataset. The computation of the leaching started at 0000 UTC, 10/29/2012. It continued for three days, till 0000 UTC, 11/1/2012. Time step for simulation of leaching was 10 sec. After three-day leaching during the period of inundation by Sandy, the As concentration distributions in water at 0000 UTC 11/1/2012 are shown in Figure 66 (Scenario 1) and Figure 67 (Scenario 2).

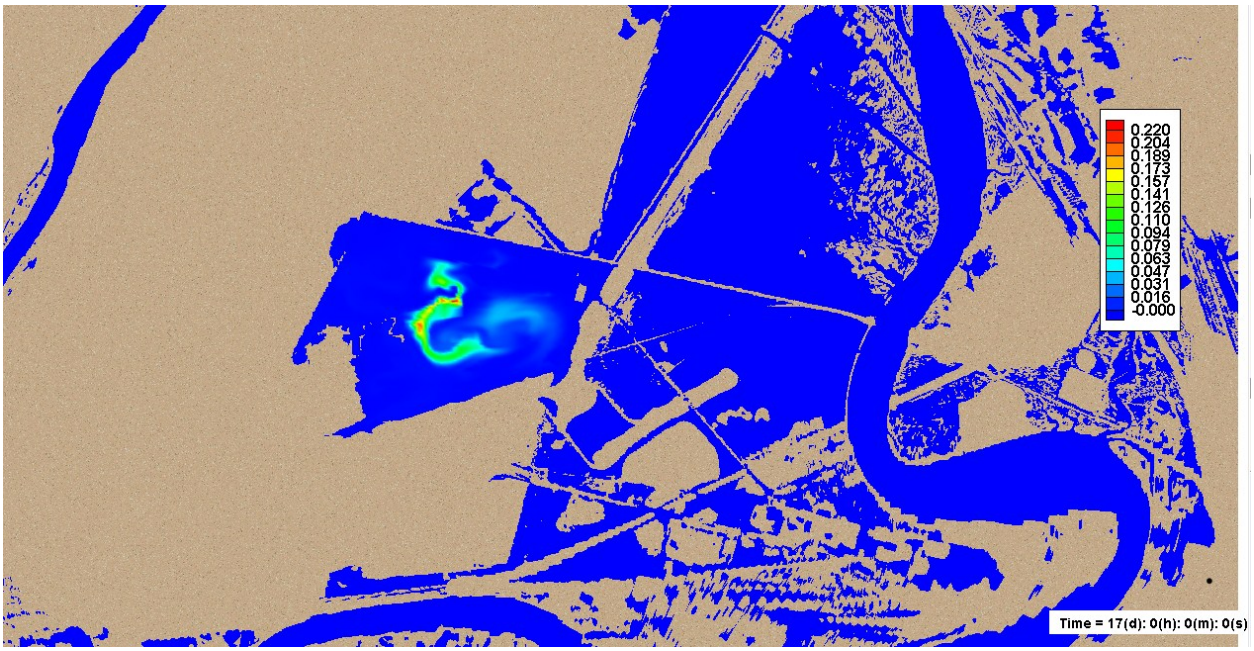

Figure 66 As Concentration distribution in water at 0000 UTC 11/1/2012 (Scenario 1)

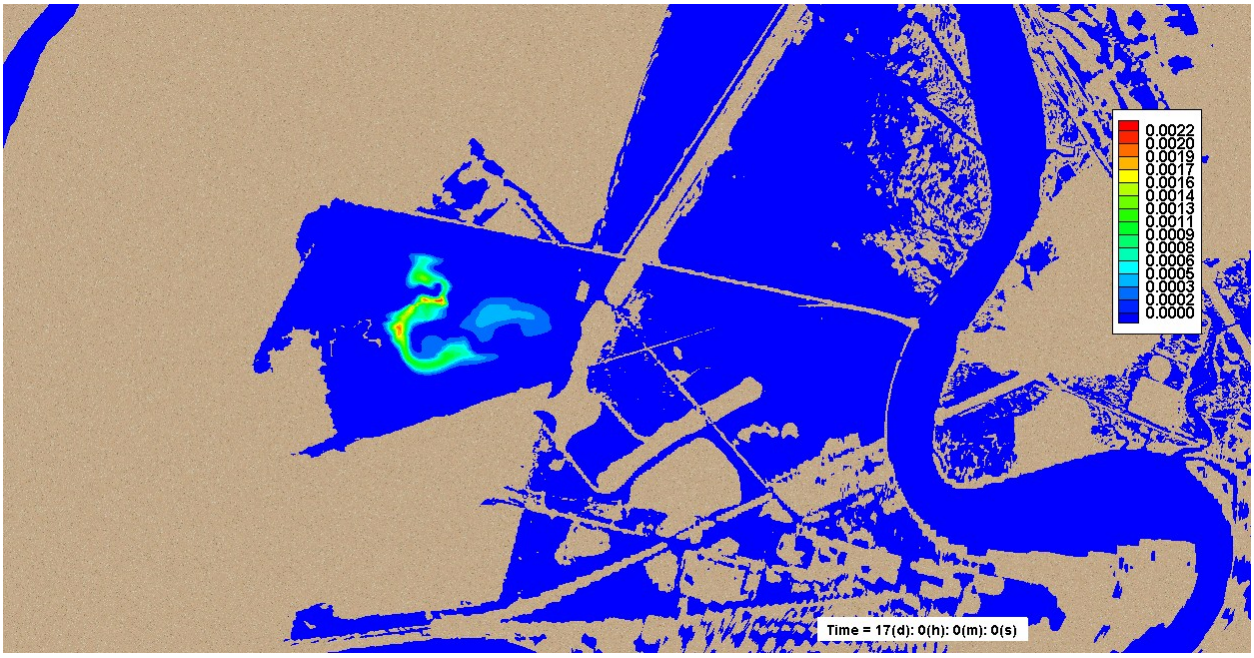

Figure 67 As Concentration distribution in water at 0000 UTC 11/1/2012 (Scenario 2)

It can be seen that the As distribution patterns are similar for both scenarios. Scenario 1 with high leaching rate resulted in a peak concentration level of 0.22 ppb compared with 0.0022 ppb in Scenario 2. There is no violation of the drinking water quality standard for As of 10 ppb (10 µg/L).

The distribution patterns are determined by the hydraulic conditions. The area near the marsh was flooded and then quite isolated from the other flooded area. As a result, the leached As is remained in the isolated area after inundation for both scenarios.

5 Acknowledgements

This work was a result of research sponsored by New Jersey Institute of Technology and the New Jersey Department of Environmental Protection. The authors thank Dr. Fadi A. Karaa for managing this project, Dr. Laramie Potts and Dr. John Miima for providing DEM data, and all other team members of this project who supported our simulation tasks.

6 References

Blake, Eric S., Kimberlain, Todd B., Berg, Robert J., Cangialosi, John P., and Beven II, John L. (2013). Tropical Cyclone Report - Hurricane Sandy (AL182012), 22 – 29 October 2012, NOAA/Hurricane Research Center, 157p., Available at http://www.nhc.noaa.gov/data/tcr/AL182012_Sandy.pdf

Cooper, M. J. P., M.D. Beevers, and M. Oppenheimer (2005). Future sea level rise and the New Jersey coast – Assessing potential impacts and opportunities, Science, Technology and Environmental Policy Program. Woodrow Wilson School of Public and International Affairs, Princeton University, a pdf file available at http://www.princeton.edu/step/people/faculty/michael-oppenheimer/recent-publications/Future-Sea-Level-Rise-and-the-New-Jersey-Coast-Assessing-Potential-Impacts-and-Opportunities.pdf

DeMaria, M., Knaff, J. A., and Kaplan, J. (2006). On the Decay of Tropical Cyclone Winds Crossing Narrow Landmasses, Journal of Applied Meteorology and Climatology, Vol. 45, pp491-499.

Ding, T. (2012). Developing a parametric model for hurricane wind and storm surge prediction in the Gulf of Mexico, 2012 Water Environment Federation Technical Exhibition and Conference, New Orleans, LA, Sept. 29-Oct. 3, 2012, (Available at http://dl.dropbox.com/u/36531386/Ding_Hurricane.pdf)

Ding, Y., Wang, S. S. Y. and Jia, Y. (2006). Development and validation of a quasi three-dimensional coastal area morphological model. *J. Wtrway., Port, Coast. and Oc. Engrg.*, ASCE, 132(6), 462-476.

Ding, Yan, and Wang, Sam S. Y. (2008a). Development and application of coastal and estuarine morphological process modeling system, Journal of Coastal Research, Special Issue No. 52, pp127-140.

Ding, Yan and Wang, Sam S. Y. (2008b). Numerical simulations of coastal flood and morphological change due to hazardous hydrological conditions at coast and estuary, In:

Solutions to Coastal Disasters 2008, Ed. By Louise Wallendorf et al., ASCE, Proceeding of Solutions to Coastal Disasters 2008 Conference, April 13-16, 2008, Oahu, Hawaii, pp. 349-360 (ISBN: 978-0-7844-0968-8).

Ding, Y., Kuiry, S.N., Elgohry M., Jia, Y., Altinakar, M.S., and Yeh, K.-C. (2013a). Impact Assessment of Sea-Level Rise and Hazardous Storms on Coasts and Estuaries Using Integrated Processes Model, Ocean Engineering, Vol.71, pp.74–95

Ding, Y., Ding, T., Jia, Y., Altinakar, M. S. (2013b). Prediction of Wind, Wave, and Storm Surge due to Hurricane ISAAC in the northern Gulf Coast, In: Proceedings of ASCE-EWRI Congress 2013 – Showcasing the Future, Cincinnati, OH, May 20-23, 2013, pp. 1793-1807.

Ding, Y., Zhang, Y.-X., and Jia, Y. (2013c). Graphical User Interface for CCHE2D-Coast − Quick Start Guide, August, 2013.

Ding, Y. (2013). CCHE2D-COAST for forecasting, planning, and investigating coastal disasters due to flooding and inundation induced by tropical cyclones, White Paper, National Center for Computational Hydroscience and Engineering, The University of Mississippi, Oxford, MS, October, 2013, 20 p.

Dubey, B., Solo-Gabriele, H., and Townsend, T., 2007. “Quantities of arsenic-treated wood in demolition debris generated by Hurricane Katrina”, J. of Environmental Science and Technology, Vol. 41, No. 5, pp 1533-1536.

Elliott, H.A., M.R. Liberati, and C.P. Huang. 1986. “Competitive adsorbtion of heavy metals by soils”. J. Environ. Qual. 15:214-219.

Frumhoff, P.C., J.J. McCarthy, J.M. Melillo, S.C. Moser, and D.J. Wuebbles. (2007). Confronting Climate Change in the U.S. Northeast: Science, Impacts, and Solutions. Synthesis report of the Northeast Climate Impacts Assessment (NECIA). Cambridge, MA: Union of Concerned Scientists (UCS). A pdf file available at http://www.climatechoices.org/assets/documents/climatechoices/confronting-climate-change-in-the-u-s-northeast.pdf

Halverson, J.B., and Rabenhorst, T. (2013). Hurricane Sandy, the science and impacts of a superstorm, Weatherwise, Vol. 66, Issue 2, pp 14-23.

Hasselmann, K., Ross, D. B., Muller, P., and Sell, W. (1976). A parametric wave prediction model, *J. Phys. Oceanogr*. 6, 200-228.

Holland, G. (1980). “An Analytic Model of the Wind and Pressure Profiles in Hurricanes”. *Journal of Applied Meteorology*, 108 (8), pp. 1212-1218.

Hwang, P.A. (2005). Drag coefficient, dynamic roughness and reference wind speed, Journal of Oceanography, 61, 399-413.

Jia, Y., Chao, X., Zhang, Y.-X., and Zhu, T. (2013). Technical Manual of CCHE2D Version 4.1, Technical Report, NCCHE-TR-02-2013, National Center for Computational Hydroscience of Engineering, The University of Mississippi, University, MS 38677, 2013.

Jia, Y and Wang, S.S.Y., (1999). "Numerical model for channel flow and morphological change studies", Journal of Hydraulic Engineering, ASCE, Vol. 125, No. 9, pp. 924-933.

Jia, Y., Wang, S.Y.Y., and Xu, Yichun, (2002). "Validation and application of a 2D model to channels with complex geometry", International Journal of Computational Engineering Science, Vol. 3, No. 1, pp.57-71.

Kaplan, J and DeMaria, M., (1995). A Simple Empirical Model for Predicting the Decay of Tropical Cyclone Winds after Landfall. Journal of Applied Meteorology, Vol. 32 (11), pp. 2499-2513.

Kuo, S., E.J. Jellum, and A.S. Baker. 1985. “Effects of soil type, liming, and sludge application on zinc and cadmium availability to Swiss chard”. Soil Sci. 122:350-359.

Large, W.G., and Pond, S. (1981). Open ocean momentum fluxes in moderate to strong winds. Journal of Physical Oceanography, 11, 324-336.

Lin, L., and Lin, R.-Q. (2004a). Wave breaking function. Proceedings 8th International Workshop on Wave Hindcasting and Prediction, Oahu, Hawaii: North Shore. Nov. 14-19, 2004.

Lin, R.-Q., and Lin, L. (2004b). Wind input function. Proceedings 8th International Workshop on Wave Hindcasting and Prediction, North Shore, Oahu, Hawaii, Nov. 14-19, 2004.

Marks, F. D., and Shay, L. K. (1998). Landfalling tropical cyclones: Forecast problems and associated research opportunities. Bull. Amer. Meteor. Soc., 79, 305–323.

Mattocks, C., and C. Forbes, (2008): A real-time, event-triggered storm surge forecasting system for the state of North Carolina, Ocean Modelling, vol. 25, pp95–119

McCallum, B.E., Wicklein, S.M., Reiser, R.G., Busciolano, R., Morrison, J.,Verdi, R. J., Painter, J. A., Frantz, E. R., and Gotvald, A. J. (2014). Monitoring Storm Tide and Flooding from Hurricane Sandy, U.S. Geological Survey Open-File Report 2013-1043, U.S. Department of the Interior, Feb. 22, 2014.

McLaren, R.G., and D.V. Crawford. 1973. "Studies on soil copper: 2. The specific adsorption of copper by soils". J. Soil Sci. 24:443-452.

Mitsuyasu, H. (1970). On the growth of spectrum of wind-generated waves (2) – spectral shapes of wind waves at finite fetch. Proc. 17th Japanese Conf. on Coastal Engrg., 1-7 (in Japanese).

NJMC (2014). New Jersey Meadowlands Commission (NJMC) real-time tide gate monitoring, http://www.frontlineaqua.com/aqua/dashboard.html.

NOAA (2014), HURDAT Re-analysis Data, Hurricane Research Division, NOAA, http://www.aoml.noaa.gov/hrd/hurdat/Data_Storm.html, accessed on February 25, 2014.

Powell, M. D. (2006). Drag coefficient distribution and wind speed dependence in tropical cyclones. Final report to the NOAA Joint Hurricane Testbed (JHT) Program, 26 pp.

Shen, W., Ginis, I., and Tuleya, R. E. (2002). A numerical investigation of land surface water on landfalling tropical cyclones. J. Atmos. Sci., 59, 789–802.

Smedley P.L., and Kinniburgh D.G., 2002. "A review of the source, behaviour and distribution of arsenic in natural waters", Applied Geochemistry 17 (2002) 517–568.

Solomon, Keith R. and John E. Warner. 1990. "Persistence, leaching, and bioavailability of CCA and pentachlorophenol wood preservatives". Final report to the Ontario Minis-try of the Environment. July 2.

Tyler, L.D., and M.B. McBride. 1982. "Mobility and extractability of cadmium, copper, nickel and zinc in organic and mineral soil columns". Soil Sci. 134:198-205.

USEPA, 2005. http://www.epa.gov/katrina/testresults/katrina_env_assessment_summary.htm

USGS (2013). Hurricane Sandy Storm Tide Mapper, http://54.243.149.253/home/webmap/viewer.html?webmap=c07fae08c20c4117bdb8e92e3239837e

Vickery, P.J., Skerlj, P. F., Steckley, A.C., and Twisdale, L. A. (2000a). Hurricane wind field model for use in hurricane simulations, Journal of Structural Engineering, Vol.126, No.10, pp.1203–1221.

Vickery, P.J., Skerlj, P.F., Twisdale, L.A. (2000b). "Simulation of Hurricane Risk in the U.S. Using Empirical Track Model". Journal of Structural Engineering, Vol. 126, No. 10, pp.1222-1237.

Young, I.R. (1988). A parametric hurricane wave prediction model. *J. Waterw. Port Coastal Ocean Eng.*, ASCE, 114, 637-652.

Young, I. R. and Burchell, G.P. (1996). Hurricane generated waves as observed by satellite, *Ocean Engng.*, 23 (8) 761-776.

Zhang, Y.-X., and Jia, Y. (2009). CCHE-MESH 2D Structured Mesh Generator Users Manual--version 3.x, NCCHE Technical Report, NCCHE-TR-2009-01, Feb. 2009. Available at https://www.ncche.olemiss.edu/research/basic/gui.

Zhang, Y.-X. (2013). CCHE-GUI – Graphical Users Interface for CCHE Models User's Manual – Version 4.0, Technical Report No. NCCHE-TR-2013-01, National Center for Computational Hydroscience and Engineering, The University of Mississippi, University, U.S.A., Jan. 2013.

Zhu, T., Jia, Y., and Wang, S.S.Y. 2011. "Arsenic Pollution by Chromated-Copper-Arsenate Treated Woody Debris," , ASCE Conf. Proc. of the 2011 World Environmental and Water Resources Congress, doi:http://dx.doi.org/10.1061/41173(414)181 , June 2011.

Zhu, T. , Jia, Y., Altinakar, M.S., Pommerenk, P., Dabak, T., and Ryon, A. (2012). "Study of Potential Impacts of Radioactive Contamination on Drinking Water Quality in Two Collinear Reservoirs Using CCHE2D Model", ICHE 2012 conference, Orlando, FL.